An ecological carrying capacity assessment for shellfish aquaculture in Baynes Sound, British Columbia

Technical Report · January 2022

5 authors, including:

Thomas Guyondet
Fisheries and Oceans Canada, Gulf Region
53 PUBLICATIONS **983** CITATIONS

Some of the authors of this publication are also working on these related projects:

Project Chlorophyll fluxes in relation with shellfish aquaculture View project

Project Picophytoplankton contribution to shellfish aquaculture View project

An ecological carrying capacity assessment for shellfish aquaculture in Baynes Sound, British Columbia

T. Guyondet[1], M.V. Krassovski[2], T.F. Sutherland[3], M.G.G. Foreman[2], and R. Filgueira[4]

[1]Fisheries and Oceans Canada
Gulf Fisheries Centre
343 Université Avenue
Moncton, NB E1C 9B6

[2]Fisheries and Oceans Canada
Institute of Ocean Sciences
9860 West Saanich Road
Sidney, BC V8L 5T5

[3]Fisheries and Oceans Canada
Pacific Science Enterprise Centre
4160 Marine Drive
West Vancouver, BC V7V 1N6

[4]Dalhousie University
Marine Affairs Program
Life Sciences Centre
1355 Oxford Street
Halifax, NS B3H 4R2

Canada

Foreword

This series documents the scientific basis for the evaluation of aquatic resources and ecosystems in Canada. As such, it addresses the issues of the day in the time frames required and the documents it contains are not intended as definitive statements on the subjects addressed but rather as progress reports on ongoing investigations.

Correct citation for this publication:

Guyondet, T., Krassovski, M.V., Sutherland, T.F., Foreman, M.G.G., Filgueira, R. 2022. An ecological carrying capacity assessment for shellfish aquaculture in Baynes Sound, British Columbia. DFO Can. Sci. Advis. Sec. Res. Doc. 2022/003. xi + 119 p.

Aussi disponible en français :

Guyondet, T., Krassovski, M.V., Sutherland, T.F., Foreman, M.G.G., Filgueira, R. 2022. Une évaluation de la capacité de charge écologique pour la conchyliculture dans le détroit de Baynes en Colombie-Britannique. Secr. can. des avis sci. du MPO. Doc. de rech. 2022/003. xii + 128 p.

TABLE OF CONTENTS

LIST OF TABLES

LIST OF FIGURES

ABSTRACT

Baynes Sound (BS), located in the waters of Georgia Strait, British Columbia (B.C.), is considered one of the most prolific production sites for bivalve culture in B.C.. Bivalve production is influenced by a balance of water quality, hydrodynamics (bay flushing), and food supply (plankton). An ecological carrying capacity assessment is required to assess this balance, where mathematical models can integrate these complex interactions using a high-resolution spatially-explicit model. The Finite Volume Community Ocean Model (FVCOM) was coupled with a Bivalve Culture Ecosystem Model (BiCEM) resorting to the Dynamic Energy Budget (DEB) to simulate bivalve physiology and their interactions with the ecosystem. These models were previously developed to address aquaculture issues in the Broughton Archipelago and Discovery Islands regions of B.C. The physical oceanographic conditions are simulated using FVCOM, analogous to previous aquaculture-motivated applications in the Broughton Archipelago and Discovery Islands. Both oceanographic observations and FVCOM outputs show a characteristic two-layered estuarine circulation over BS. This estuarine circulation appears to be strengthened or weakened by river run-off and atmospheric forcing on a seasonal scale and constitutes an overall key feature for the Sound's water inner circulation and exchange with the Strait of Georgia (SoG). The biogeochemical processes are simulated using BiCEM, which predicted that wind forcing, tidal mixing, and estuarine residual circulation contribute to the regular nutrient replenishment from the deep waters of the SoG, leading to high levels of pelagic primary productivity (phytoplankton). In turn, this phytoplankton productivity supports the potential for secondary production of zooplankton and bivalve culture. In general, the response of zooplankton and wild bivalve populations to the existing shellfish aquaculture activity indicates a system within the bounds of its ecological carrying capacity. Although the planned expansion of additional farm coverage and stock, currently under review, would impose an increased demand on the Sound's pelagic resources, the results do not indicate that the additional bivalve production could not be sustained. However, a precautionary approach should be considered with high-stocking scenarios and concentrated areas, such as, Fanny, Mud, and Deep Bays. Gradual aquaculture development in concert with proper monitoring of environmental and cultured shellfish conditions (Research Paper #2) in sensitive areas may provide sustainability of BS.

1. INTRODUCTION

Bivalve aquaculture is usually promoted as one of the greenest animal protein sources, and it has been proposed as a way to sustainably extract more food and biomass from the ocean (SAPEA, 2017). In addition to food provisioning, bivalve aquaculture can provide other ecosystem services like water clarity (Cranford 2019) and nutrient extraction (Petersen et al. 2019). Despite these services, the cultivation of bivalves at high densities could potentially cause negative effects on the environment (reviewed by Weitzman et al. 2019). Some of these potential ecosystem effects are common to most human activities carried out in the ocean, e.g. deployment of gear, marine litter, etc. Some are common to other aquaculture activities, e.g. introduction of invasive or exotic species, and the spread of disease, pathogens, and genes. Finally, some of the potential effects are specific to bivalve aquaculture and are related to the potential alteration of flows of energy and matter via bivalve physiology: (1) the filtration activity of the bivalves can exert a top-down control of phytoplankton populations (Dame 1996, Timmermann et al. 2019); (2) the differential retention capacity of particles of different size can modify the structure of the planktonic community (Jiang et al. 2016, Froján et al. 2016); (3) the excretion and egestion can modify nutrient dynamics and, in turn, affect phytoplankton populations (Smaal 1991, Cranford et al. 2007); (4) the organic deposition can affect benthic habitat and nutrient dynamics (Newell 2004, Smyth et al. 2018); furthermore (5), these potential effects on nutrient dynamics and planktonic communities can cause cascading effects on higher trophic levels (Jiang and Gibbs 2005, Kluger et al. 2017).

Although all these potential impacts are relevant, and to a certain degree most of them have been covered in the scientific literature, the bivalve-phytoplankton interaction has captured most of the attention. The rationale for this emphasis on phytoplankton is two-fold. First, phytoplankton is the main food source for bivalves, and an impact on phytoplankton abundance can affect the growth of the farmed population, which is crucial for the viability of the activity (Bacher et al. 2003, Ferreira et al. 2007). Second, phytoplankton is the base of the food web, and as it has been stated above, an impact on phytoplankton can cause cascading effects through the food web, and consequently lead to ecosystem-level impacts. Furthermore, the focus on ecosystem-level effects is at the core of the Ecosystem Approach to Aquaculture (EAA, Soto et al. 2008), the state-of-the-art understanding on how aquaculture should be managed. Following the guiding principles of the EAA, management should focus on far-field effects that can impact ecosystem functioning rather than on near-field effects in the vicinity of the farm. Accordingly, taking into account the potential for phytoplankton to capture ecosystem-level effects and the EAA guiding principles, the bivalve-phytoplankton interaction has become mainstream for assessing the potential impacts of bivalve aquaculture (DFO 2015, Filgueira et al. 2015a).

Ecological Carrying Capacity (ECC) has been proposed as a tool to operationalize the EAA from the natural ecosystem standpoint (Weitzman and Filgueira 2020), and it has been defined as the magnitude of aquaculture activity in a given area that can be supported without leading to unacceptable changes in ecological processes, species, populations, communities, and habitats in the aquatic environment (DFO 2015*). A priori,* ECC calls for the analysis of the full range of ecosystem-level interactions, but according to the EAA guiding principles, ECC is usually assessed by focusing on the bivalve-phytoplankton interaction. Furthermore, this decision is also guided by the law of parsimony, which suggests that the analysis of a problem should focus on the relevant system features, critical dynamics, and scales to the problem to be solved, avoiding unnecessary complexity (Food and Agriculture Organization [FAO] 2008, Fulton 2010). This is particularly relevant when ECC is assessed using ecosystem models, as the increase of model complexity to bolster realism inherently leads to greater scientific uncertainty (FAO 2008).

Accordingly, most models to assess ECC in bivalve aquaculture sites have focused on coupling a hydrodynamic model, representing the water circulation of the system, to a low trophic model representing the nutrient, phytoplankton, and zooplankton dynamics with the addition of the bivalve component (e.g. Guyondet et al. 2010, Dabrowski et al. 2013, Pete et al. 2020). The physical oceanographic conditions in BS are simulated using the same Finite Volume Community Ocean Model (FVCOM; Chen et al. 2006) that was previously developed and applied to assist in addressing aquaculture issues in the Broughton Archipelago and Discovery Islands regions of B.C. (Foreman et al. 2015).

BS is one of the most relevant farming areas for bivalves in British Columbia (B.C.), Canada. Over the last five years the clam and oyster industry in B.C. has contributed significantly to the total Canadian production in terms of harvest landings (clam: 67%; oyster: 60%) and dollar value (clam: 85%; oyster: 39%) (DFO 2019). Common clams that are harvested include butter, littleneck, Manila, geoduck and varnish clams, while the oyster taxa that are cultivated in BS consist of Pacific, European, and Eastern oysters. Although aquaculture monitoring in the near-field occurs following aquaculture regulations, an ECC assessment of BS for potential future expansion of aquaculture is lacking; however, this estimation is crucial to determine the ecological sustainability and to ensure that farming is carried out according to an EAA approach. Accordingly, the overarching goal of this study is to create a spatially-explicit hydrodynamic-biogeochemical coupled model to ultimately estimate the ECC of BS for current and hypothetical aquaculture scenarios. This will be addressed by coupling a Finite Volume Community Ocean Model (FVCOM) for BS with a novel low-trophic model, Bivalve Culture Ecosystem Model (BiCEM), which includes a Dynamic Energy Budget (DEB) model to simulate bivalve physiology and growth, and their interactions with the ecosystem. This overarching goal will be addressed by tackling the following objectives:

1. Evaluate the hydrodynamic accuracy of the FVCOM model component and discuss the biological applicability of the biogeochemical (BiCEM) component in the coupled BS model (Appendix A and C).

    a. Compare modelled and observed water properties.

    b. Identify uncertainties and consequences associated with data availability and modelling parameterizations through sensitivity analyses for this Pacific region application of FVCOM-BiCEM.

2. Assess ecological carrying capacity for bivalve aquaculture in BS at a bay wide scale using a high-resolution, spatially-explicit hydrodynamic-biogeochemical coupled model (FVCOM-BiCEM) (Main document and Appendix B).

3. Include an assessment of the potential influence of new site applications on existing farms across varying spatial scales for use in management decision-making with respect to shellfish aquaculture facilities (Main document).

2. SITE DESCRIPTION

2.1. DESCRIPTION

BS is a coastal embayment located in the northern SoG, which is bordered by Vancouver Island and the southwestern mainland of B.C., Canada (Figure 1). In turn, BS consists of a channel bound by Vancouver Island and Denman Island and oriented along a northwest-southeast axis (40 km). The Sound has an area of 90 km^2 which includes sheltered bays, intertidal mud- and sand-flats, marshes, and rocky substrates (Carswell et al. 2006). While the majority of the subtidal area is between 20-30 m in depth, the upper reach consists of a wide, deep basin (40-

80 m) and the lower reach widens into Mud and Deep Bays upstream of the restricted southern entrance. A diverse intertidal zone borders the shoreline and dominates the western shore with wide mud- and sand-flats that experience a 4-metre (spring) tidal range.
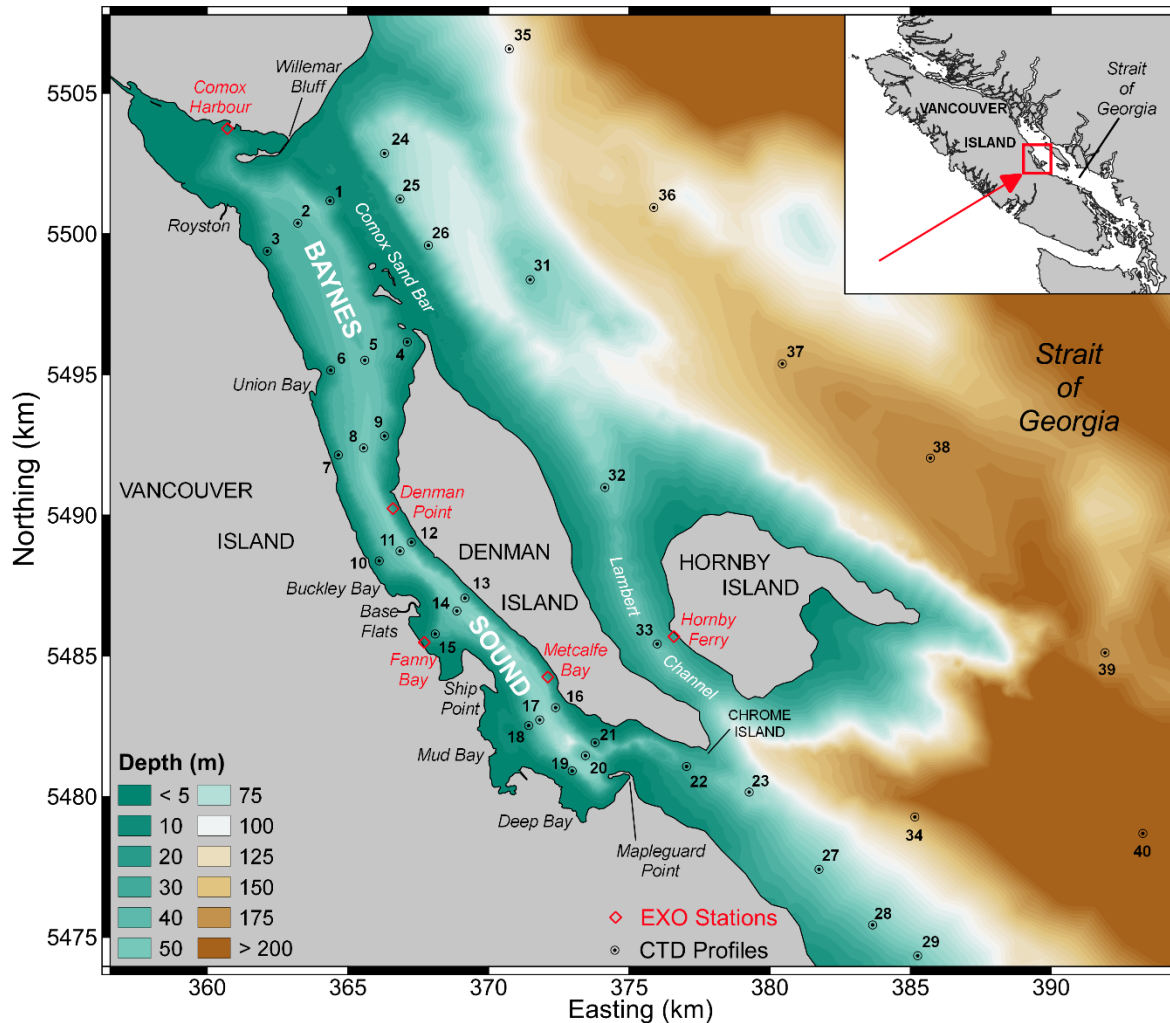
Figure 1: Map of the Baynes Sound study area showing water depths and locations of the main sites of interest as well as sampling stations.

2.2. OCEANOGRAPHY

BS follows a traditional estuarine definition where a semi-enclosed water body exchanges with the open sea and is diluted by terrestrial inflows of freshwater that drives the 2-layer estuarine convection (Pritchard, 1967). The Courtenay River, located at the head of the Sound and fueled by both the Tsolum and Puntledge Rivers, provides the largest input of freshwater runoff with a mean annual discharge of 51-54 m^3 s^{-1} (Morris et al. 1979; Riddell and Bryden, 1996). Water exchange between BS and the SoG occurs at two locations: 1) the northeastern Comox Sandbar provides a wide (>5 km) and shallow (4 m) intertidal connection between Denman Island and Comox; and 2) the southeastern 20 m-deep entrance between the southern tip of Denman Island and Mapleguard Point (Vancouver Island). Although volume fluxes of water are substantial at the northern Comox Sandbar entrance within the upper 4 m of the water column, the southern entrance serves as the primary conduit for deep-water exchange.

Denman Island provides protection from wind-induced wave action from the SoG and promotes seasonal stratification of the water column. Winter winds are predominantly from the southeast and relatively stronger than other seasons due to the unobstructed southeast stretch across the SoG. Although the summer winds are predominantly from the northwest and relatively weaker having developed across an obstructed land-sea stretch, this wind bearing provides a down-Sound force driving the surface layer towards the southeastern entrance and promoting a counter-flow at depth. Under certain tidal conditions, this scenario appears to facilitate deep-water renewal and vertical exchange across the southern semi-restricted sill entrance. In addition, vertical mixing may take place with southeasterly wind-driven upwelling at the western shore induced by an east-west temperature differential influenced by cold-water intrusions across the Comox Bar (Waldie 1951). In general, BS is considered to be well ventilated where the bottom-water is replaced approximately every two months, based on dissolved oxygen distributions, modest river runoff, and tidal exchange (Morris et al. 1979). These mixing scenarios influence nutrient availability for phytoplankton production.

2.3. PHYTOPLANKTON

Phytoplankton biomass varies along the down-Sound hydrodynamic gradient depending on the season. In the spring time, the protected upper-reach basin promotes stratified conditions that support the formation of a phytoplankton lens and strong chlorophyll maxima. Alternately, uniform profiles of phytoplankton biomass are observed in the lower reach of the Sound as they are influenced by the narrow entrance tidal jet and boundary water conditions. However, during summer conditions, pronounced sub-surface chlorophyll maxima (5-15 m) can extend across the entire Sound with varying levels of production.

2.4. BENTHOS

Within the subtidal zone, sediment texture, geochemical attributes, and meiofauna abundance patterns follow a strong hydrodynamic gradient along the length of the central axis of BS (Sutherland et al. 2018). Sediment texture transitions from a cohesive muddy sediment in the deeper floc-dominated depositional basin (upper reach of BS) to a non-cohesive sandy sediment in the tidally-dominated southern entrance. In turn, this trend aligns with decreases in 1) sediment erodibility (Sutherland and Amos, 2020); and 2) hydrodynamic control of eroded particle size (Kassem et al. 2021), with an increasing seabed sand component towards the southern entrance. A combination of local terrestrial sand-based landforms (e.g. Willemar Bluff) and high-energy hydrodynamic conditions maintain the well-sorted Comox sand-bar and dune-rippled sandy shoal located at the northern and southeastern entrances, respectively (Clague 1976; Pritchard, 1967).

2.5. INTERTIDAL

BS serves as a sheltered estuary with a vast intertidal zone, characterized by a range of substrate types and hydrographic conditions, that provides sufficient habitat for a wide variety of bivalve populations. Extensive tidal flats exist on the western shore at Ship Point, Fanny Bay, Mud Bay and Deep Bay, while a large sand bar at the northeastern entrance harbours significant populations of both wild and cultured clams.

3. METHODS

3.1. SUPPORTING DATA

Ecosystem variables supporting bivalve ecological carrying capacity assessments were collected with varying frequency and spatial resolution depending on modelling requirements and resources available. Sampling and data collection can be divided into the following components:

- Vertical profiles of oceanographic and biological variables (temperature, salinity, dissolved oxygen, turbidity, *in vivo* fluorescence, and photosynthetically active radiation (PAR)) were collected using a Seabird-911 profiling CTD (conductivity, temperature, depth) equipped with a 24 Niskin-bottle Rosette. The location, timing, and frequency of physical oceanographic data collection (temperature, salinity, and dissolved oxygen) are described in Appendix A and mapped on Figure 1. In general, CTD profiles were carried out in the spring (April) and summer (June-August) periods fairly consistently between 2009 and 2019, with an increase in station coverage within the boundary zone of the SoG in 2014. Central-axis stations (2, 5, 8, 11, 14, 17, 20, 22, 23) were surveyed annually with the exception of 2010, 2015, and 2017. Additional CTD data acquired from local Fisheries and Oceans (DFO) monitoring programs provided an increase in spatial and temporal coverage within the modelling domain.

- Vertical profiles of plankton and nutrient variables were collected with congruent water samples during the CTD Niskin-Rosette deployments, where bottles were triggered independently at standard oceanographic depths to capture a profile of both physical and biological analyses. (0, 5, 10, 15, 25, 50, 75, 100, 150, 200, 250, 300, 350 m; Water Properties Section, Institute of Ocean Sciences, Fisheries and Oceans Canada). Each water sample was analyzed for seston (suspended particulate matter), organic/inorganic fractions, particulate carbon and nitrogen, phytoplankton production (chl-a) and dissolved nutrients [nitrate/nitrite (NO_3/NO_2), phosphate (PO_4), silicate (SiO_3)] concentrations. In addition, phytoplankton primary productivity incubations were carried out at the upper, lower, and outer reach of BS. The laboratory analyses for these sampled variables are outlined in Appendix C.

- Time-series CTD data at fixed depth on oyster rafts were carried out using YSI-EXO2 Sondes. Deployment at 5 m depth (oyster-rack height) at each oyster growout site in the upper (Denman Point) and lower (Metcalfe Bay) reaches of BS. Other non-growout deployment locations included Comox Harbour, Fanny Bay, and Lambert Channel (between Denman and Hornby Islands) (Figure 1). Water samples were collected in 1-L Nalgene bottles from a portable Niskin bottle deployed at the depth of the oyster rafts (5m) during the oyster growout trials. These water samples were collected to support the CTD time-series data and both DEB (Appendix B) and BiCEM modelling.

- Time-series temperature data were collected at three fixed racks on oyster stacks using HOBO pendants. HOBOs attached to the top, middle, and bottom oyster racks within each replicate oyster stack deployed at both Denman Point and Metcalfe Bay (Table 1; Figure 1). This data supported the oyster DEB modelling outlined in Appendix B.

Table 1: Physical and biological oceanographic variables collected from CTD vertical profiles and fixed-depth, time-series deployments. Chl = chlorophyll, Diss = dissolved; PAR = photosynthetically active radiation, CTD = Conductivity, temperature, depth.

Deployment	Vertical Profiles		Time-series 5m depth		Time-series, 5m-depth, oyster racks # 2, 8, 14
Instrument-probe / Water-samples	CTD Seabird-911	Water samples	YSI-EXO-CTD	Water samples	HOBO Temp probe
Time period	2009-2019	2009-2019	2016-2017	2016-2017	2016-2017
Temperature	X	X	X	-	X
Salinity	X	X	X	-	-
Oxygen	X	X	X	-	-
Fluorescence	X	-	X	-	-
Turbidity	X	Seston	X	Seston	-
PAR	X	-	-	-	X
Chl extraction	-	X	-	X	-
Diss nutrients	-	X	-	-	-
Locations	Selected stations (see Appendix A)	Selected stations (see Appendix A)	Comox Harbour	Comox Harbour	-
			Denman Point	Denman Point	Denman Point
			Fanny Bay	Fanny Bay	-
			Metcalfe Bay	Metcalfe Bay	Metcalfe Bay
			Lambert Channel	Lambert Channel	-

Methods associated with zooplankton abundance and biomass, oyster growth rates, and intertidal bivalve diversity are outlined in the methods section in Appendix C.

3.2. THE OCEAN CIRCULATION MODEL

The physical oceanographic conditions in BS are simulated using the same Finite Volume Community Ocean Model (FVCOM, Chen et al. 2006) that was previously developed and applied to help address aquaculture issues in the Broughton Archipelago and Discovery Islands regions of B.C. (Foreman et al. 2015). FVCOM solves the three-dimensional (3D) primitive equations for velocity and surface elevation in combination with the 3D transport/diffusion equations for salinity and temperature in the presence of turbulent mixing. This is done on a spatial grid that approximates the region of interest with triangular columns of varying size and orientation. FVCOM is coupled to the bivalve culture ecosystem model (BiCEM) by simply employing regularly stored values of temperature, salinity, velocity, and mixing as BICEM input. The feedback of suspended aquaculture structures on water circulation was not accounted for in the present implementation of FVCOM for Baynes Sound (Grant and Bacher. 2001). These effects are thought to be very localized in the direct vicinity of such farms. Moreover, this type of culture is only practiced on a very limited portion of the Sound (0.37 and 2.26% of the Sound's area in the Current and Expansion scenarios, respectively). Consequently, it was concluded that omitting these feedback processes would represent a minor bias in the carrying capacity

assessment that is conducted at much wider scale (bay or sound). Further details on FVCOM's application to BS and its evaluation can be found in Appendix A.

3.3. BIVALVE CULTURE ECOSYSTEM MODEL (BICEM)

The present study relies on the off-line coupling of FVCOM with a biogeochemical model as detailed in Appendix C. Briefly, BiCEM simulates the nitrogen cycle, considered as the limiting element for BS productivity, through inorganic nutrients, phytoplankton, non-living suspended organic matter, zooplankton, and wild and cultivated bivalves. Bivalve eco-physiology is addressed with specific Dynamic Energy Budget (DEB) models that were first evaluated separately (Appendix B and Filgueira et al. 2016a) and then incorporated in the BiCEM structure. Hence, the coupled model provides a dynamic and spatially-explicit representation of the ecosystem resulting from the interactions between all variables.

The model verification was conducted by comparison with *in situ* observations of the different variables as detailed in Appendix C. The model agreed reasonably well with the data available over the 2016-17 annual cycle and was deemed suitable to further explore the functioning of the BS system.

In particular, model outputs were analysed to assess the ecological carrying capacity of BS for shellfish aquaculture based on 5 specific scenarios:

- Current: meant to be as representative as possible of BS conditions in 2016-2017, this scenario was used for comparison with field observations during the model calibration procedure (see Appendix C).

- No aquaculture: all shellfish farms are removed from the Current scenario. In terms of bivalves, only wild clam beds remain.

- Current – Max: all existing farms in the Current scenario operate at a maximum stocking density that was derived from the maximum production criteria provided by the Aquaculture Management Directorate (AMD) at DFO, which corresponded to 50 t ha^{-1} for bottom culture and 200 t ha^{-1} for culture in suspension.

- Expansion: farms that were not included in the Current scenario either because they did not exist in 2016-17 or existed but did not report any production in 2015 and 2016. This scenario includes new applications currently (as of December 2020) under review by AMD.

- Expansion – Max: combines the two previous scenarios by considering all farms (existing + new) at maximum stocking density.

The overall cultivated bivalve stocks and farm coverage for each scenario are summarized in Table 2.

Scenarios were compared to one another using relative change indices (RCI) for various variables (X) as follows:

$$RCI = 100 \times \frac{X_S - X_R}{X_R}$$

Where S refers to the specific scenario tested and R is a reference scenario. As for the sensitivity analysis results presented in Appendix C, RCI were calculated on temporally and spatially explicit bases, i.e. at each time step and depth-integrated at each model grid node, but were then consolidated through temporal and spatial statistics (mean, absolute mean, maximum, minimum and standard deviation) for presentation. Spatial mean calculations of depth-integrated values were weighted by grid cell areas to account for the irregular resolution.

The distribution of bivalve farms considered in the Current and Current – Max scenarios as well as farms added to the Expansion and Expansion – Max scenarios are presented in Figure 2 for reference.

Table 2: Summary of cultured bivalve stocks and farm coverage per culture type/species and for all scenarios tested.

Scenario	Bivalve stocks ($\times 10^6$ ind)						
	Wild Clams	Cultivated Clams	Bottom Oysters	Suspended Oysters	Total Cultivated	Total	Change in Total (%)
Current	996.36	1006.09	97.98	99.61	1203.68	2200.04	-
Current - Max	996.36	1257.62	275.56	137.50	1670.68	2667.04	21.23
Expansion	917.92	1290.71	112.98	534.13	1937.82	2855.75	29.80
Expansion - Max	917.92	1613.38	317.76	737.30	2668.43	3586.36	63.01

Scenario	Area coverage (ha)					
	Wild Clams	Cultivated Clams	Bottom Oysters	Suspended Oysters	Total Cultivated	Fraction of BS under culture (%)
Current & Current - Max	884.07	269.04	248.02	34.67	551.72	5.84
Expansion & Expansion - Max	829.90	338.93	283.34	213.74	836.01	8.84
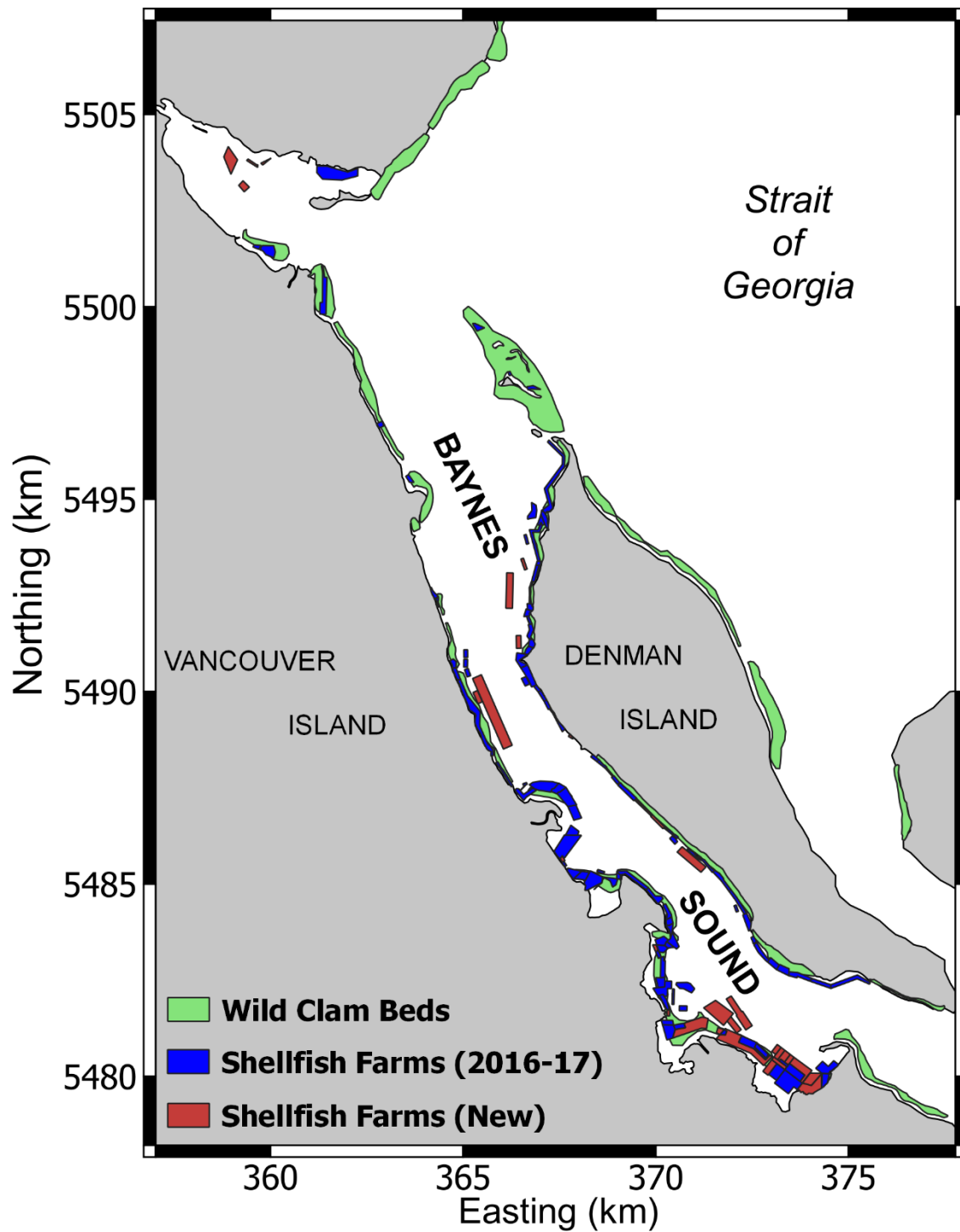
Figure 2: Spatial distribution of wild clam beds (green, source: iMapBC,) and bivalve farms considered in the Current and Current - Max scenarios (blue) and added to the Expansion and Expansion - Max scenarios (red).

4. EVALUATING BAYNES SOUND ECOLOGICAL CARRYING CAPACITY FOR SHELLFISH AQUACULTURE

The objectives of the present section are to answer questions related to the second and third Terms of Reference objectives of this Canadian Science Advisory Secretariat (CSAS) process.

4.1. MAIN FEATURES OF BAYNES SOUND PELAGIC ECOSYSTEM

The present study focuses on the 2016-17 annual cycle, spanning May 2016 to April 2017, as it provided the best available data set to force and validate the biogeochemical component (BiCEM) of the coupled model, in particular simultaneous information on most pelagic variables (nutrients, phytoplankton, particulate organic matter and zooplankton) and suspended oyster growth. As such the present assessment is somewhat constrained to the 2016-17 observed biological conditions. In an effort to assess the inter-annual variability of these conditions and highlight more persistent features, all nitrate and phytoplankton data collected in recent summers (spanning 2011 – 2019) through vertical profiles along the main central axis of BS were compared (Figure 3).

Given the dynamic nature of pelagic ecosystems and the fast turnover rate of phytoplankton, it is difficult to draw any strong conclusions regarding the inter-annual variability of BS's conditions from these data. However, a strong vertical stratification is characteristic of these summer conditions, as also observed for physical variables. Phytoplankton productivity, confined to the euphotic zone (depth of 1% surface light level), results in the larger concentrations observed in the top 10 meters of the water column. Exceptions seem to occur during periods of strong production (blooms in 2018 and 2019) when large biomasses extend over a thicker top layer and down to 15–20 m depth throughout the Sound. As a consequence of the phytoplankton biomass aggregation, surface waters are depleted of nitrate over a similar depth, which most likely limits further production in summer conditions. Nutrient depletion is common during calm summer conditions of B.C. surface waters due to the seasonal appearance of flagellate phytoplankton blooms. These flagellate blooms deplete and then exploit the upper water-column via daily vertical migration down to the nutrient-rich dense subsurface layer to pick up nutrients and then up to the water surface to harvest sunlight for photosynthesis (Haigh and Taylor, 1990). Below an often sharp change in density (pycnocline) and nutrients (nutricline) in the water column, deeper waters exhibit higher nitrate concentrations with, in all sampling occasions, a wedge-like water mass of highest nutrient concentrations extending to diverse degrees from the southern entrance into the Sound. This pattern suggests the intrusion of nutrient-rich, high-density, deep-waters from the SoG over the BS sill at the southern entrance as an important pathway for nutrient renewal and subsequent sustained productivity of BS's ecosystem. Deep-water renewal is common in local B.C. inlets where restricted, shallow-silled entrances create strong tidal jets that facilitate deep-water exchanges under certain tidal conditions (Haigh et al. 1992; Lazier, 1963). In addition, FVCOM-derived volume-fluxes revealed a Coriolis-influenced vertical stratification of incoming and outgoing fluxes across the southern entrance (Figure A14b). Given this vertical water-column structure between April and June, absence of phytoplankton in light-intense surface waters (photo-inhibition), and the chlorophyll maxima depths (4-10 m) observed on either side of the entrance, both deep-water nutrient intrusion and the seeding of surface-dwelling phytoplankton may help maintain phytoplankton production in the Sound. FVCOM-derived volume-fluxes confirm a residual circulation allowing deep water to enter the southern entrance in all seasons (Figure A14b).

The Northern SoG that encompasses our model boundary zone has been observed to have relatively higher nutrients and flagellate phytoplankton concentrations along the western Vancouver Island shoreline, in proximity of BS entrances, during the typical summer stratified, nutrient-depleted conditions that are observed on the SoG northern shore (Haigh and Taylor,

1990, 1991; Olson et al. 2020). This pattern is attributed to the entrainment of nutrients and micro-algae from tidal turbulence of northern passages, including Discovery Passage, and may provide favourable forcing conditions for BS's sustained productivity. Although river run-off represents another potential source of new nutrients, using annual cycles of discharge and concentration of the four principal rivers, nitrogen loading appears fairly low when scaled to the Sound's surface area (DIN = 0.97 and DON = 1.41 gN m^{-2} yr^{-1}). The low sensitivity of BiCEM variables to these river inputs, reported in Appendix C, suggests that they also have a limited influence in the model ecosystem.
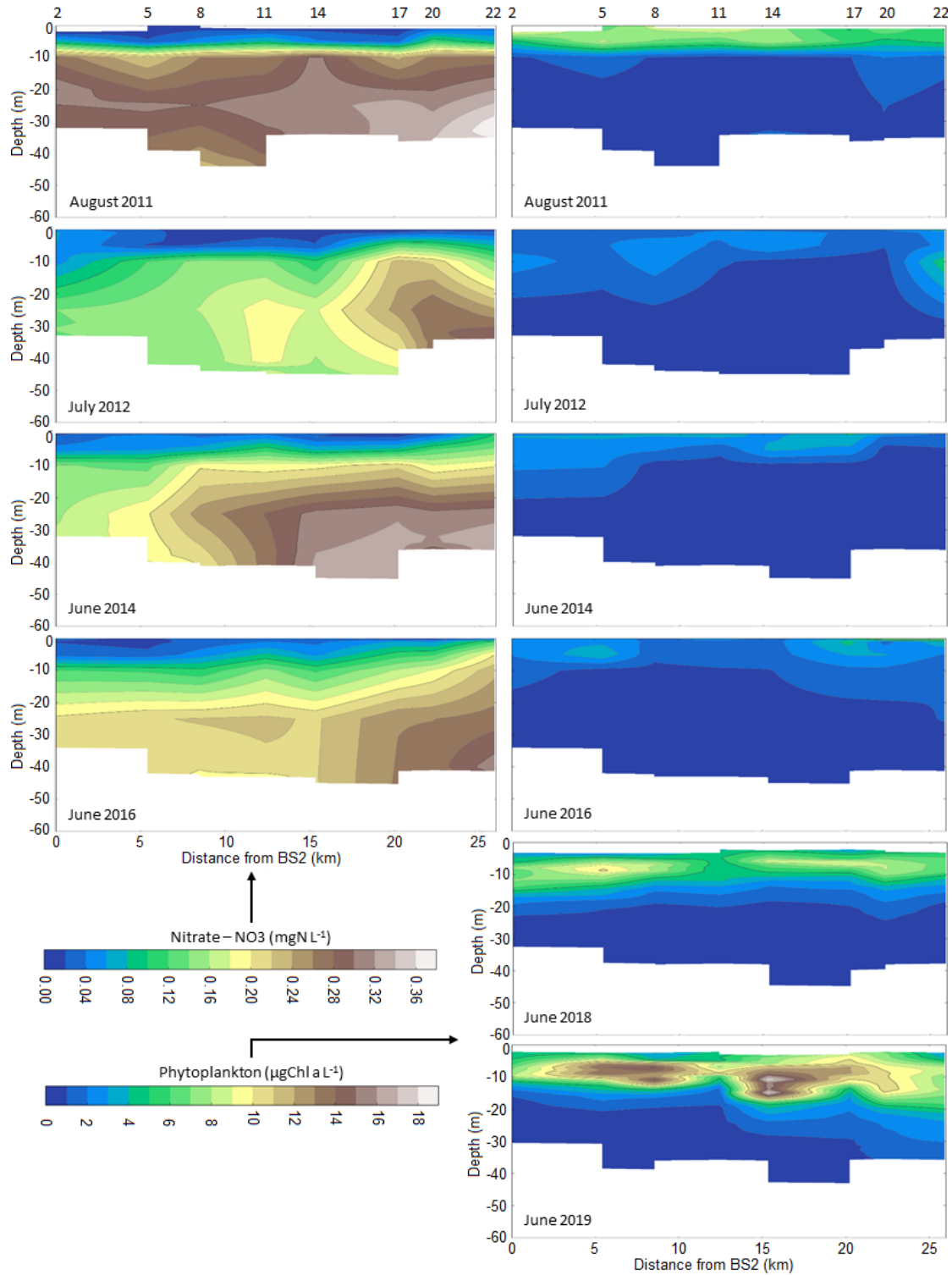
Figure 3: Thalweg plots of nitrate (left) and phytoplankton (right) concentrations from summer surveys conducted in BS in recent years (besides August 2011, sampling was conducted in late June – early July). Station BS2 in the upper Sound is used as the origin of all transects extending southward through stations BS 5, 8, 11, 14, 17, 20, 22 (shown above top row panels, see Figure1 for locations).

The bottom-rich water intrusions just mentioned would require some mixing mechanism in order to bring the nutrients up in the euphotic zone and fuel new phytoplankton production. One logical candidate for such mixing is tidal forcing. Figure 4 matches the daily time series of continuously recorded phytoplankton concentrations (Chl-a; YSI-EXO2 Sonde fluorometer probes; Table 1) at 5-m depth at both upper (Lucky-7) and lower (Mac's Oysters) Sound monitoring stations, with the daily tidal range simulated by FVCOM at the lower Sound location, an indicator of the Neap-Spring cycle. Looking at the summer period (late June to early September) when nutrients are most likely to limit primary production in surface waters, it is striking to see how the peaks in phytoplankton biomass tend to coincide with lows in the tidal range (Neap phase). A hypothesis to explain this pattern is that the Spring phase contributes enough mixing to bring some replenishment of nutrients to the surface layers and disperse phytoplankton across the water column, preventing accumulation in the euphotic zone. Only the following Neap phase brings enough water-column stability for the phytoplankton to take advantage of the new nutrients and produce the observed peaks in biomass. Such a physical control on phytoplankton, common in deep estuarine systems (Therriault et al. 1990; Winter et al. 1975), combined with the intrusion of nutrient-rich bottom waters and/or tidal-jet seeding of flagellate phytoplankton (Taylor et al. 1994) from the SoG, seems to constitute an important process for the overall productivity of BS.
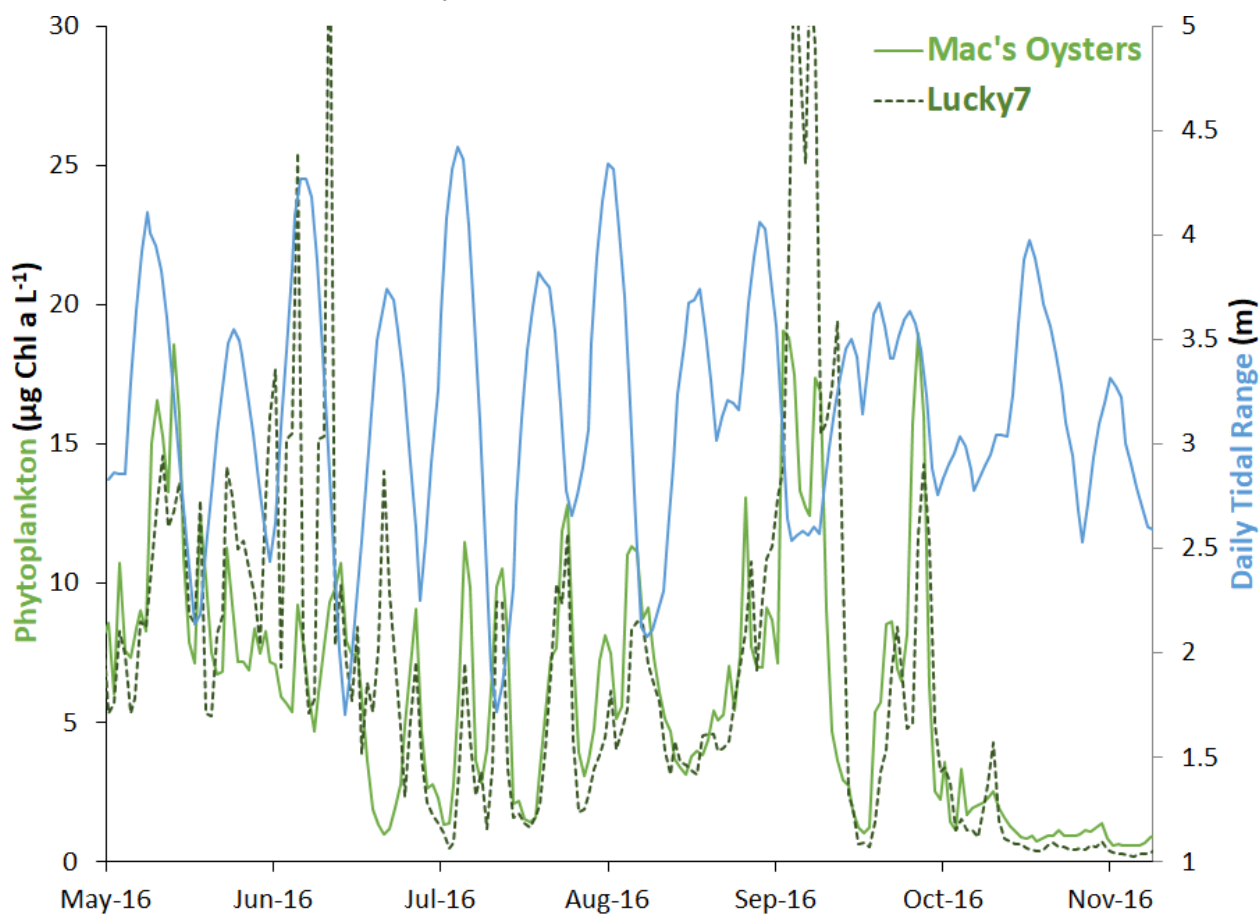
Figure 4: Time-series of phytoplankton concentration (left axis) as measured with moored fluorometers at a fixed depth of 5 m at both the upper (Lucky7) and lower (Mac's oysters) BS monitoring sites. Daily tidal ranges simulated by FVCOM at the Mac's Oyster site are also shown as an indicator of the Neap-Spring tidal cycle (right axis).

The combined influence of the southern-entrance tidal jet along with the northern Courtenay River outflow and Comox Bar surface exchange could potentially lead to differences in the upper vs lower Sound dynamics. The analysis of BiCEM results in Appendix C indicated that the upper Sound seemed generally more sensitive to changes in contrast to a more resilient lower Sound. Spatial distribution maps of annual phytoplankton net primary productivity and mean biomass estimated over the water column from the model results also reveal some heterogeneity across the entire Sound (Figure 5). Primary productivity is markedly stronger in the upper portion of the Sound. The Neap-Spring dynamics and nutrient-rich water intrusions from the south described earlier, coupled with the bottom topography gently sloping up towards the upper Sound (Figure 1), bringing nutrient-rich waters closer to the surface may explain this latitudinal gradient. Although not very influential at the Sound scale, direct river nutrient inputs and longer residence times (Figure A15) could also contribute to the stronger productivity at the upper end. The geographical contrast in productivity does not translate into a similar upper/lower Sound distinction for mean phytoplankton biomass (Figure 5). Such a discrepancy suggests that part of the upper production gets exported either directly to the SOG through the Comox Bar but also likely towards the lower Sound given the direction of the residual circulation in the surface layers (Figure A14).
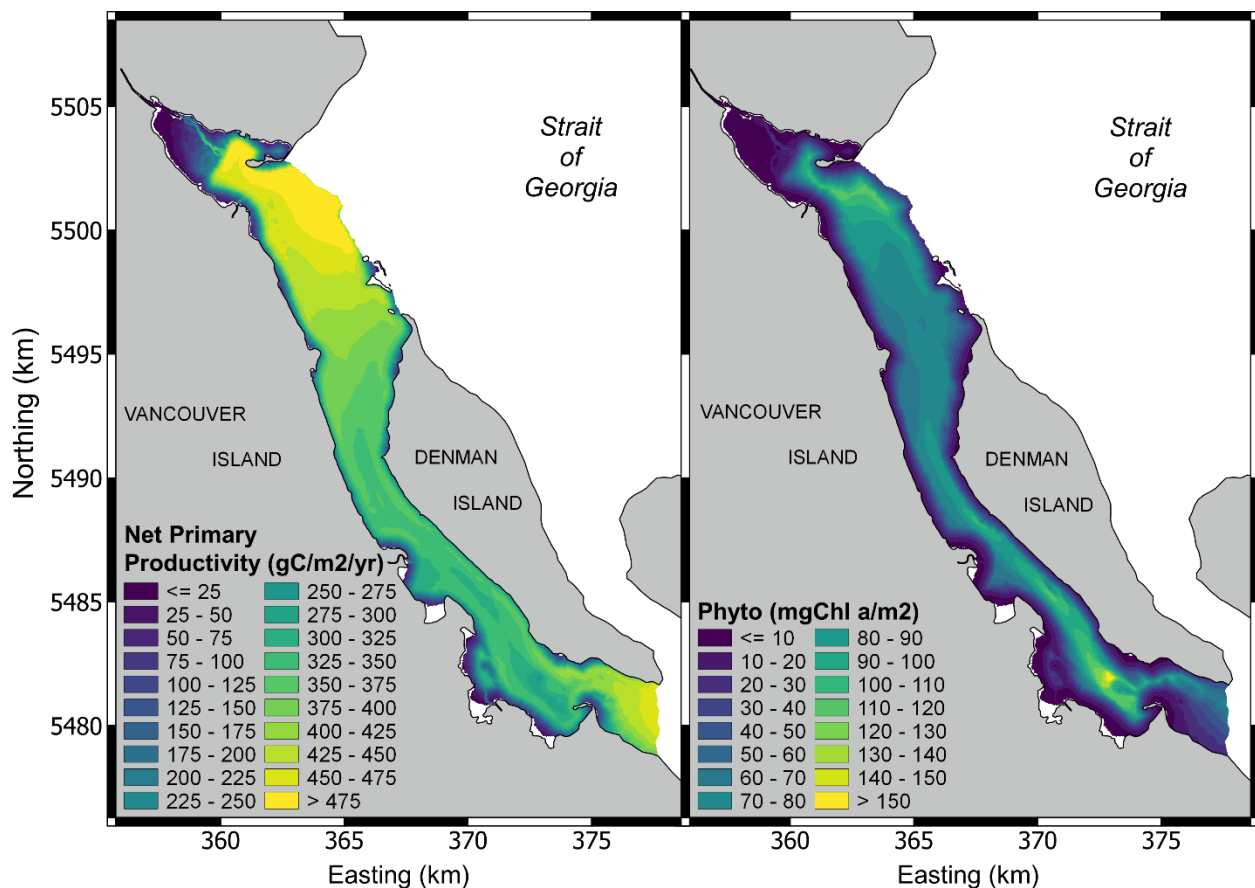
Figure 5: Spatial distribution of annual phytoplankton net primary productivity (left) and mean biomass (right) in Baynes Sound estimated from BiCEM results over the whole water column for 2016-17 providing a reference for scenario-building.

Finally, the BiCEM outputs were processed to compare the uptake of phytoplankton resources by zooplankton and cultured and wild bivalve populations against phytoplankton renewal through primary productivity at the whole BS scale (Table 3). Although some uncertainty is associated with these model estimates as discussed in Appendix C, their relative magnitude provides a strong indication that cultured bivalves at the 2016-17 level of aquaculture development exert a much smaller filtering pressure than zooplankton and only utilize a small fraction of the pelagic resources produced at the Sound scale. Further analysis of cultured bivalve influence is provided in the following sections.

Table 3: Comparison of phytoplankton production (net primary productivity) and consumption by cultured bivalves and zooplankton at Baynes Sound scale and on a seasonal and annual basis as estimated from BiCEM outputs in the 2016-17 reference conditions. Winter: January, February, March; Spring: April, May, June; Summer: July, August, September; Fall: October, November, December.

Season	net Primary Productivity	Phyto uptake by wild clams		Phyto uptake by cultured bivalves		Phyto uptake by zooplankton	
	$(gC\ m^{-2})$	$(gC\ m^{-2})$	% netPP	$(gC\ m^{-2})$	% netPP	$(gC\ m^{-2})$	% netPP
Winter	3.31	0.04	1.17	0.07	2.15	1.76	53.00
Spring	176.31	0.15	0.08	0.37	0.21	110.52	62.69
Summer	140.53	0.15	0.10	0.37	0.26	122.38	87.09
Fall	8.47	0.04	0.53	0.09	1.08	12.22	144.32
Year	328.61	0.38	0.11	0.90	0.28	246.88	75.13

4.2. CARRYING CAPACITY ASSESSMENT

Carrying capacity for shellfish aquaculture of a specific body of water is commonly evaluated by the comparison of bivalve food renewal rate, through primary productivity and exchange of water, and food consumption rate by the entire cultured bivalve population in the study area (Dame and Prins, 1998). Hay and Co (2003) used this approach for their BS carrying capacity estimate, considering the whole Sound as a single homogenous body of water and using model outputs to derive average (both in time and space) food renewal rates and limited experimental data to provide the bivalve filtration rate. In the present study, the same conceptual approach of rate comparison was applied although through a validated dynamic and high-resolution, spatially-explicit framework (see triangular grid-structure in Figure A2). This integrated modelling approach provides spatial fine-scale outputs to further explore the response of BS's pelagic ecosystem and wild and cultured bivalves to various scenarios of aquaculture development.

4.2.1. General Scenario Comparisons

Reference conditions are necessary to assess each aquaculture development scenario. In the present study, a specific model scenario where all cultured bivalves were removed from the ecosystem (No Aquaculture) was first used as such a common reference.

4.2.1.1. Current scenario

The Current scenario was first evaluated as representative of 2016-17 conditions in BS.

Pelagic variables

Figure 6 summarizes the response of phytoplankton, particulate organic nitrogen (PON) and zooplankton as maps of time-averaged relative change indices (RCI). Following the farm

distribution along the edges of the Sound and aggregation towards the south, reductions in these three variables are generally stronger in the nearshore and in the lower half of the Sound. Phytoplankton reduction remains below 2% over most of the open water areas and below 15-20% in the nearshore, except for a few limited areas where it can reach 30% and above (Figure 6a). It is to be noted that for a given filtering pressure the RCI would be more sensitive in shallower areas where the volume of water available to absorb this pressure is smaller. This does not constitute a model nor index artefact but follows from the logical increase in sensitivity to food reduction in shallower waters. Nonetheless, slightly more pronounced effects are predicted by the model for all variables in the inner portions of Deep Bay, Mud Bay and Fanny Bay, despite significant water exchanges (4-5 m tidal range) relative to maximum water height/volume.

Although PON represents a secondary food source for cultured bivalves, it exhibits stronger reductions in open and deeper water areas that promote settlement (Figure 6b). On the contrary, PON reductions in shallow regions are not as marked as for phytoplankton that can maintain their position in the water-column at varying degrees (higher for flagellates, lower for diatoms). In deeper areas where PON reductions are more diffuse, actually resulting from filtration occurring remotely, the RCI for PON combines the effects of this PON filtration but also further indirect reduction caused by the reduction in phytoplankton, which then contributes less to the PON dynamics (through mortality). In the shallower areas, inside or close to the farms, the direct filtering dominates the RCI response and PON reductions are less severe as bivalves feed preferentially on phytoplankton.

In addition to the slower turnover rates of zooplankton (secondary producer) compared to phytoplankton (primary producer), zooplankton responds to both competition for food and a marginal filtering pressure from the cultured bivalves (secondary or tertiary). All these factors lead to overall slightly stronger reductions for this secondary producer than for either Phyto or PON (Figure 6c). As stated in Appendix C (Section 10.3.4), any attempt to interpret zooplankton outputs further should be discouraged given the model limitations. This single model variable accounts for a variety of groups and species with their own different seasonal cycles and feeding behaviour. As such, not much zooplankton ecology value is retained in the model. This variable is included primarily to provide a closure to the model trophic web at a higher level than phytoplankton through a somewhat realistic top-down pressure. Although there is uncertainty in how well this zooplankton filtering pressure is captured by the model, according to the sensitivity analysis performed in Appendix C (Section 10.4.3), the influence of this uncertainty on the overall model results seems limited.

BS scale RCI statistics for these three pelagic variables are summarized in Table 4 for all scenarios. In Current conditions (2016-17), the influence of cultured bivalves appears very limited when reported to the whole Sound with mean RCI above -10% for all variables.
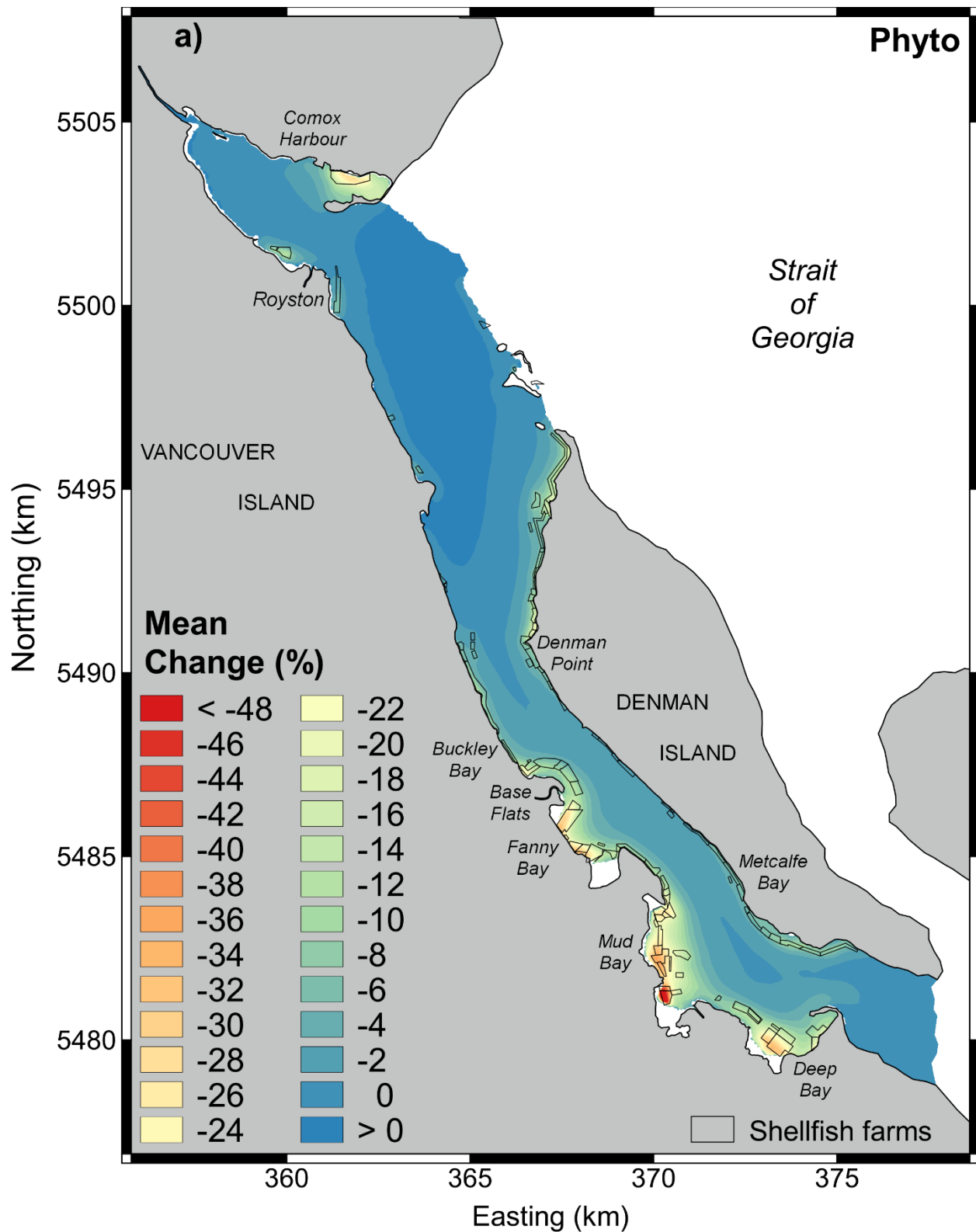
Figure 6: Spatial distribution of time-averaged relative change index as a result of the addition of active 2016-17 bivalve farms (Current scenario) in the Baynes Sound model ecosystem for a) Phytoplankton, b) Particulate Organic Nitrogen (PON), and c) Zooplankton (reference: No Aquaculture scenario). Maps b and c appear on the following two pages.
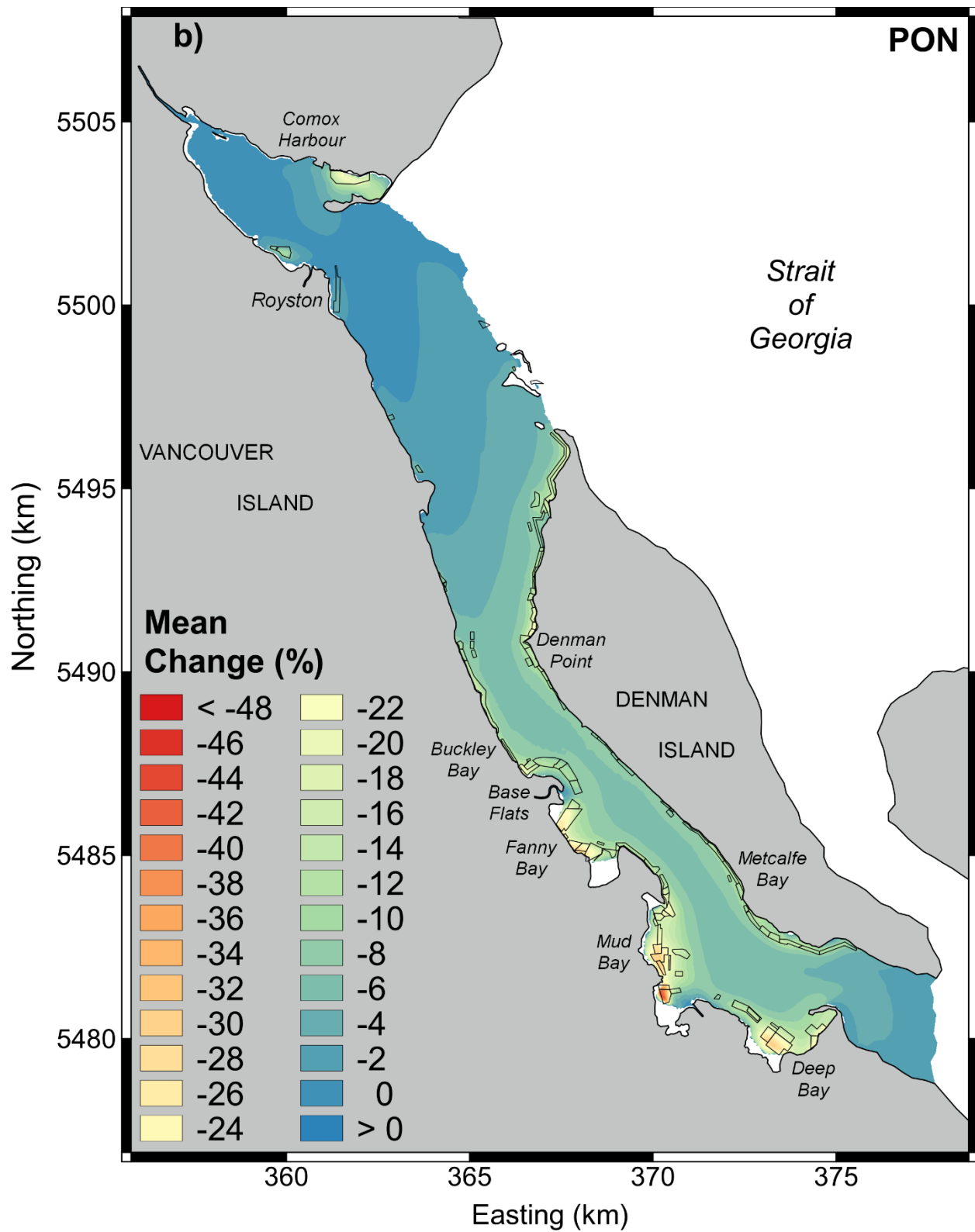
Figure 6 (continued)
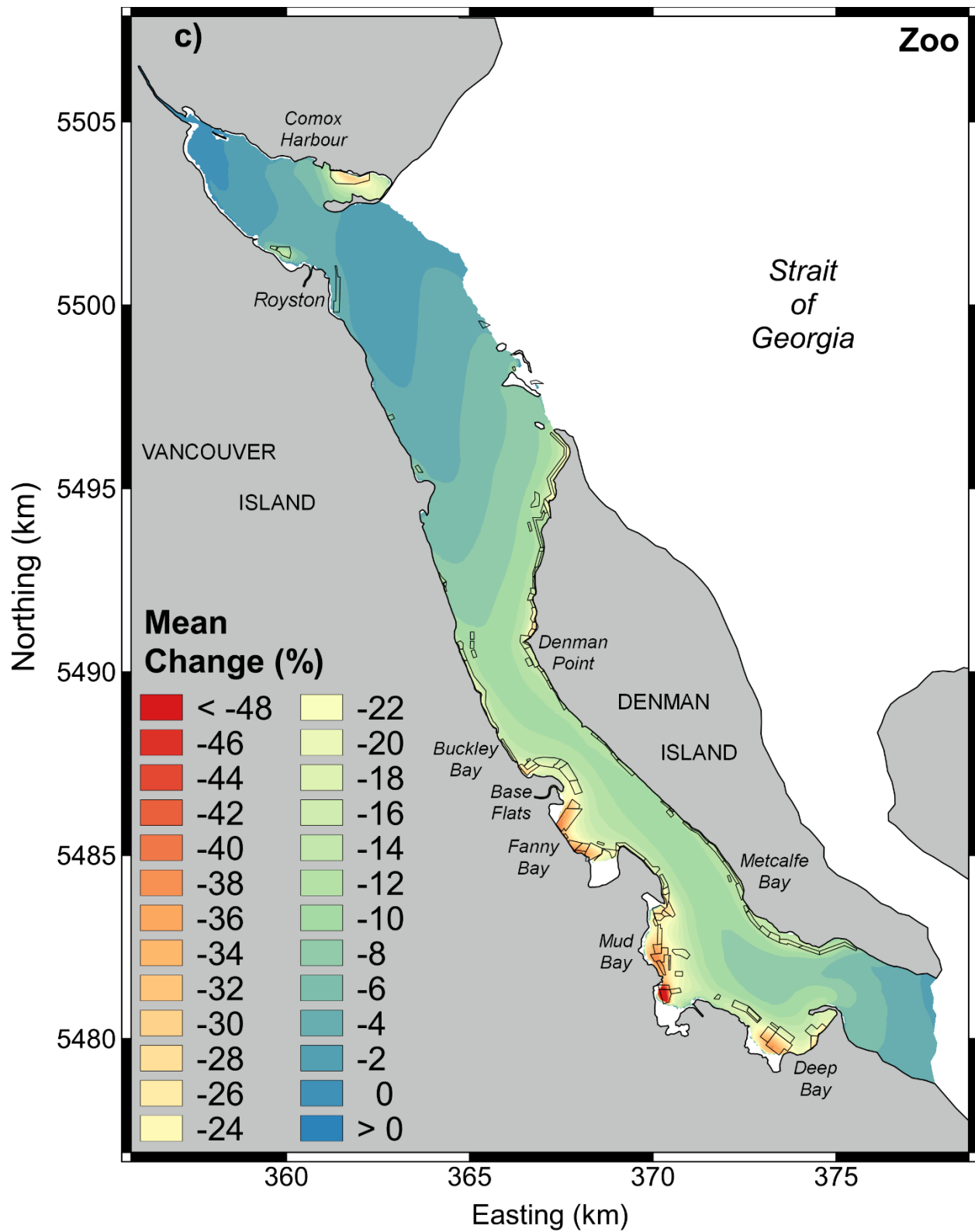
Figure 6 (continued)

Table 4: Summary of Relative Change Index statistics for pelagic variables. The reference is the No Aquaculture scenario. Mean and Absolute mean (mean of absolute values) represent both time (over 1 year) and space (over Baynes Sound) averages, while other statistics account for the spatial variability (over BS) of time-averaged change. SD: standard deviation.

Scenario	Relative Change Index (%)									
	Phyto					*PON*				
	Mean	Abs. Mean	Max.	Min.	SD	Mean	Abs. Mean	Max.	Min.	SD
Current	-3.27	3.43	1.74	-56.20	6.27	-6.05	6.05	0.12	-44.53	5.40
Current - Max	-3.03	3.93	3.99	-61.55	7.98	-8.15	8.15	0.00	-50.20	7.08
Expansion	-5.58	5.73	3.61	-63.62	8.02	-10.08	10.08	0.00	-50.93	7.47
Expansion - Max	-5.61	6.56	6.76	-69.50	10.05	-12.95	12.95	0.00	-56.99	9.49

Scenario	Relative Change Index (%)				
	Zoo				
	Mean	Abs. Mean	Max.	Min.	SD
Current	-9.49	9.49	0.00	-57.60	7.10
Current - Max	-12.53	12.53	0.00	-63.86	8.99
Expansion	-14.12	14.12	0.00	-65.46	8.96
Expansion - Max	-17.89	17.89	0.00	-71.31	11.11

Primary Productivity

The response of this key parameter, indicative of the local (i.e. within BS) renewal rate of bivalve food, was assessed using a RCI estimate, similarly to other pelagic components. As for phytoplankton biomass the effects of cultured bivalve on primary productivity are limited to the very nearshore areas and slightly more prominent in the lower Sound with maximum reductions generally below 20% with the exception of a small shallow area in Mud Bay reaching 30% (Figure 7). The overall lower relative reductions in net primary productivity (netPP) compared to phytoplankton biomass are to be expected as cultured bivalves can contribute two positive feedbacks to primary producers. First, bivalve excretion mainly as ammonia (NH_4) can locally enhance primary productivity in waters otherwise depleted in inorganic nitrogen. The second mechanism is through the filtration of phytoplankton and PON that may increase water clarity and alleviate some of the light limitation to primary productivity. As a result, some areas of the Sound outside the farming zones see an actual slight increase (positive RCI) in primary productivity in the presence of the cultured bivalves (Figure 7). When averaged over BS, the model predicts a relative phytoplankton primary productivity decrease of 4.12% for the current (2016-17) aquaculture activity level.
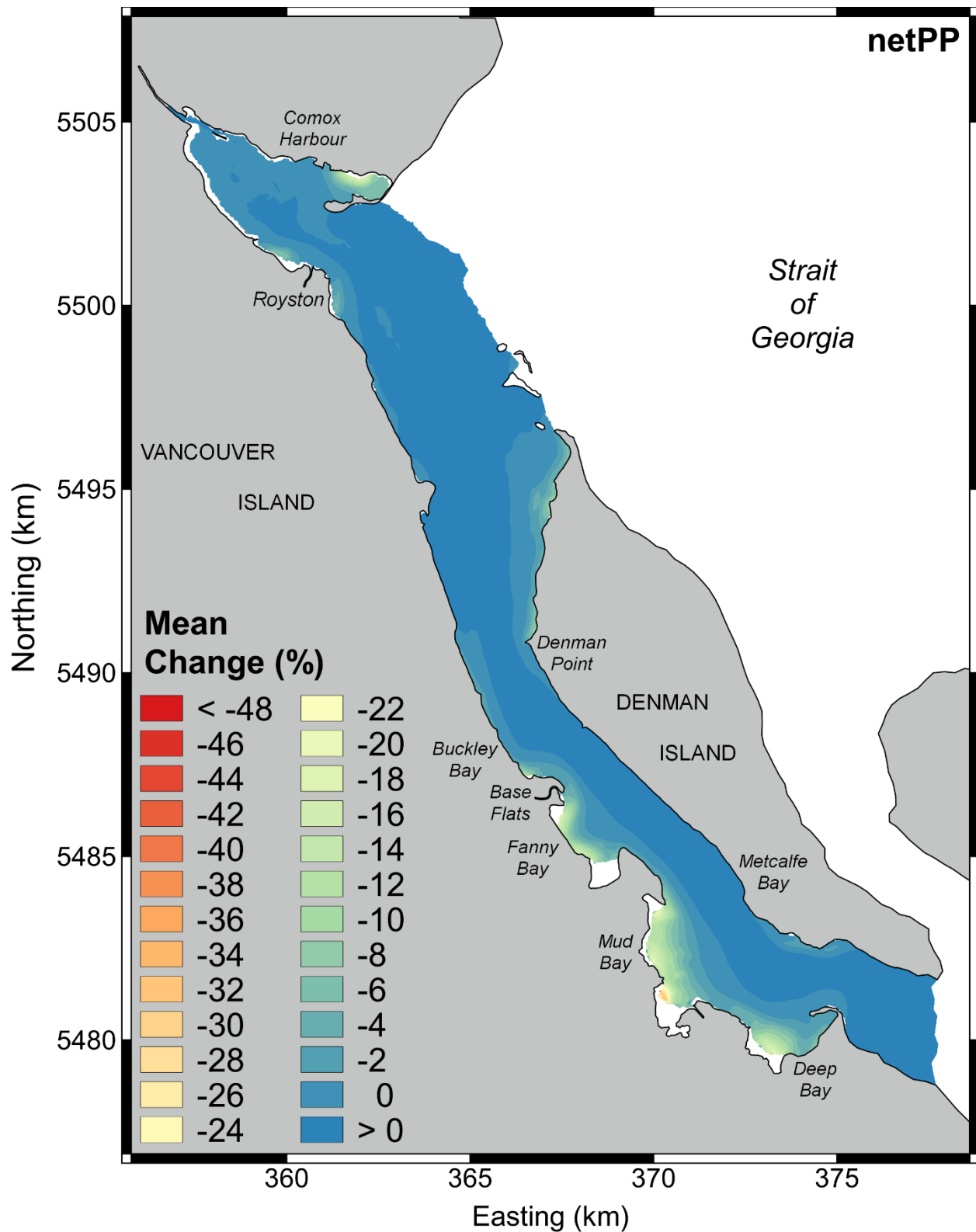
Figure 7: Spatial distribution of time-averaged relative change index for the entire water column net primary productivity (netPP) in the Current scenario (reference: No Aquaculture scenario).

Wild bivalves

In addition to zooplankton, wild clam beds included in the model can provide a preliminary assessment of the influence of cultured bivalves on other resources of the ecosystem. The response of wild clams was assessed by comparing their final shell length and tissue dry weight at the end of the simulations with the reference No Aquaculture scenario (Table 5). Although these beds are located in the nearshore areas where bivalves farms were shown to have the larger influence on food particles, very low decreases in clam shell growth are predicted with a maximum reduction of 2.45%. Clam tissue weight seems to respond more strongly to the presence of cultured bivalves but it must be noted that this variable is highly sensitive to the reproduction cycle of the animals. The combination of this sensitivity with the comparison of scenarios made at a specific date (end of simulation) results in tissue weight being a much less consistent measure of growth change than shell length. The large tissue weight RCI values in both the increase (Max) and decrease (Min) directions are another indication that the interpretation of this metric is strongly affected by the reproduction cycle.

Table 5: Summary of Relative Change Index statistics for wild clams. The reference is the No Aquaculture scenario. Mean and Absolute mean (mean of absolute values) represent both time (over 1 year) and space (over Baynes Sound) averages, while other statistics account for the spatial variability (over BS) of time-averaged change. SD: standard deviation.SL: shell length, TDW: tissue dry weight

Scenario	Relative Change Index (%)									
	Wild Clams									
	Mean		Abs. Mean		Max.		Min.		SD	
	SL	TDW	SL	TDW	SL	TDW	SL	TDW	SL	TDW
Current	-0.32	-4.23	0.32	4.38	0.00	97.91	-2.45	-23.20	0.34	4.90
Current - Max	-0.48	-5.40	0.48	5.62	0.00	122.29	-2.98	-28.81	0.50	6.13
Expansion	-0.42	-5.51	0.42	5.70	0.00	161.44	-3.12	-28.83	0.46	6.43
Expansion - Max	-0.60	-6.89	0.60	7.18	0.00	192.17	-3.92	-35.81	0.67	7.99

4.2.1.2. Current – Maximum stocking scenario

Pelagic variables and primary productivity

The increase of bivalve stocks in existing farms to a level providing the maximum allowed production leads to similar spatial patterns of reduction in pelagic variables and primary productivity than in the Current scenario (Figure 8). Reduction levels are slightly increased for all parameters and in most areas. Inside and directly around farms where reductions are strongest, both intensity and extent slightly increase as a consequence of the larger stock. Typical reductions in the vicinity of the farms reach 22, 25 and 30% for phytoplankton, PON and zooplankton, respectively and up to 40, 35 and 45% over small portions of inner Deep Bay, Mud Bay and Fanny Bay. Comparatively, netPP is only reduced by 15% and up to 25% over the same areas, relative to the No Aquaculture scenario. Also visible from the PON and zooplankton RCI distributions in deeper open waters is an area of strongest reduction in the mid-lower Sound compared to both the northern and southern ends. This spatial pattern may be explained by both extremities benefiting from water exchange with the SOG and lower farm coverage. When expressed at BS scale, reductions in pelagic variable concentrations exceed 10% only for zooplankton (12.5%, Table 4). In contrast, net primary productivity reduction at the Sound scale barely increased compared to the Current scenario (4.3 vs 4.1%) owing to the feedback mechanisms from bivalve culture mentioned earlier. Notably, despite the increase in cultured bivalve stocks, phytoplankton concentrations increased overall (lower reduction)

compared to the Current scenario (Table 4) as a consequence of these feedback mechanisms and the further reduced filtering pressure from stronger reduction in zooplankton biomass.

Wild bivalves

Again, the decrease in food particle concentrations associated with the larger stocks of cultured bivalves in this scenario only marginally reduces the growth of clams on wild beds, as measured by the change in shell length, with maximum reductions below 3% at the end of the simulated year (Table 5). Such relative reductions correspond to only just above 1 mm decreases in length. Despite the general proximity of wild clam beds to farmed areas where the strongest reductions in food particle concentrations are predicted (Figure 2), it seems that the wild clams do not experience any substantial food limitation even from the increased cultured bivalve stocks tested in this scenario.
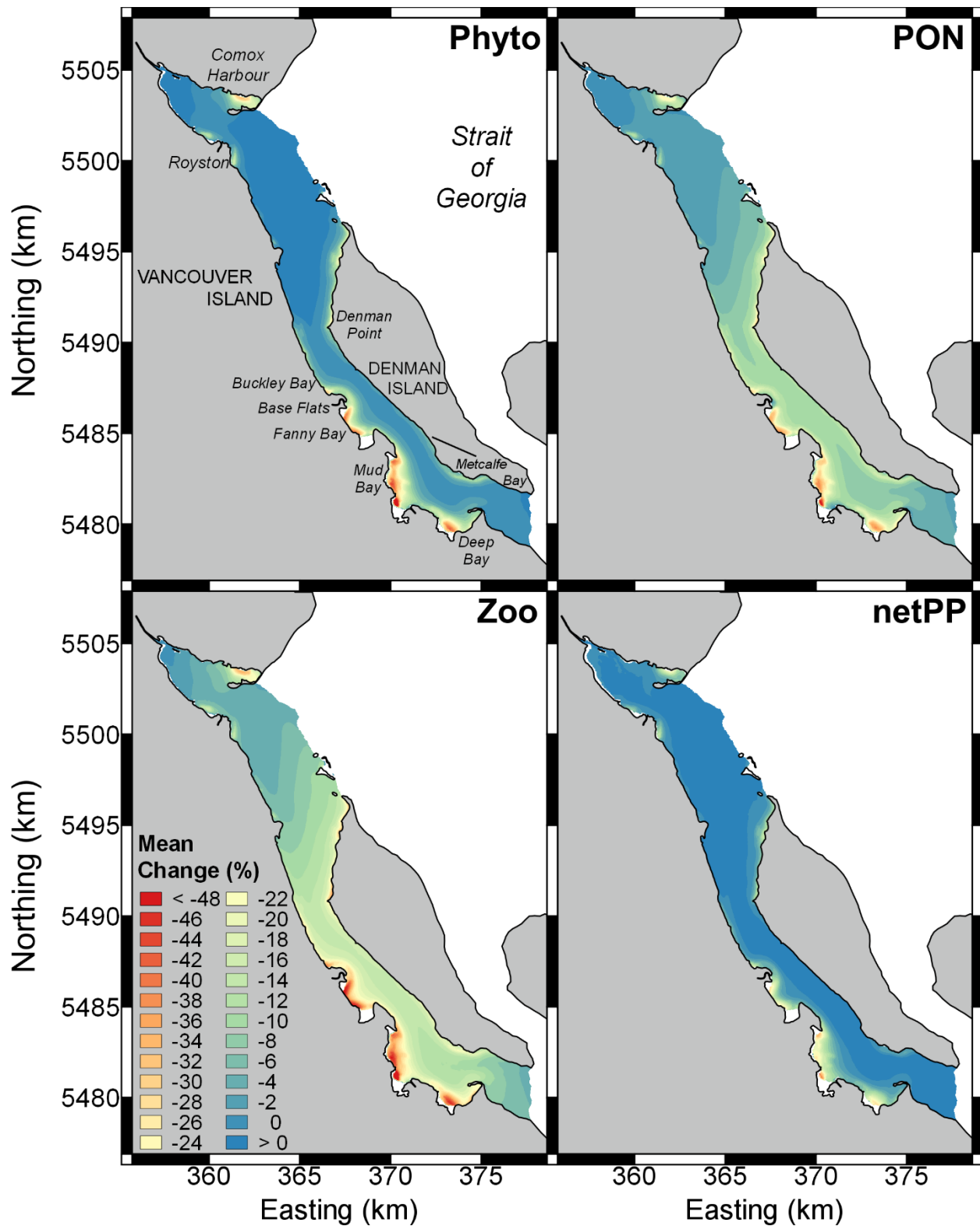
Figure 8: Spatial distribution of time-averaged relative change index for pelagic variables (Phyto: phytoplankton, PON: particulate organic nitrogen, Zoo: zooplankton and netPP: net primary productivity) in the Current - Max scenario (reference: No Aquaculture scenario).

4.2.1.3. Expansion scenario

Pelagic variables and primary productivity

The principal effect of the introduction of new farms is to extend the areas of reduced pelagic variable concentrations and accentuate these reductions, especially in Deep and Mud Bay where existing farm coverage and planned expansions are substantial (compare Figure 9 and Figure 6). In this expansion scenario, reductions in phytoplankton, PON and zooplankton stronger than 20, 22.5 and 25%, respectively, cover much of these two embayments. In Fanny Bay, however, expansion is limited to a single new farm covering 1 ha, which limits further reductions in pelagic variables to the diffuse effects of remote farms. The same pattern of extended and slightly deepened reductions can be observed for phytoplankton primary productivity (Figure 10 vs. Figure 7). Assessing these results at the BS scale, it appears that the addition of new farm coverage exerts a stronger pressure on the pelagic resources compared to the increase in stocks imposed in the Current – Max scenario (Table 4). While the stocking density increase of the Current – Max scenario is testing the capacity of food renewal at the local scale through advection and mixing, potentially leading to stronger local reductions, the farm coverage increase of the Expansion scenario is rather testing the ability of the whole system to renew food particles through exchange with the SOG and inner primary productivity (Guyondet et al. 2010; Heip et al. 1995). Moreover, the Expansion scenario actually results in a higher overall stock of cultured bivalves in BS, as it corresponds to a 61.0% increase from the Current scenario compared to a 38.8% increase for the Current – Max scenario.
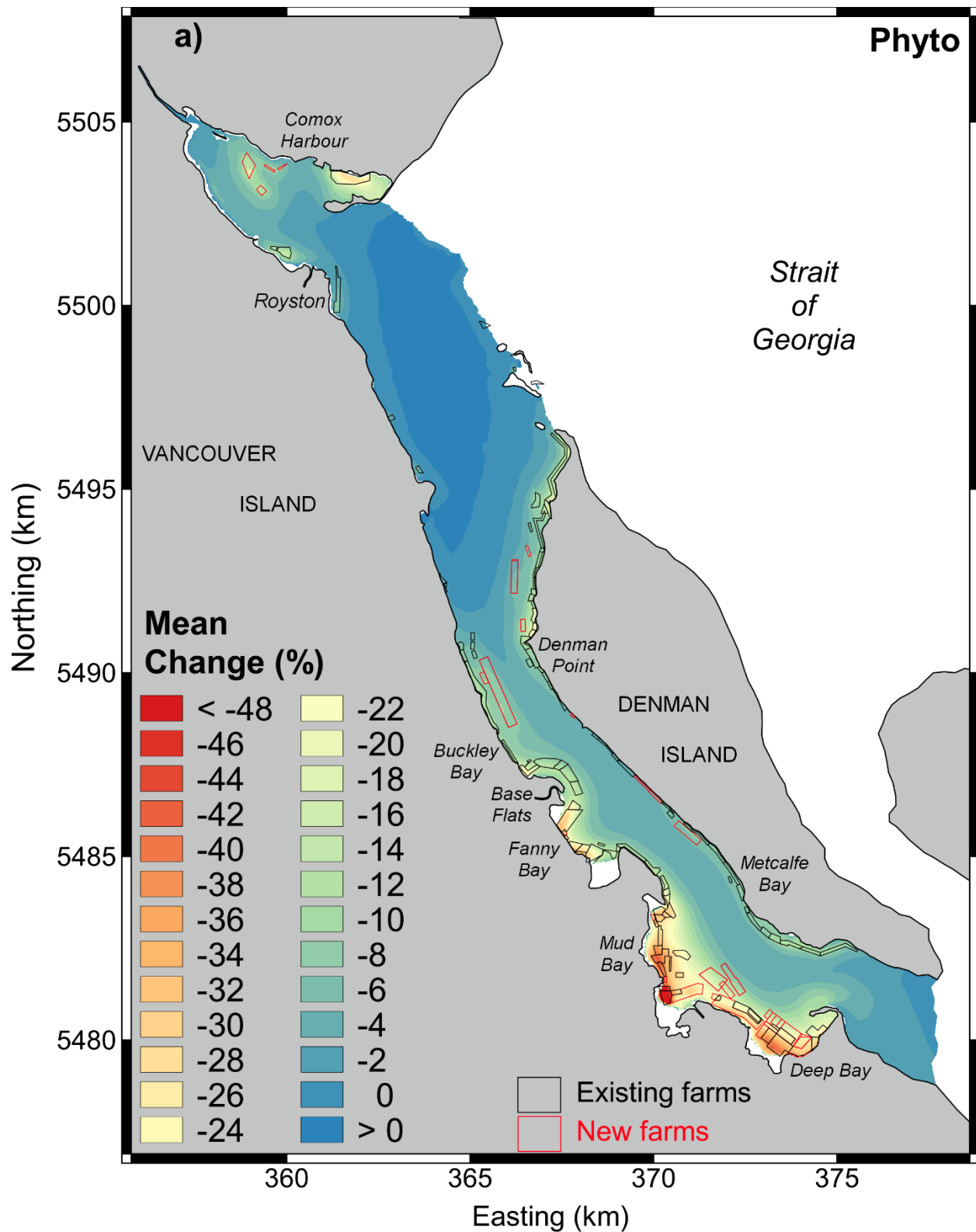
Figure 9: Spatial distribution of time-averaged relative change index as a result of the addition of existing (black polygons) and new bivalve farms (red polygons, Expansion scenario) in the Baynes Sound model ecosystem for a) Phytoplankton, b) Particulate Organic Nitrogen (PON), and c) Zooplankton (reference: No Aquaculture scenario). Maps b and c appear on the following two pages.
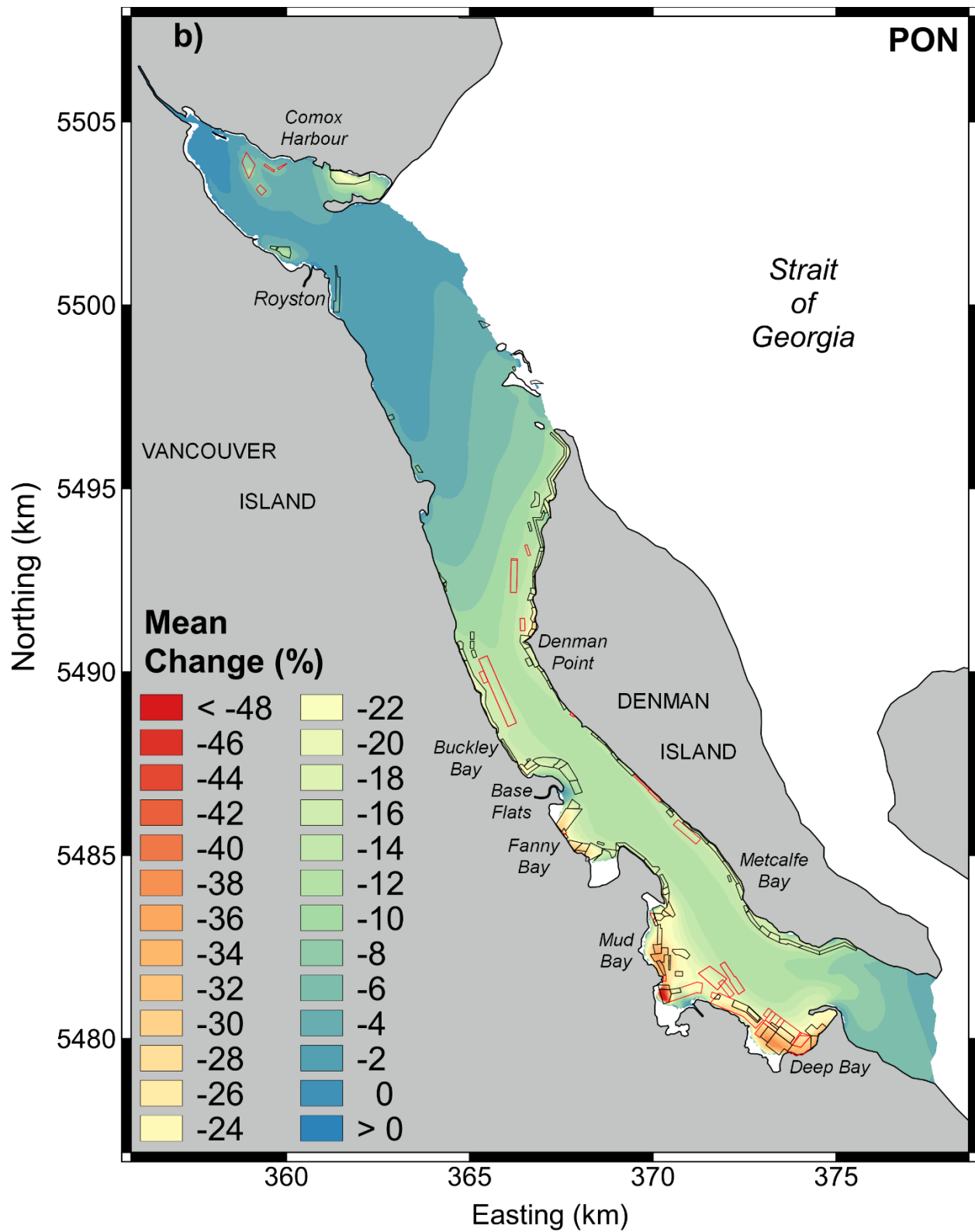
Figure 9 (continued)
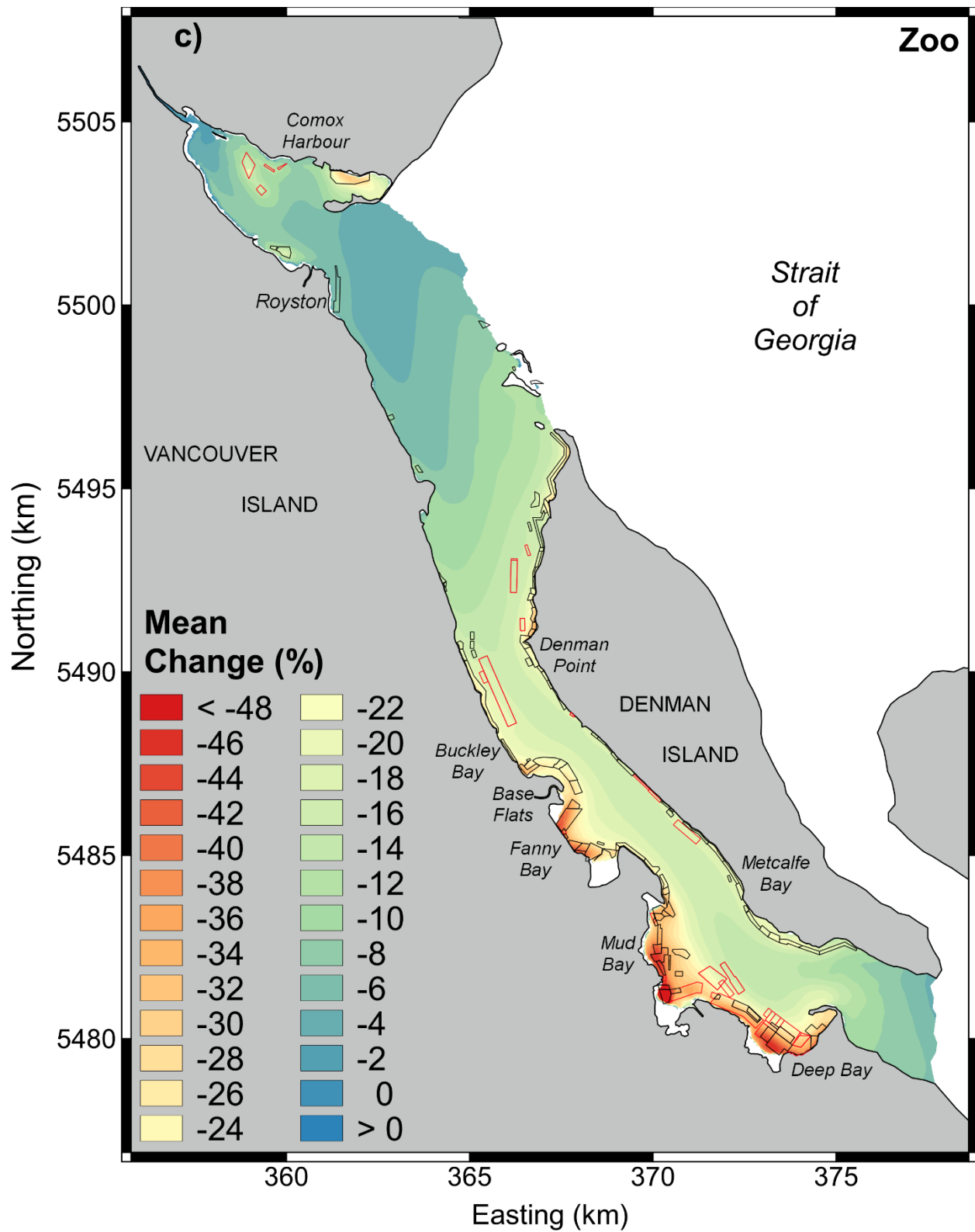
Figure 9 (continued)
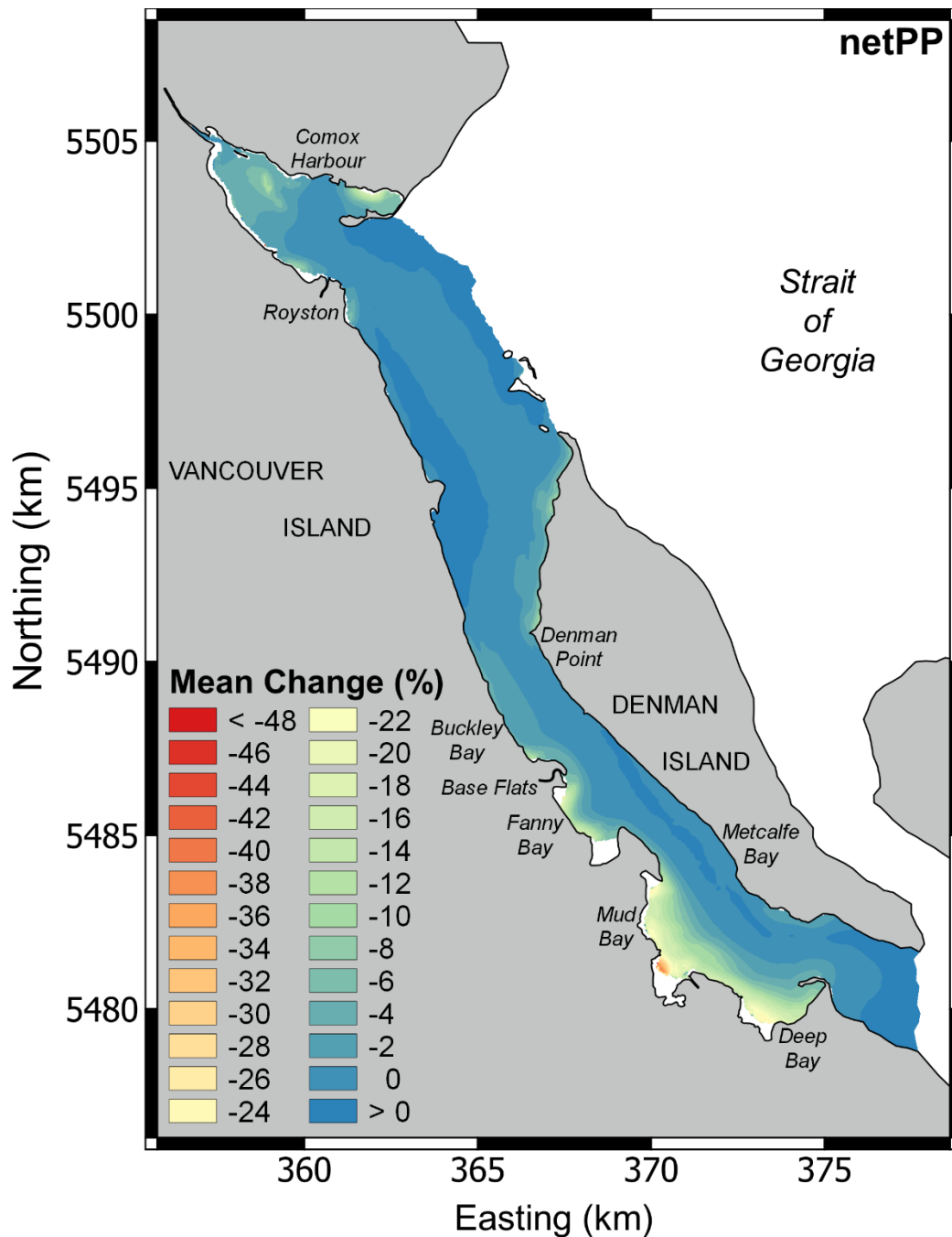
Figure 10: Spatial distribution of time-averaged relative change index for net primary productivity (netPP) as a result of the addition of existing and new bivalve farms (Expansion scenario) in the BS model ecosystem (reference: No Aquaculture scenario).

Wild bivalves

In agreement with the hypothesis that the Expansion scenario is not as stringent on the local food concentration reductions as the Current – Max scenario, wild clams experience an overall slightly lower reduction in growth, measured in shell length, following the farming expansion (Table 5). However, the maximum growth reduction reaching just above 3.1%, in excess of the

3.0% predicted for the Current – Max scenario is an indication that expansion can still impose stronger food limitations in specific areas, in this case the southern end of Mud Bay.

4.2.1.4. Expansion at maximum stocking scenario

Pelagic variables and primary productivity

This final scenario includes the largest stock of cultured bivalves of all scenarios tested in the present study with more than double the stock of the Current conditions. Even in these high stocking conditions, most of the upper Sound, except for Comox Harbour, remains barely affected with regards to phytoplankton concentration and primary productivity (Figure 11). Low reductions in primary productivity persist over the majority of the deeper open waters of the Sound, only increasing in the nearshore in close proximity to the farmed areas. Reductions in PON and zooplankton are also limited to below 7 and 10%, respectively, over the northern basin. These variables, however, experience reductions over 15 to 20% in the lower two thirds of the Sound indicating that pelagic resources are getting exploited at the Sound scale in these high stocking conditions. Furthermore, pelagic variable concentrations are decreased by more than 30% and primary productivity by more than 15% over the main culture areas, i.e. Fanny, Mud and Deep Bays. At the scale of the entire Sound, a very limited effect on phytoplankton is confirmed while PON and zooplankton exhibit 3 to 4% further reduction compared to the Expansion lower stocking scenario (Table 4).

Wild bivalves

Growth of wild clams continues to be little affected even by the largest stocking scenario. Shell lengths are only reduced by 0.6% on average over BS and to a maximum of less than 4% at a local scale (Table 5), corresponding to average and maximum absolute reductions of 0.2 and 1.6 mm, respectively.
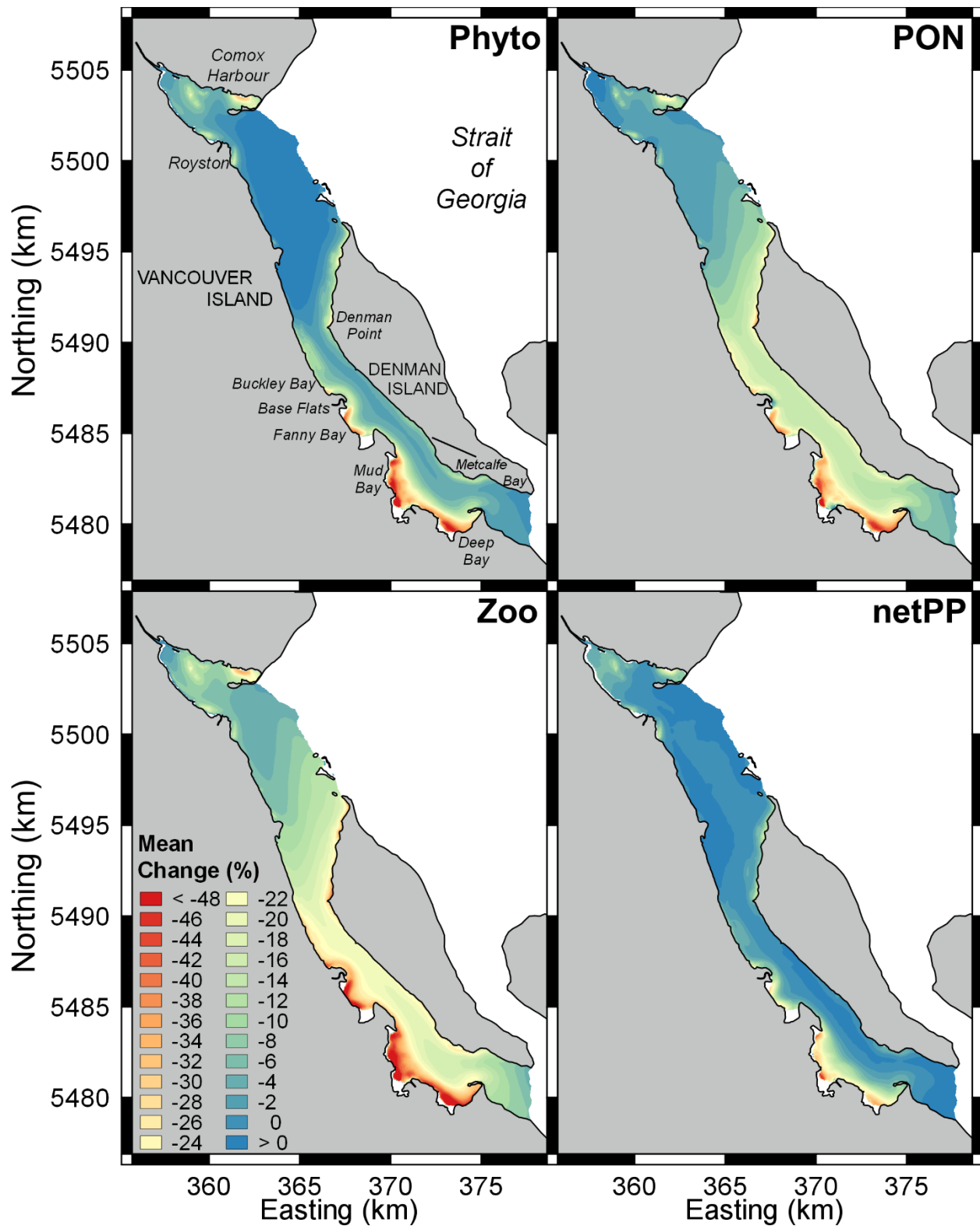
Figure 11: Spatial distribution of time-averaged relative change index for pelagic variables (Phyto: phytoplankton, PON: particulate organic nitrogen, Zoo: zooplankton and netPP: net primary productivity) in the Expansion - Max scenario (reference: No Aquaculture scenario).

In Summary, BS is a large coastal system that still experiences a fairly rapid water renewal through efficient wind-driven and tidal exchange and estuarine residual circulation. Intense flushing usually provides the foundation for a strong resilience of aquatic ecosystems to any kind of perturbation (Filgueira et al. 2016b; Panda et al. 2013; Roselli et al. 2013). Moreover, these physical drivers also contribute to the high phytoplankton primary productivity of the Sound through the replenishment of nutrients and their delivery to surface euphotic waters. The combination of fast water renewal and high local primary productivity is the perfect mix for the realization of a high carrying capacity for shellfish culture (Dame and Prins, 1998).

The scenarios tested in the present study provided a framework to evaluate the response of BS's pelagic ecosystem to increases in both intensity and coverage of shellfish aquaculture. The assessment of BiCEM outcomes at the scale of the entire Sound suggests cultured bivalves exert a very limited influence as highlighted by overall low reductions in phytoplankton biomass (< 6%, Table 4) and productivity (< 1.5%, Table 6) for all stocking scenarios tested. Moreover, even in the highest stocking conditions, the total uptake of phytoplankton, their main source of food, by cultured bivalves still represents less than 1% of the Sound's primary productivity capacity (Table 6). Such a limited influence can be expected from the farm coverage, which only amounts to 5.85% of the total Sound surface area in current conditions and would only increase to 8.9% in the Expansion scenario. Although different hydrodynamic conditions and culture practices prevent a direct comparison, regions that have experienced carrying capacity issues from shellfish farming were usually sustaining much wider farm coverages (see Table 7 placing BS in the context of strongly exploited coastal systems). Another contributing factor is the distribution of most of the farms in shallower waters along the edges of the Sound that contribute a limited portion of the pelagic primary productivity (Figure 5). From these peripheral locations, the control natural and cultured bivalve populations may exert on pelagic resources at the system scale appears limited.

Table 6: Summary of annual net primary productivity and phytoplankton uptakes by zooplankton and wild and cultured bivalves over Baynes Sound for all scenarios tested.

Scenario	net Primary Productivity	net PP Mean Change	Phyto uptake by wild clams		Phyto uptake by cultured bivalves		Phyto uptake by zooplankton	
	(gC m^{-2} yr^{-1})	(%)	(gC m^{-2} yr^{-1})	% netPP	(gC m^{-2} yr^{-1})	% netPP	(gC m^{-2} yr^{-1})	% netPP
No Aquaculture	329.48	-	0.39	0.12	-	-	254.03	77.10
Current	328.61	-0.26	0.38	0.11	0.90	0.28	246.88	75.13
Current - Max	328.34	-0.35	0.38	0.11	1.43	0.44	242.65	73.90
Expansion	326.07	-1.04	0.36	0.11	1.47	0.45	241.07	73.93
Expansion - Max	324.96	-1.37	0.36	0.11	2.17	0.67	235.17	72.37

Table 7: Intensity of bivalve aquaculture at system scale in important production areas, P.E.I. = Prince Edward Island.

Site	Total Area (km²)	Bivalve Culture Coverage (%)	Water Renewal Time (d)	Species	Reference
Baynes Sound (B.C., Canada)	90.0	5.8	10 – 16	*Crassostrea gigas Ruditapes philippinarum*	This study
St Peter's Bay (P.E.I., Canada)	15.8	39.6	15 – 80	*Mytilus edulis*	Guyondet et al. 2015
Tracadie Bay (P.E.I., Canada)	19.3	40.0	10 – 40	*Mytilus edulis*	Comeau et al. 2008, Filgueira et al. 2014b
Sacca di Goro (Italy)	26.0	34.1	2 – 13	*Ruditapes philippinarum*	Marinov et al. 2007, Maicu et al. 2018
Sungo Bay (China)	144.0	32.1	5 – 20	*Crassostrea gigas, Chlamys farreri*	Zhang et al. 2009, Wang et al. 2018
Willapa Bay (USA)	347.0	10.0	10 – 24	*Crassostrea gigas, Ruditapes philippinarum*	Banas and Hickey 2005, Feist and Simenstad 2000, Wheat and Ruesink 2013

Compiling the total surface area of the Sound that experiences a given level of phytoplankton concentration reduction provides an indication of the ecological footprint of cultured bivalves (Table 8), based on the premise that strong reductions can only be sustained if restricted to a small portion of the system (Gibbs, 2007). The overall footprint, i.e. area with reductions higher than 5%, is limited to about 20 and 40% of the entire Sound for the current and expansion farm coverages, respectively. Moreover, the reductions stronger than 20%, are restricted more or less to the areas actually covered by farms (6 and 9% in current and expanded conditions). Furthermore, comparing the Expansion and Current – Max scenarios reveals that while an overall larger fraction of the Sound's productivity gets exploited by the extended farm coverage (Expansion scenario, Table 6), areas of stronger reduction in pelagic resources barely expand (Table 8), limiting the risk for acute impacts. In that respect, extending coverage seems preferable to intensifying stocking, though other considerations, in particular broader spatial planning, would have to be accounted for in any development plans.

Previous studies have suggested natural variation of phytoplankton as a threshold for aquaculture-induced reductions in biomass that would provide a precautionary approach ensuring the system operates within its limits of resilience (Grant and Filgueira, 2011). This definition of ecological carrying capacity relies on the determination of phytoplankton natural variation that requires large amounts of data and can be site specific. Nonetheless, previous reports of natural phytoplankton variation used in this context are fairly consistent with variations in the 32 – 49 % range (Bricker et al. 2016; Filgueira et al. 2013b; Filgueira et al. 2015b). Assuming this variation criterion can be applied to BS waters would provide another indication that the Sound would remain within the limits of ECC for all scenarios tested. Furthermore, using the criterion proposed in the Bivalve Standard of the Aquaculture Stewardship Council (ASC, 2019), that no more than one third of phytoplankton primary productivity should be used by cultured shellfish would lead to the same conclusion.

Despite the limited extent of stronger reduction areas just mentioned, the distribution maps included in the present document identified the cultivation zones of Fanny, Mud and Deep Bays as the most sensitive for all pelagic variables and primary productivity. Although somewhat surprising given that these bays are fairly wide open, this result can be explained by the larger farm coverage in these specific locations. In current conditions, Fanny, Mud and Deep Bays shelter respectively 10.9, 14.0 and 13.7% of all BS farmed areas. On a local scale, shellfish farms cover 30.9% of Fanny Bay and 21.1% of Mud and Deep Bays combined and these

proportions would increase to 31.5% and 44.3% following the planned expansion. These coverage considerations and BiCEM outputs warrant particular attention to be paid on these three embayments.

Table 8: Fraction of Baynes Sound surface area experiencing various levels of phytoplankton concentration relative change in each of the aquaculture development scenarios tested. For example, reductions are stronger than 5% over only 21.12% of the Sound in the Current scenario.

Scenario	% Area of Phytoplankton Relative Change			
	< -5%	< -10%	< -20%	< -30%
Current	21.12	11.95	6.15	3.92
Current - Max	21.49	14.08	7.43	5.12
Expansion	40.74	17.76	9.28	5.22
Expansion - Max	38.59	20.33	10.71	7.34

4.2.2. Farm Interactions

Related to Terms of Reference (ToR) #3 is the notion of localised effects of new farms on food availability and decrease in existing farm production. In addition to the direct relevance for spatial planning of aquaculture and other coastal activities, the response of cultured bivalves can provide a reliable indication of the overall state of the receiving ecosystem in terms of pelagic food resources utilization (Filgueira et al. 2013a, 2014a). The assessment is based here on the comparison of BiCEM results from the Expansion and Current scenarios. As new farm expansions are planned in different areas of BS that can potentially respond differently based on local hydrodynamics and current farm coverage, outcomes were detailed in three separate zones: Comox Harbour, the mid Sound down to Base Flats and the lower Sound.

Model outputs for the Comox Harbour region are shown on Figure 12. Following the Courtenay river outflow forcing, the area of reduced phytoplankton concentration is pushed against the south shore and extends up to the southeastern corner of the harbour. The maximum reductions do not reach 20% and are restricted to a small area directly within the new farm polygons, as a result of the fast water exchange provided by that same river outflow and the rather small addition in farm coverage (~19 ha). As a consequence of the southeastern extension, a single existing shellfish farm located in the Royston area is affected by the reduction footprint. However, the food availability reduction is already sufficiently diluted that BiCEM predicts a maximum decrease in shellfish growth of only 0.3%, measured as the relative change in shell length in this farm.
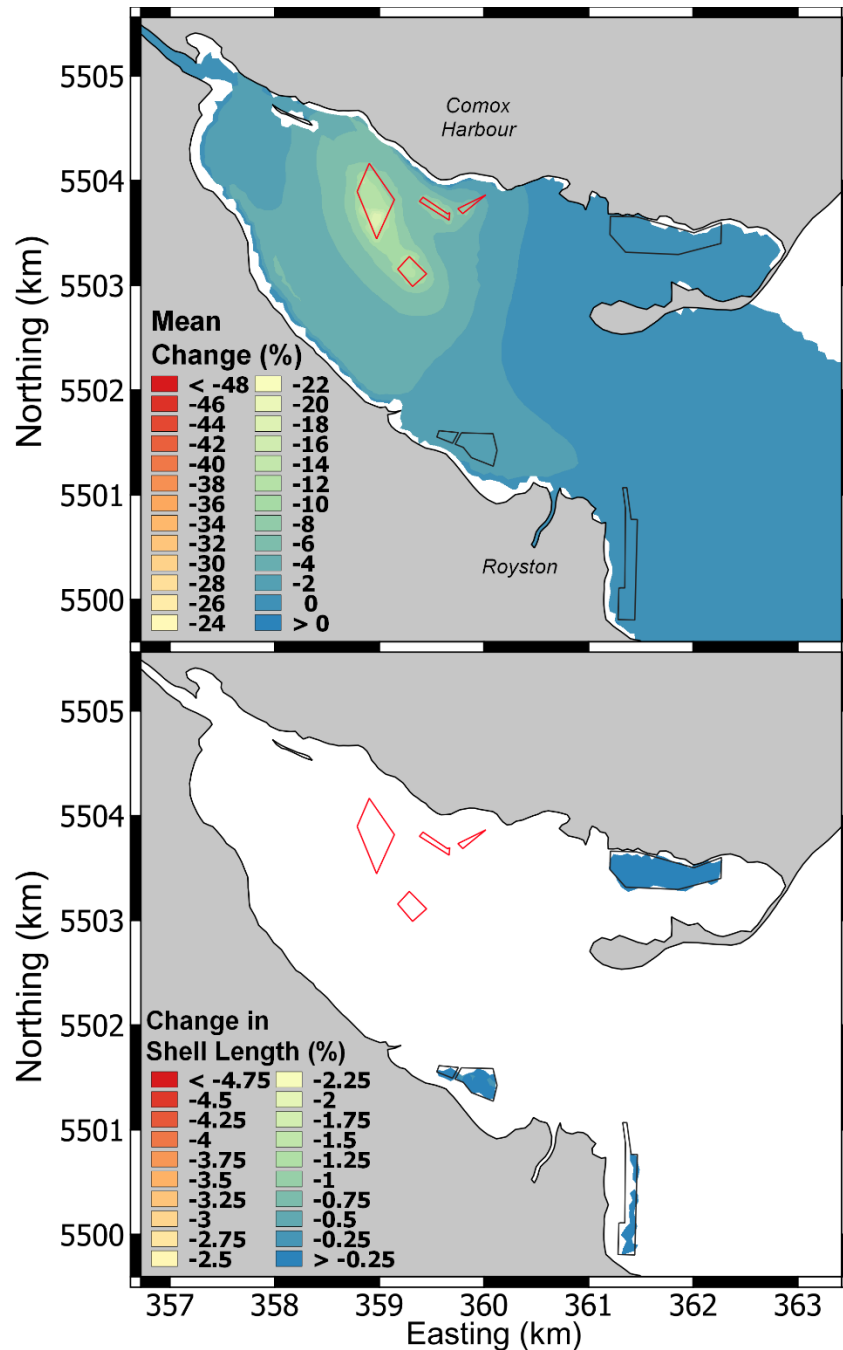
Figure 12: Spatial distribution of time-averaged relative change index (RCI) for phytoplankton (top) and associated RCI for the shell length of cultured bivalves (bottom) in the Comox Harbour area for the farm Expansion scenario (red polygons). The Current scenario (black farm polygons) is the reference for RCI calculations.

The planned expansions in the mid-Sound region consist in new farms for culture in suspension located in deeper areas just north of Denman Point on the eastern side of the Sound and north of Buckley Bay on the opposite side, for a total additional coverage of about 76 ha. Although slower water renewal can be expected in this central segment of the Sound, local mixing and the large volumes of water available in these deeper areas contribute to limiting maximum phytoplankton reductions to about 8% (Figure 13). Reduction footprints associated with new

farms are elongated in the southward direction following the general estuarine residual circulation of the Sound that drives surface waters to the south (Figure A14). Moreover, new farms in this section of the Sound contribute to a uniform low reduction (2 – 4%) area that extends down to the southern entrance over the deeper open waters. The resulting pattern of cultured shellfish growth reduction appears very patchy with neighbouring farms showing substantially different responses. The reason for this patchiness is the species actually cultured on each of these farms. As also observed for wild clams, cultured clams are fairly insensitive to the predicted levels of food reduction. On the other hand, cultured oysters seem more affected by these same reductions in food availability. However, the overall growth decreases predicted by BiCEM stay marginal for both clams (0.15 – 0.25%) and oysters (0.75 – 1.1% for bottom culture and 1 – 1.6% for culture in suspension) over all existing farms in this section of the Sound.
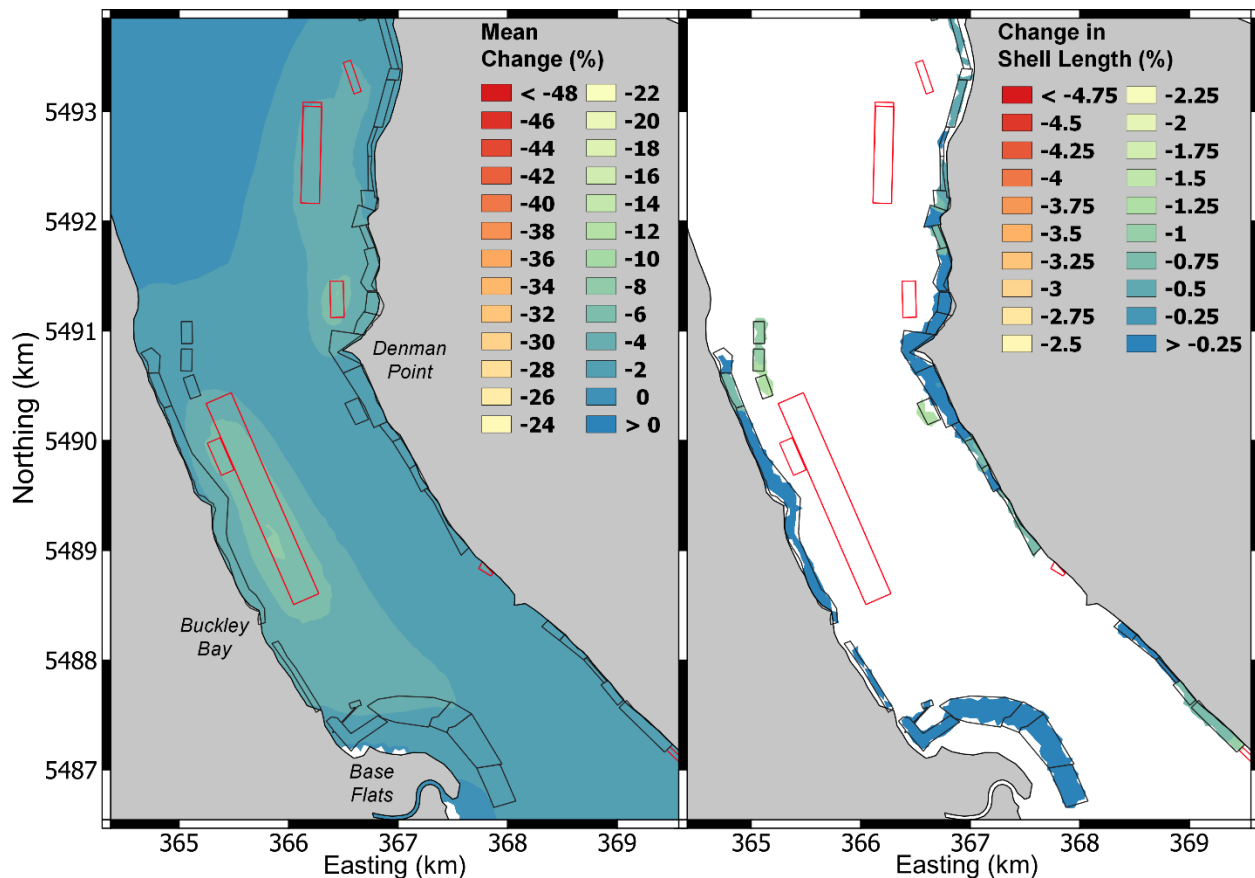
Figure 13: Spatial distribution of time-averaged relative change index (RCI) for phytoplankton (left) and associated RCI for the shell length of cultured bivalves (right) in the mid Baynes Sound area for the farm Expansion scenario (red polygons). The Current scenario (black farm polygons) is the reference for RCI calculations.

Finally, it is over the lower Sound that the largest part of the new farm coverage is planned with a total increase of 190 ha from which more than 88% or 168 ha are concentrated in the Mud Bay-Deep Bay sub-region. Consequently, BiCEM predicts higher phytoplankton reductions to cover most of this sub-region following the introduction of the new farms (Figure 14). Phytoplankton reduction levels stronger than 7% extend over the majority of these two bays and increase up to 25 – 30% on small portions of the inshore shallower reaches. Again, there is appearance of patchiness in the response of cultured shellfish growth because of the different

species reared on the different farms and the higher sensitivity of model oysters to a decrease in food availability. Cultured clams are still the least affected but they experience stronger growth reductions in Mud Bay and Deep Bay than anywhere else in the Sound. Cultured clam reductions in growth range from 0.15 – 0.2% outside Mud and Deep Bays to maximum reductions of 1.3% in the inner areas of Deep Bay. Intermediate growth reductions are for bottom culture oysters ranging from 0.3 – 1.6% and 1.3 – 5.2% outside and inside the Mud-Deep Bay sub-region, respectively. The response of suspended oysters is even slightly stronger with shell growth reductions ranging from 1.1 – 2% outside Mud-Deep Bays and from 3.4 – 5.8% inside. Even these strongest reductions remain small in comparison to the inter-individual variability generally observed in shellfish populations even cultured ones (Filgueira et al. 2013a; Tamayo et al. 2011). For reference, the normalised standard deviation (SD/mean) of suspended oyster shell length measured in our two partner farms at the end of our *in situ* growth monitoring were 12.0 and 15.9%, which would make even the largest reductions predicted for the Expansion scenario difficult to detect in the field.
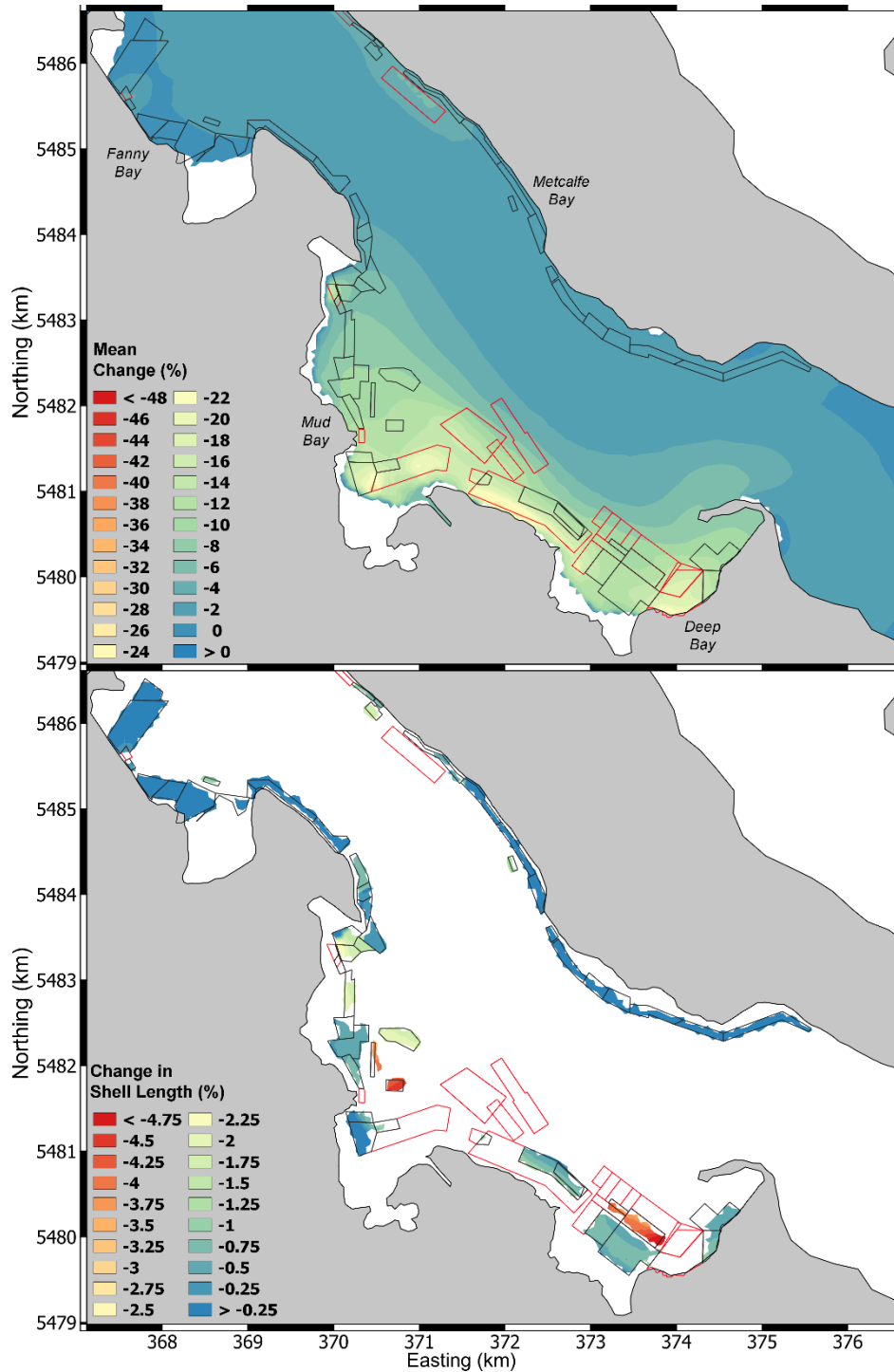
Figure 14: Spatial distribution of time-averaged relative change index (RCI) for phytoplankton (top) and associated RCI for the shell length of cultured bivalves (bottom) in the lower Baynes Sound area for the farm Expansion scenario (red polygons). The Current scenario (black farm polygons) is the reference for RCI calculations.

General statistics over BS for all tested scenarios are reported in Table 9 to complement the information relative to the response of cultured bivalves to the different levels of aquaculture development. These Sound-scale measures confirm the lower sensitivity of cultivated clams

compared to bottom cultured oysters that experience similar intensities of food availability reduction. Suspended oysters show slightly lower reductions in growth than their bottom counterparts but are also exposed to the lower food reductions generally occurring over the deeper parts of the Sound. Comparing the results obtained for the Current – Max and Expansion scenarios for the different species/culture techniques, bottom cultivated bivalves appear more affected by an increase in local stocking density, while suspended oysters respond more strongly to an increase in farm coverage. In addition to the different relative increases in stocking density imposed among the different species/techniques in the Current – Max scenario, several other factors may explain this bottom – suspension discrepancy. First, a large proportion of existing farms are used for bottom culture (> 93 % of total farmed area). Hence, the increase in local stocking introduced by the Current – Max scenario is more likely to affect these culture areas, which are also more sensitive to food reductions from the lower volume available compared to deeper areas where suspension culture is practiced. On the other hand, the majority of planned expansions correspond to farms in suspension (61.5% of additional farmed area), which are less likely to affect bottom culture from their remote locations but do seem to interact more with existing farms in suspension.

Table 9: Summary of relative change indices (RCI) for shell length (SL) and tissue dry weight (TDW) of cultured bivalves in Baynes Sound at the end of each scenario. The Current scenario was used as the reference for the RCI calculations.

Bottom Oysters

Scenario	Relative Change Index (%)									
	Mean		Abs. Mean		Max.		Min.		SD	
	SL	TDW	SL	TDW	SL	TDW	SL	TDW	SL	TDW
Current - Max	-4.97	-14.90	4.97	14.90	0.00	0.00	-8.72	-39.29	1.63	7.78
Expansion	-1.16	-3.96	1.16	3.96	0.00	0.00	-6.07	-35.54	0.96	5.12
Expansion - Max	-6.52	-19.52	6.52	19.52	0.00	0.00	-13.36	-48.76	2.31	9.96

Suspended Oysters

Scenario	Relative Change Index (%)									
	Mean		Abs. Mean		Max.		Min.		SD	
	SL	TDW	SL	TDW	SL	TDW	SL	TDW	SL	TDW
Current - Max	-1.92	-4.42	1.92	4.42	-0.82	-1.87	-3.83	-8.42	0.77	1.64
Expansion	-2.51	-5.71	2.51	5.71	-0.66	-1.60	-5.80	-13.03	1.57	3.39
Expansion - Max	-5.15	-11.42	5.15	11.42	-1.99	-4.53	-9.98	-21.57	2.73	5.62

Cultivated Clams

Scenario	Relative Change Index (%)									
	Mean		Abs. Mean		Max.		Min.		SD	
	SL	TDW	SL	TDW	SL	TDW	SL	TDW	SL	TDW
Current - Max	-0.79	-5.96	0.79	6.92	0.00	39.47	-2.11	-14.93	0.41	5.27
Expansion	-0.27	-3.79	0.27	4.05	0.00	36.28	-1.92	-28.07	0.25	3.69
Expansion - Max	-1.18	-10.19	1.18	11.33	0.00	34.77	-3.21	-39.88	0.65	7.39

5. SUMMARY

A state-of-the-art spatially-explicit coupled hydrodynamic-biogeochemical modelling approach supported by the most recent available field observations was used to evaluate the influence of cultured shellfish on the pelagic ecosystem of BS. The particular hydrodynamics involving wind and tidal mixing and the estuarine residual circulation contribute to the regular replenishment of nutrients from the neighbouring rich deep waters of the SoG, leading to high levels of pelagic primary productivity. In combination with an efficient water renewal, this primary productivity confers a high potential for secondary production to BS and in particular the ability to sustain a large bivalve culture production.

The general assessment provided by BiCEM outputs in terms of changes in pelagic resources (biomass and productivity) with the level of aquaculture development as well as the responses of zooplankton and wild bivalves indicate a low influence of shellfish aquaculture and that this activity currently operates within the ecological carrying capacity of BS. The planned expansions are substantial in terms of additional farm coverage and stock and would exploit a larger fraction of the Sound's pelagic resources. However, the present results do not provide any indication that the additional production could not be sustained, especially when compared to similar studies conducted in more intensively exploited systems (Filgueira et al. 2014a; Guyondet et al. 2015).

Caution must be exerted in the interpretation of BiCEM results, especially for variables and parameters identified in the sensitivity analysis of Appendix C. In particular, higher uncertainty is associated with zooplankton results given their sensitivity and the scarcity of data to constrain the choice of related parameters. However, this variable still provides an indication of the limited influence of shellfish aquaculture towards higher trophic levels in BS, which is confirmed by the more robust results obtained for cultured bivalves.

Finally, the present results are conditioned to some extent by the specific annual cycle studied, spanning May 2016 to April 2017, that exhibited some uncharacteristic environmental conditions and forcing for part of the period. Inter-annual variability is, however, intrinsic to any coastal ecosystem and defines carrying capacity as a moving target. Nevertheless, the very limited influence of current stocks and the high stocking scenarios reported provide relevant information for a precautionary approach to shellfish aquaculture development in BS. Such development should proceed gradually and in conjunction with proper monitoring of environmental (see Working Paper #2 of this CSAS process) and cultured shellfish conditions. Particular attention should be paid to Fanny, Mud and Deep Bays, which already concentrate a large proportion of the production and have been identified as the most sensitive to further development.

Analyses of long time-series and results from forecast models suggest that bivalve cultures in Baynes Sound will be impacted by climate change. In their analyses of sea surface temperatures along the B.C. coast, Amos et al. (2015) computed a trend of 0.42°C per decade in the 1961-2012 Chrome Island lighthouse observations. Masson and Cummins (2007) conducted a similar analysis of 1970-2005 temperature observations over the entire water column at a site in the central SoG and found depth-averaged and near-surface warming trends of 0.24°C per decade and 0.33°C per decade, respectively. However, possible harmful trends in ocean acidification and hypoxia are more concerning. In this regard, Ianson et al (2016) found that while the SOG has a higher carbon content and lower pH than surrounding waters in the NE Pacific, intense mixing in the physically restricted channels connecting the SOG to the outer coast allows significant oxygen uptake but minimal CO_2 out gassing, thereby protecting the SOG from hypoxia but not from ocean acidification. As a matter of fact, similar acidification trends have been reported for the northern SOG area surrounding Baynes Sound (Evans et al. 2019). Finally, in a recent paper Khangaonkar et al. (2021) combined their FVCOM application

for the Salish Sea with the high emissions scenario RCP8.5 from the Intergovernmental Panel on Climate Change Fifth Assessment Report (IPCC 2014) to study impacts on hypoxia, acidification, algae, zooplankton and eelgrass over the period of 2000 to 2095. Though their results indicated substantial area-day increases in exposition to hypoxic waters for benthic and near-bed pelagic species in the southern Salish Sea by 2095, their grid was not sufficiently refined in the Baynes Sound region to accurately capture the relatively strong tidal currents at the two entrances. Thus, the model would not have included the strong mixing that Ianson et al. (2016) claimed should preclude hypoxia. Khangaonkar et al. (2021) also found that even though nutrient loads from both oceanic and land-based sources were projected to increase and fuel stronger phytoplankton primary productivity, there was little increase in micro-algal biomass due to increased predation from larger biomass levels of micro and mesozooplankton.

All these predicted changes outlined above may affect bivalves in Baynes Sound. For example, larval stages are considered the most sensitive to ocean acidification (Waldbusser et al. 2015) exposing natural populations and bivalve aquaculture relying on natural spat recruitment to the earliest and strongest negative impacts from pH and calcite/aragonite saturation changes. As predicted for zooplankton, warming waters may lead to increased filtering pressure from bivalves, especially considering that the two most abundant species in Baynes Sound (i.e. Manila clams and Pacific oysters) are found and cultivated in warmer climates (e.g. Mediterranean Sea). The potential faster growth and increased production could however be hindered by an overall decrease in the Sound's carrying capacity, following the increased pressure on phytoplankton resources. In addition to an increase in mean water temperature, climate change could potentially lead to temporal shifts in the temperature seasonal cycle and planktonic communities (Mackas et al. 2011, 2013; Allen and Wolfe, 2013; Filgueira et al. 2015). Such shifts may affect the phenology of different species or group of species in different ways and lead to new match/mismatch between supply and demand for pelagic resources. As for any climate-driven change further research is warranted to understand the ultimate consequences of these shifts on coastal ecosystems in general and their carrying capacity for bivalve aquaculture in particular.

6. ACKNOWLEDGMENTS

practices. Comox Marina and BC Ferries provided platform space to deploy YSI-EXO2 Sondes. Stephanie Palmer provided satellite derived chlorophyll values in our area of interest for BiCEM model groundtruthing. Mac's Oyster, Rob Marshall, Daphne Munroe, and the Pacific Biological Shellfish Data Unit provided both cultured and wild bivalve population data for the intertidal zone in Baynes Sound, where possible. Theraesa Coyle collated the intertidal bivalve data according to georeferenced locations. Shani Rousseau pre-processed all CTD and sample data for input into BiCEM. Both the Aquaculture Management Division (Adrienne Paylor, Shelley Jepps, and Chris Marrie) and the Aquaculture Resource Management Division (Melinda Scott, Krista Sandberg, Michelle Charboneau, and Chris Grady) provided guidance with the Terms of Reference and licencing information, respectively.

7. REFERENCES CITED

Allen, S.E., and Wolfe, M.A. 2013. Hindcast of the timing of the spring phytoplankton bloom in the Strait of Georgia, 1968 – 2010. Progr. Oceanogr. 115:6-13.

Amos, C.L., Martino, S., Sutherland, T.F., and Al Rashidi, T. 2015. Sea Surface Temperature Trends in the Coastal Zone of British Columbia, Canada. J. Coast. Res. 31(2):434-446.

ASC (Aquaculture Stewardship Council). 2019. ASC bivalve standard–version 1.1. March 2019. ASC, Utrecht. The Netherlands, 53 p.

Bacher, C., Grant, J., Hawkins, A., Fang, J., Zhu, P., and Besnard, M. 2003 Modeling the effect of food depletion on scallop growth in Sungo Bay (China). Aquat. Living. Resour. 16:10-24.

Banas, N.S., and Hickey, B.M. 2005. Mapping exchange and residence time in a model of Willapa Bay, Washington, a branching, macrotidal estuary. J. Geophy, Res: Oceans. 110: C11011.

Bricker, S.B., Getchis, T.L., Chadwick, C.B., Rose, C.M., and Rose, J.M. 2016. Integration of ecosystem-based models into an existing interactive web-based tool for improved aquaculture decision-making. Aquaculture, 453:135-146.

Carswell, B., Cheeseman, S., and Anderson, J. 2006. The use of spatial analysis for environmental assessment of shellfish aquaculture in Baynes Sound, Vancouver Island, British Columbia, Canada. Aquaculture, 253 (1–4):408-414.

Chen, C., Beardsley, R.C., and Cowles, G. 2006. An unstructured grid, finite-volume coastal ocean model (FVCOM) system. Oceanogr. Spec. Iss. on Advanc. in Computat. Oceanogr. 19 (1):78-89.

Clague, J.J. 1976. Sedimentology and Geochemistry of Marine Sediments near Comox, British Columbia. Ottawa, Ontario: Energy, Mines and Resources Canada, Geol. Surv. Can. Pap. 76-21, 21p.

Comeau, L.A., Drapeau, A., Landry, T., and Davidson, J. 2008. Development of longline mussel farming and the influence of sleeve spacing in Prince Edward Island, Canada. Aquaculture, 281: 56–62.

Cranford, P. J. 2019. Magnitude and extent of water clarification services provided by bivalve suspension feeding. In: Goods and Services of Marine Bivalves. Springer, Cham. pp. 119-141.

Cranford, P.J., Strain, P.M., Dowd, M., Hargrave, B.T., Grant J., and Archambault M.-C. 2007 Influence of mussel aquaculture on nitrogen dynamics in a nutrient enriched coastal embayment. Mar. Ecol. Prog. Ser. 347:61-78.

Dabrowski, T., Lyons, K., Curé, M., Berry, A., and Nolan, G. 2013. Numerical modelling of spatio-temporal variability of growth of *Mytilus edulis* (L.) and influence of its cultivation on ecosystem functioning. J. Sea Res. 76, 5-21.

Dame, R. F. 1996 Ecology of Marine Bivalves. An Ecosystem Approach. CRC Press, Boca Raton.

Dame, R. F., and Prins, T.C. 1998. Bivalve carrying capacity in coastal ecosystems. Aquat. Ecol. 31(4):409-421.

DFO. 2015. Carrying capacity for shellfish aquaculture with reference to mussel aquaculture in Malpeque Bay, Prince Edward Island. DFO Can. Sci. Advis. Sec. Sci. Advis. Rep. 2015/003.

DFO. 2019. Aquaculture Production and Values.

Evans, W., Pocock, K., Hare, A., Weekes, C., Hales, B., Jackson, J., Gurney-Smith, H., Mathis, J.T., Alin, S.R. and Feely, R.A. 2019. Marine CO_2 Patterns in the Northern Salish Sea. Front. Mar. Sci. 5: 536.

FAO. 2008. Fisheries Management. 2. The ecosystem approach to fisheries. 2.1 Best practices in ecosystem modelling for informing an ecosystem approach to fisheries. Technical Guidelines for Responsible Fisheries 4. Suppl. 2 Add 1. FAO, Rome. X + 72 p.

Feist, B.E., and Simenstad, C.A. 2000. Expansion rates and recruitment frequency of exotic smooth cordgrass, *Spartina altemiflora* (Loisel), colonizing unvegetated littoral flats in Willapa Bay, Washington. Estuaries, 23:267-274.

Ferreira, J.G., Hawkins, A.J.S., and Bricker, S.B. 2007. Management of productivity, environmental effects and profitability of shellfish aquaculture – the Farm Aquaculture Resource Management FARM model. Aquaculture, 264:160-174.

Filgueira, R., Comeau, L. A., Landry, T., Grant, J., Guyondet, T., and Mallet, A. 2013a. Bivalve condition index as an indicator of aquaculture intensity: A meta-analysis. Ecol. Ind. 25:215-229.

Filgueira, R., Grant, J., Stuart, R., and Brown, M.S. 2013b. Ecosystem modelling for ecosystem-based management of bivalve aquaculture sites in data-poor environments. Aquac. Environ. Inter. 4:117–133.

Filgueira, R., Guyondet, T., Comeau, L. A., and Grant, J. 2014a. Physiological indices as indicators of ecosystem status in shellfish aquaculture sites. Ecol. Ind. 39: 134 - 143

Filgueira, R., Guyondet, T., Comeau, L. A., and Grant, J. 2014b. Storm-induced changes in coastal geomorphology control estuarine secondary productivity. Earth's Future. 21:1-6.

Filgueira, R., Brown, M. S., Comeau, L. A., and Grant, J. 2015. Predicting the timing of the pediveliger stage of *Mytilus edulis* based on ocean temperature. J. Mollusc. Stud. 81(2):269-273.

Filgueira, R., Comeau, L. A., and Guyondet, T. 2015a. Modelling carrying capacity of bivalve aquaculture: a review of definitions and methods. DFO Can. Sci. Advis. Sec. Res. Doc. 2015/002. v + 31p.

Filgueira, R., Guyondet, T., Bacher, C., and Comeau, L.A. 2015b. Informing marine spatial planning (MSP) with numerical modelling: a case-study on shellfish aquaculture in Malpeque Bay (Eastern Canada). Mar. Pollut. Bull. 100 (1):200-216.

Filgueira, R., Guyondet, T., Comeau, L.A., and Sutherland, T.F. 2016a. Dynamic Energy Budget DEB models of bivalve molluscs inhabiting British Columbia coastal waters: Review of existing data and further directions for data collection. Can. Tech. Rep. Fish. Aquat. Sci. 3173: vii + 28 p.

Filgueira, R., Guyondet, T., Comeau, L.A., and Tremblay, R. 2016b. Bivalve aquaculture-environment interactions in the context of climate change. Global Change Biol. 22 (12):3901 -3913.

Foreman, M.G.G., Chandler, P.C., Stucchi, D.J., Garver, K.A., Guo, M., Morrison, J., and Tuele, D. 2015. The ability of hydrodynamic models to inform decisions on the siting and management of aquaculture facilities in British Columbia. DFO Can. Sci. Advis. Sec. Res. Doc. 2015/005. vii + 49 p.

Froján, M., Figueiras, F. G., Zúñiga, D., Alonso-Pérez, F., Arbones, B., and Castro, C. G. 2016. Influence of mussel culture on the vertical export of phytoplankton carbon in a coastal upwelling embayment Ría de Vigo, NW Iberia. Est. Coast. 395: 1449-1462.

Fulton, E.A. 2010 Approaches to end-to-end ecosystem models. J. Ma.r Syst. 81:171-18.

Gibbs, M.T. 2007. Sustainability performance indicators for suspended bivalve aquaculture activities. Ecol. Ind. 71:94-107.

Grant, J., and Bacher, C. 2001. A numerical model of flow modification induced by suspended aquaculture in a Chinese bay. Canadian Journal of Fisheries and Aquatic Sciences, 585, 1003-1011.

Grant, J., and Filgueira, R. 2011. The application of dynamic modelling carrying capacity in shellfish farming. In: Shumway, S.E. (Ed.) Shellfish Culture and the Environment. Wiley-Blackwell, New York, 135 – 154.

Guyondet, T., Roy, S., Koutitonsky, V. G., Grant, J., and Tita, G. 2010. Integrating multiple spatial scales in the carrying capacity assessment of a coastal ecosystem for bivalve aquaculture. J. Sea Res. 643:341-359.

Guyondet, T., Comeau, L. A., Bacher, C., Grant, J., Rosland, R., Sonier, R., and Filgueira, R. 2015. Climate Change Influences Carrying Capacity in a Coastal Embayment Dedicated to Shellfish Aquaculture. Est. Coast. 385:1593-1618.

Haigh, R,. and Taylor, F.J.R. 1990. Distribution of potentially harmful phytoplankton species in the northern Strait of Georgia, British Columbia. Distribution of potentially harmful phytoplankton species in the northern Strait of Georgia, British Columbia. Can. J. Fish. Aquat. Sci. 47:2339-2350.

Haigh, R., and Taylor, F.J.R. 1991. Mosaicism of microplankton communities in the northern Strait of Georgia, British Columbia. Mar. Biol. 110:301-314.

Haigh, R., Taylor, F.J.R., and Sutherland, T.F. 1992. Phytoplankton ecology of Sechelt Inlet, a fjord system on the British Columbia coast. I. General features of the nano- and microplankton. Mar. Ecol. Progr. Ser. 89:117-134.

Hay and Company Consultants Inc. 2003. Baynes Sound Carrying Capacity Study Technical Report, MAFF.001, Ministry of Agriculture, Food and Fisheries, Ministry of Sustainable Resource Management and Environment Canada, Environmental Protection, Pacific and Yukon Region, vii + 24 p. (unpublished).

Heip, C.H.R., Goosen, N.K., Herman, P.M.J., Kromkamp, J., Middelburg, J.J., and Soetaert, K. 1995. Production and consumption of biological particles in temperate tidal estuaries. Oceanogr. Mar. Biol. Ann. Rev. 33:1-149.

Ianson, D., Allen, S.E., Moore-Maley, B.L., Johannessen, S.C., and Macdonald, R.W. 2016. Vulnerability of a semi-enclosed estuarine sea to ocean acidification in contrast with hypoxia. Geophys. Res. Lett. 43:5793-5801. doi:10.1002/2016GL06899

IPCC, 2014. Climate Change, 2014: Synthesis Report. Contribution of Working Groups I, II and III to the Fifth Assessment Report of the Intergovernmental Panel on Climate Change [Core Writing Team. Pachauri, R.K., Meyer, L.A. (Eds.)], IPCC, Geneva, Switzerland, 151 pp.

Jiang, W., and Gibbs, M.T. 2005. Predicting the carrying capacity of bivalve shellfish culture using a steady, linear food web model. Aquaculture, 244:171-185.

Jiang, T., Chen F., Yu Z., Lu, L., and Wang, Z. 2016. Size-dependent depletion and community disturbance of phytoplankton under intensive oyster mariculture based on HPLC pigment analysis in Daya bay, South China Sea. Env. Poll. 219:804-814.

Kassem, H., Sutherland, T.F., and Amos, C.L. 2021. Hydrodynamic controls on particle size of resuspended sediment from sandy and muddy substrates in British Columbia, Canada. J. Coast. Res. 37(3):691-707.

Khangaonkar, T., Nugraha, A., Premathilake, L., Keister, J., and Borde, A. 2021. Projections of algae, eelgrass, and zooplankton ecological interactions in the inner Salish Sea – for future climate, and altered oceanic states. Ecol. Model. 441 (C):109420.

Kluger, L. C., Filgueira, R., and Wolff, M. 2017. Integrating the concept of resilience into an ecosystem approach to bivalve aquaculture management. Ecosystems, 207:1364-1382.

Lazier, J.R.N., 1963. Some Aspects of the Oceanographic Structure in the Jervis Inlet System. University of British Columbia, Vancouver, B.C. MSc. Thesis.

Mackas, D.L., Thomson, R, and Galbraith, M. 2011. Changes in the zooplankton community of the British Columbia continental margin, 1985-1999. Can. J. Fish. Aquat. Sci. 58:685-702.

Mackas, D., Galbraith, M., Faust, D., Masson, D., Young, K., Shaw, W., Romaine, S., Trudel, M., Dower, J., Campbell, R., Sastri, A., Bornhold-Pechter, E.A., Pakhomov, E., and El-Sabaawi, R. 2013. Zooplankton time-series from the Strait of Georgia: Results from year-round sampling at deep water locations, 1990-2010. Progr. Oceanogr. 115:129-159.

Maicu, F., De Pascalis, F., Ferrarin, C., and Umgiesser, G. 2018. Hydrodynamics of the Po River-Delta-Sea system. J. Geophy, Res. Oceans. 123:6349-6372.

Marinov, D., Galbiati, L., Giordani, G., Viaroli, P., Norro, A., Bencivelli, S., and Zaldívar, J.M. 2007. An integrated modelling approach for the management of clam farming in coastal lagoons. Aquaculture, 269:306-320.

Masson, D., and Cummins, P.F. 2007. Temperature trends and interannual variability in the Strait of Georgia, British Columbia, Cont. Shelf Res. 27:634-649.

Morris, S. Leaney, A.J. Bell, A.J., and Thompson, J.M. 1979. The Courtney River estuary, status of environmental knowledge to 1978: Report of the Estuary Working Group. Fisheries and Environment Canada, Special Estuary Series 8. 355p.

Newell, R.I. 2004. Ecosystem influences of natural and cultivated populations of suspension-feeding bivalve molluscs: a review. J. Shellfish Res. 231, 51-62.

Olson, E.M., Allen, S.E., Do, V., Dunphy, M., and Ianson, D. 2020. Assessment of nutrient supply by a tidal jet in the Northern Strait of Georgia based on a biogeochemical model. J. Geophy, Res. Oceans. 125. e2019JC015766.

Panda, U.S., Mohanty, P. K., and Samal, R. N. 2013. Impact of tidal inlet and its geomorphological changes on lagoon environment: A numerical model study. Est. Coast. Shelf. Sci. 116, 29–40.

Pete, R., Guyondet, T., Bec, B., Derolez, V., Cesmat, L., Lagarde, F., Pouvreau, S., Fiandrino, A., and Richard, M. 2020. A box-model of carrying capacity of the Thau lagoon in the context of ecological status regulations and sustainable shellfish cultures. Ecol. Model. 426 (C):109049.

Petersen, J. K., Holmer, M., Termansen, M., and Hasler, B. 2019. Nutrient Extraction Through Bivalves. Smaal, S., Ferreira J., Grant J., Petersen J., Strand, O. (Eds). In: Goods and Services of Marine Bivalves. Springer, Cham. pp. 179-208.

Pritchard, D.W. 1967. What is an estuary: Physical viewpoint. Lauff, G.H. (Ed), In: Estuaries. Washington, D.C.:American Association for the Advancement of Science, AAAS Publication 83, pp. 3-5.

Riddell, A., and Bryden, G. 1996. Courtenay River Water Allocation Plan. Nanaimo, British Columbia: BC Ministry of Environment, Lands and Parks, Regional Water Management, Vancouver Island Region, 80p.

Roselli, L., Cañedo-Argüelles, M., Costa-Goela, P., Cristina, S., Rieradevall, M., D'Adamo, R., and Newton, A. 2013. Do physiography and hydrology determine the physico-chemical properties and trophic status of coastal lagoons? A comparative approach. Est. Coast. Shelf. Sci. 117: 29-36.

SAPEA, Science Advice for Policy by European Academies. 2017. How can more food and biomass be obtained from the oceans in a way that does not deprive future generations of their benefits? Evidence Review Report No. 1. SAPEA, Berlin. ISBN 978-3-9819415-1-7.

Smaal, A. C. 1991 The ecology and cultivation of mussels: new advances. Aquaculture, 94: 245-261.

Smyth, A. R., Murphy, A. E., Anderson, I. C., and Song, B. 2018. Differential effects of bivalves on sediment nitrogen cycling in a shallow coastal bay. Est. Coast. 414: 1147-1163.

Soto, D., Aguilar-Manjarrez, J., Brugère, C., Angel, D., Bailey, C., Black, K., Edwards, P., Costa-Pierce, B., Chopin, T., Deudero, S., Freeman, S., Hambrey, J., Hishamunda, N., Knowler, D., Silvert, W., Marba, N., Mathe, S., Norambuena, R., Simard, F., Tett, P., Troell, M. and Wainberg, A. 2008. Applying an ecosystem-based approach to aquaculture: principles, scales and some management measures, In: Soto, D., Aguilar-Manjarrez, J., Hishamunda, N. Eds., Building an ecosystem approach to aquaculture. In: Building an ecosystem approach to aquaculture. FAO/Universitat de les Illes Balears Expert Workshop. 7–11 May 2007, Palma de Mallorca, Spain. FAO Fisheries and Aquaculture Proceedings. No.14. Rome, FAO. pp 15-35.

Sutherland, T.F., and Amos, C.L. 2020. An *in situ* assessment of seabed stability in Baynes Sound, British Columbia, Canada. J. Coast. Res. 36 (3):472-486.

Sutherland, T.F., Garcia-Hoyos, L.M., Poon, P., Krassovski, M.V., Foreman, M.G.G., Martin, A.J., and Amos, C.L. 2018. Seabed attributes and meiofaunal abundance associated with a hydrodynamic gradient in Baynes Sound, British Columbia, Canada. J. Coast. Res. 34 (5):1021-1034.

Tamayo, D., Ibarrola, I., Urrutia, M.B., and Navarro, E. 2011. The physiological basis for inter-individual growth variability in the spat of clams *Ruditapes philippinarum*. Aquaculture, 321 (1/2):113-120.

Taylor, F.J.R., Haigh, R., and Sutherland, T.F. 1994. Phytoplankton ecology of Sechelt Inlet, a fjord system on the British Columbia coast. II Potentially harmful species. Mar. Ecol. Progr. Ser. 103:151-164.

Therriault, J.-C., Legendre, L., and Demers, S. 1990. Oceanography and Ecology of Phytoplankton in the St.Lawrence Estuary. In: Oceanography of a Large-Scale Estuarine System. 39 (Issue June 1992):269-295.

Timmermann, K., Maar, M., Bolding, K., Larsen, J., Nielsen, P., and Petersen, J. K. 2019. Mussel production as a nutrient mitigation tool for improving marine water quality. Aquacult. Env.. Interact. 11:191-204.

Waldbusser, G.G., Hales, B., Langdon, C.J., Haley, B.A., Schrader, P., Brunner, E.L., Gray, M.W., Miller, C.A., and Gimenez, I. 2015. Saturation-state sensitivity of marine bivalve larvae to ocean acidification. Nat. Climate Change. 5 (3):273-280.

Waldie, R.J. 1951. Winter Oceanography of Baynes Sound and the Lazo Bight. Fish. Res. Brd. of Can. Manuscript Reports of the Biological Stations. No.441, 27p.

Wang, B., Cao, L., Micheli, F., Naylor, R.L., and Fringer, O.B. 2018. The effects of intensive aquaculture on nutrient residence time and transport in a coastal embayment. Environ. Fluid. Mech. 18:1321-1349.

Weitzman, J., and Filgueira, R. 2020. The evolution and application of carrying capacity in aquaculture: towards a research agenda. Rev. Aquacult. 123:1297-1322.

Weitzman, J., Steeves, L., Bradford, J., and Filgueira, R. 2019. Far-field and near-field effects of marine aquaculture. World Seas: An Env. Eval. 197-220.

Wheat, E., and Ruesink, J.L. 2013. Commercially-cultured oysters (*Crassostrea gigas*) exert top-down control on intertidal pelagic resources in Willapa Bay, Washington, USA. J. Sea Res. 81:33–39.

Winter, D. F., Banse, K., and Anderson, G.C. 1975. The dynamics of phytoplankton blooms in Puget Sound a fjord in the northwestern United States. Mar. Biol. 292:139-176.

Zhang, J., Hansen, P.K., Fang, J., Wang, W., and Jiang, Z. 2009. Assessment of the local environmental impact of intensive marine shellfish and seaweed farming—application of the MOM system in the Sungo Bay, China. Aquaculture, 287:304=310.

8. APPENDIX A: EVALUATION OF THE HYDRODYNAMIC MODEL, FINITE VOLUME COMMUNITY OCEAN MODEL (FVCOM)

8.1. TERM OF REFERENCE OBJECTIVE #1

Evaluate the hydrodynamic accuracy of the FVCOM model component and discuss the biological applicability of the biogeochemical (BiCEM) component in the coupled Baynes Sound model.

a. Compare modelled and observed water properties

b. Identify uncertainties and consequences associated with data availability and modelling parameterization through sensitivity analysis for this Pacific region application of FVCOM-BiCEM.

8.2. INTRODUCTION

8.2.1. FVCOM overview and representativeness of the simulation period

Hydrodynamic models have become a standard tool to better understand the physical oceanographic conditions affecting aquaculture sites and the potential impacts of those sites on the surrounding environment. Foreman et al. (2015) included a literature review of many such models and presented a case for employing the Finite Volume Community Ocean Model (FVCOM), developed by Chen et al. (2003, 2004, 2006a,b), in the Broughton Archipelago and Discovery Islands regions of B.C.. Basically, all hydrodynamic models solve the three-dimensional (3D) primitive equations for velocity and surface elevation in combination with the 3D transport/diffusion equations for salinity and temperature in the presence of turbulent mixing. This is done over a grid network that covers the geographic region of interest and whose land boundary approximates the coastline as closely as possible. In the case of FVCOM, the horizontal grid is comprised of triangles of varying size and orientation that provide more flexibility in fitting complicated coastlines and bathymetric features than finite difference approaches like NEMO (Nucleus for European Modelling of the Ocean, Madec, 2015) and FG8 (Stronach et al. 1993), which typically employ rectangles of a consistent size and orientation. In the vertical, the grid is typically a column extension of the horizontal triangles (or rectangles) which allows for layers (or levels) of varying thickness that can, for example, better approximate complex dynamics near the surface and bottom. The governing partial differential equations are generally approximated either by i) replacing partial derivatives with finite differences (i.e., finite difference techniques) or, ii) assuming simple functional forms for the variables of interest (i.e., finite element or finite volume techniques), and then solving a series of equations that provide new values for all the variables at discrete time intervals as we move through a prescribed time period. See Foreman et al. (2015) for more details.

It should be noted that the modelling described herein is not the first to have been used to study the carrying capacity in Baynes Sound (Figure A1). Using results from extensive field studies carried out in 2002, Hay and Company Consultants (2003, henceforth HCC03) developed and validated a different combination of ocean circulation (H3D) and biogeochemical models for this purpose. Though their conclusion was that "the commercial bivalve population is functioning at a level well below the maximum bivalve carrying capacity of Baynes Sound" (HCC03), local oyster and clam production tonnages have respectively increased by factors of 2.6 and 1.5 from 2001 (HCC03) to 2015 (DFO, 2019). So it is timely to revisit the carrying capacity topic to update current industry practices and consider potential changes in environmental conditions related to climate change. It should be noted that Hay and Company Consultants (2001) have also applied

their carrying capacity models to assess the oyster productive capacity of Gorge Harbour, B.C. in collaboration with Richardson and Newell (2002) and Barnes (2007).
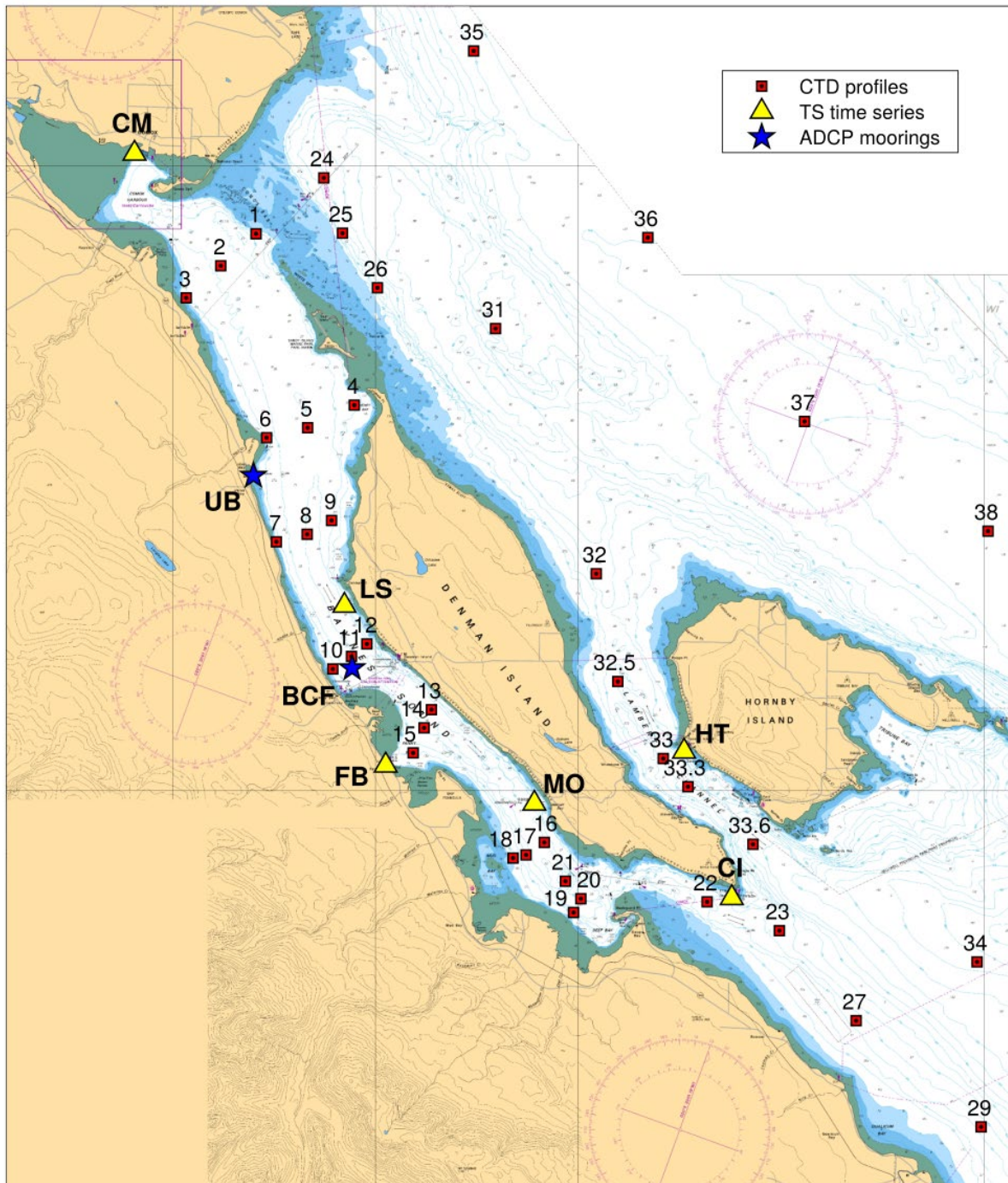
Figure A1: Regional map of Baynes Sound showing CTD stations and locations of ADCP moorings (UB; Union Bay; BCF: BC Ferries) and temperature-salinity time series observations (CM: Comox Harbour; LS: Lucky Seven; FB: Fanny Bay; MO: Mac's Oysters; CI: Chrome Island; HT: Hornby Terminal). The base map showing bathymetric contours (blue) and mudflat regions (green) was modified from the Canadian Hydrographic Service nautical chart #3527.

8.3. METHODS

FVCOM has a sizeable user community in Canada, having been applied not only to general ocean and lake circulation problems, but also to specifically help understand dispersion around salmon farms in B.C., New Brunswick (Page et al. 2014), and Newfoundland (Ratsimandresy et al. 2020). It was for this reason, and the flexibility its triangular grid allows a better fitting the coastline, that FVCOM was chosen to simulate the hydrodynamics of Baynes Sound. However, unlike the previous B.C. applications to generally steep-sided fjords and inlets, a wetting-and-drying capability was included to more accurately capture the effects of extensive mudflats in the region. The accuracy of this feature has been confirmed in the New Brunswick applications where the large Bay of Fundy tidal range plays an important role in the local hydrodynamics (Wu et al. 2014).

In the horizontal, the Baynes grid is comprised of irregularly sized triangles covering the northern half of the SoG (side lengths vary from approximately 4 km in the central strait to 40 m in Baynes Sound (Figure A2a, b)), while in the vertical there are 20 unequally-spaced layers (Figure A2c). As seen in Figure A2c, the layer thickness when expressed as a fraction of the total depth has been chosen to be much smaller near the surface in order to better resolve the freshwater lense and the transmission of wind energy and heat flux to the upper ocean. The relative thickness then increases down the water column so that the bottom layer covers approximately 8% of the total depth. As subsequent temperature and salinity plots show there is little variation in the lower portions of the water column, this coarser resolution is sufficient.

The model bathymetry was generated from Canadian Hydrographic Service (CHS) single-beam acoustic surveys with multi-beam soundings included where available. However in order to reduce the 'hydrostatic inconsistency' and spurious currents (Haney 1991) that can result with terrain-following vertical layers (like those here) and steep bathymetry, all depths were smoothed with a volume preserving technique that limits the ratio $\Delta h/h$ within each triangle, where Δh is the difference between maximum and minimum depth and h is the average depth. This smoothing follows Hannah and Wright (1995) and is similar to the criteria recommended by Mellor et al. (1994).

The model is forced with i) the five tidal constituents M_2, S_2, N_2, K_1, and O_1 comprising approximately76% of the total tidal height range at Comox, ii) freshwater discharge from four rivers emptying into Baynes Sound, and iii) winds and heat flux from the Environment and Climate Change Canada (ECCC) High Resolution Deterministic Prediction System (HRDPS) atmospheric model with 2.5 km horizontal resolution. Three-dimensional temperature and salinity fields interpolated from observations (conductivity, temperature, depth (CTD)) in the region were used to initialize the model and to specify temperatures and salinities along the northern and southern model boundaries during the model simulations.

Though including the next three largest tidal constituents would increase the percentage of tidal height range explained to 87%, it is unlikely that this additional tidal energy would make much difference to the subsequent BiCEM results. As will be seen, tidal current power measured at the two acoustic Doppler current profiler (ADCP) deployments in central Baynes Sound accounted for only a relatively small percentage of the total. Most of the power was in the sub-tidal frequency bands and attributable to variations in a combination of winds, river discharges, and inputs from the SoG.
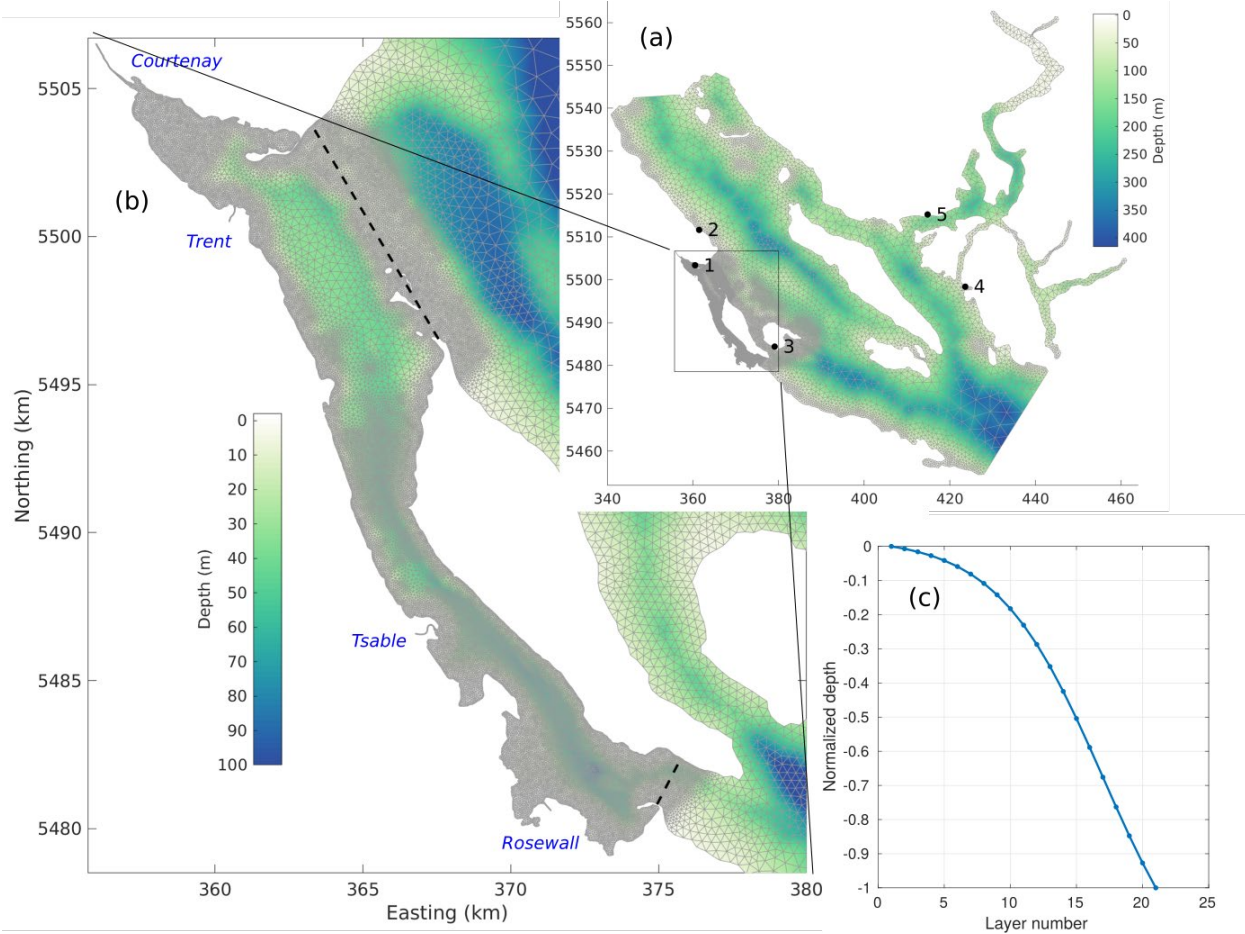
Figure A2: Triangular grid and bathymetry for the circulation model. (a) for the entire model domain, (b) close-up view of Baynes Sound area with the Courtenay, Trent, Tsable, and Rosewall Rivers included in the model, and (c) bounds of the model vertical layers. Panel (a) includes tide gauge locations later used to evaluate the model: 1 – Comox, 2 – Little River, 3 – Hornby Island, 4 – Irvines Landing, and 5 – Saltery Bay. Dashed lines in Panel (b) show transect lines across which volume fluxes are later calculated.

FVCOM is linked to the Generalized Ocean Turbulence Model (GOTM; Burchard et al. 1999; Umlauf and Burchard, 2003) which offers several vertical mixing scheme choices. The results presented here were obtained with the Mellor-Yamada 2.5 scheme (MY2.5, Mellor and Yamada, 1982) and a vertical Prandtl number of 1.0 (i.e., the same vertical mixing coefficient was used in both the velocity and temperature/salinity equations). Though FVCOM applications in other B.C. regions typically employed k-ε turbulent mixing, comparisons with results from MY2.5 in the Discovery Islands (Foreman et al. 2012) demonstrated that the particular choice made little difference to vertical profiles of velocity. Horizontal diffusion is parameterized with a Smagorinsky (1963) method whose formulation is described in Chen et al. (2008). Several coefficient values were tested before compromising on the value 0.02 m^2/s in the salinity and temperature transport/diffusion equations and 0.2 m^2/s for the momentum equations. In terms of the FVCOM parameters, this means the horizontal Prandtl number was 0.1. These values provided reasonably smooth velocity fields and attempted to minimize potential contribution that horizontal mixing can make to vertical mixing in regions with steep bathymetry. In FVCOM, horizontal diffusion "occurs only parallel to" the vertical layers and this simplification can lead to overly diffusive model thermoclines and haloclines when those layers have significant slopes (Chen et al. 2006b).

Physical water-column variables, required to support both FVCOM and BiCEM (Bivalve Culture Ecosystem Model) were collected with varying frequency and spatial resolution in Baynes Sound depending on modelling requirements and resources available. Vertical profiles of temperature, salinity, and oxygen were collected using a Seabird911 profiling CTD (conductivity, temperature, depth) equipped with a 24 Niskin-bottle Rosette. For the most part, CTD profile surveys were carried out in the spring and summer periods between 2009 and 2019 in Baynes Sound and the Northern SoG (boundary zone) as part of the Ecosystem Research Initiative (ERI), Program for Aquaculture Regulatory Research (PARR), and AMD request for advice.

In general, central-axis stations (2, 5, 8, 11, 14, 17, 20, 22, and 23) were surveyed annually with the exception of 2010, 2015, and June 2017 (3-station tidal series) (Table A1). The number of sampling stations increased during this sampling period from 23 (inside BS) to 40 in order to increase spatial coverage in the boundary zone for the modelling period (2016-2017). Hourly tidal-series of vertical CTD profiles (Seabird-911-Rosette) at 3 fixed stations (ST2-upper, ST17-lower, ST23-outer Baynes Sound) were collected in both April and June of 2017. Additional CTD data were available from local DFO monitoring programs that provided increased spatial and temporal coverage within the entire modelling domain. This long time-series of CTD data addresses ecosystem variation with respect to the TOR Objective 1a&b examining data availability and sensitivity analysis of the models FVCOM and BiCEM (Appendix C).

Table A1: CTD sampling stations for the collection of vertical profiles of temperature, salinity, and dissolved oxygen.

Year	Month	Central-axis Stations	Additional Stations
2009	April	2,5,8,11,14,17,20,22,23	1,3,4,6,7,9,10,12,13,15,16,18,19,21
2011	April	2,5,8,11,14,17,20,22,23	24,25,26
2011	August	2,5,8,11,14,17,20,22,23	1,3,4,6,7,9,10,12,13,15,16,18,19,21
2012	July	2,5,8,11,14,17,20,22,23	1,3,4,6,7,9,10,12,13,15,16,18,19,21,27,28,30,31,32
2013	April	2,5,8,11,14,17,20,22,23	31,32,33,34
2014	April	2,5,8,11,14,17,20,22,23	1,3,4,6,7,9,10,12,13,15,16,18,19,21,27,28,30,31,32-40
2014	June	2,5,8,11,14,17,20,22,23	1,3,4,6,7,9,10,12,13,15,16,18,19,21,27,28,30,31,32-40
2016	April	2,5,8,11,14,17,20,22,23	1,3,4,6,7,9,10,12,13,15,16,18,19,21,27,28,30,31,32-40
2016	June	2,5,8,11,14,17,20,22,23	1,3,4,6,7,9,10,12,13,15,16,18,19,21,27,28,30,31,32-40
2017	April	2,5,8,11,14,17,20,22,23	2, 17, 23 (Tidal series), 32.5, 33, 33.3, 33.6
2017	June	2, 17, 23 (Tidal series)	-
2018	April	2,5,8,11,14,17,20,22,23	-
2018	June	2,5,8,11,14,17,20,22,23	-
2019	April	2,5,8,11,14,17,20,22,23	-
2019	June	2,5,8,11,14,17,20,22,23	-

In addition to CTD vertical profiles, portable YSI-EXO2 CTD sondes were deployed at 5 locations (Comox Harbour, Denman Point, Fanny Bay, Metcalfe Bay, and Lambert Channel) at a water depth of 5m to provide time-series data of temperature, salinity, and dissolved oxygen between June and December 2016 (Figure A1). The CTD sonde deployments at Denman Point and Metcalfe Bay were located on oyster rafts in order to log environmental data during *in situ*

oyster growout trials. A 2017 time-series CTD data set was acquired from Hakai Institute responsible for a Fanny Bay mooring in Baynes Sound.

FVCOM was coupled with a Bivalve Culture Ecosystem Model (BiCEM) to provide the biogeochemical aspect required to assess a bivalve carrying capacity in Baynes Sound. The procedure for a coupled FVCOM/BiCEM simulation was to first run FVCOM and store values of temperature, salinity, velocity, and mixing at regular twenty minute intervals throughout the simulation period, and then use these values as input for BiCEM. Though both models could be run simultaneously, it is more computationally efficient to calibrate the circulation model first so that the biological model can be run and tuned separately. This procedure is feasible because there is no feedback from any of the BiCEM variables to those in the circulation model, which is typically more computer intensive and requires many runs to calibrate properly.

8.4. 2016-2017 TEMPERATURE AND SALINITIES IN CONTEXT OF OTHER YEARS

Our coupled FVCOM-BiCEM simulation covered the full annual cycle of May 2016 to April 2017. Though not optimal in terms of evaluating "the hydrodynamic accuracy of the FVCOM model component" (TOR1), this period was chosen because it did provide the largest set of biological data that could be used to initialize and evaluate BiCEM. Of course, this (or any other) choice raises the question of how representative that particular time period is in the context of the physical and biogeochemical fluxes. From the physical perspective, Figure A3 attempts to, at least, partially address that issue by superimposing sea surface salinities and temperatures observed at the Chrome Island lighthouse (Figure A1) for May 2016 to April 2017 on curves of the average, and average plus/minus one standard deviation, computed over its complete observational period of 1961 to 2019 (model simulation values are also shown and will be discussed later). Though not consistently within one standard deviation of the long term average, the cumulative time when the observed 2016-17 salinity curve is outside this band is considerably less than when it is inside with a significant drop from 29 psu to 25 psu in early November being notable. The 2016-17 temperatures are also generally within one standard deviation of the long term average, though the steep drop from 20.3°C on August 18 to 11.8°C on September 6 is also notable.
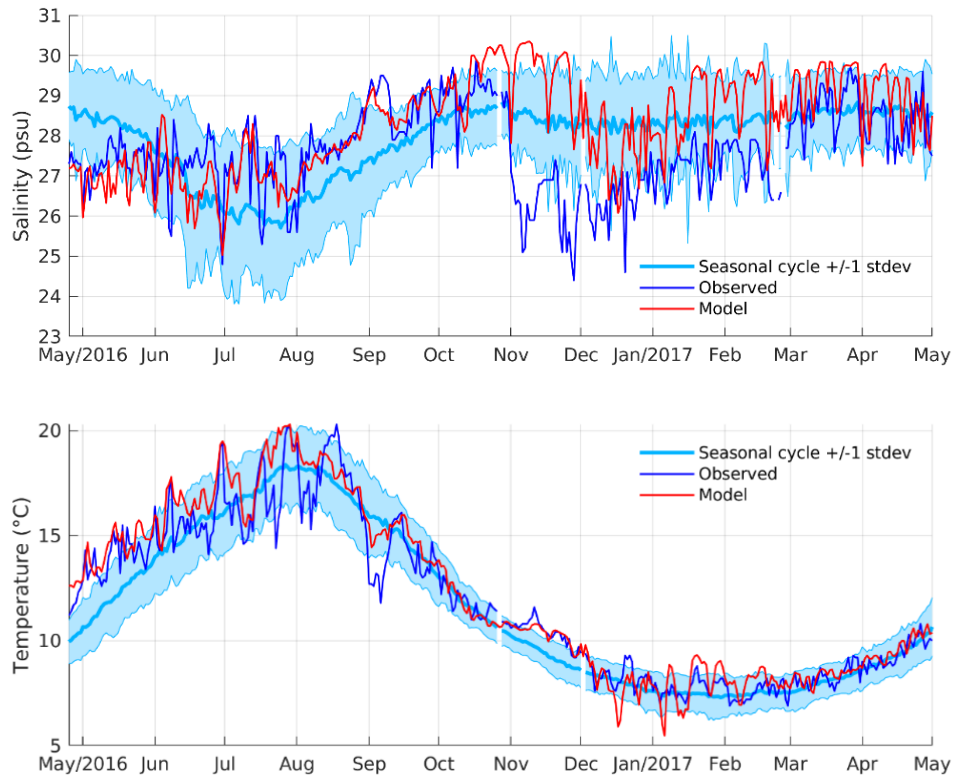
Figure A3: Chrome Island observed and modelled sea surface salinity (top) and temperature (bottom) for May 2016 to April 2017 superimposed on the average seasonal cycle plus/minus one standard deviation.

Figure A4 provides another perspective of the representativeness of our simulation period by showing the average, average plus/minus one standard deviation, and 2016-2017 Fraser River discharges at Hope. The former three values were computed over the period of 1912 to 2019. These discharges can be viewed as a proxy for the volume of low salinity water in the southern SoG that could potentially enter into Baynes Sound, primarily from the south. The 2016-17 values are generally seen to be considerably larger than average prior to mid-May, lower than average from June through August, considerably larger than average in November, and generally within one standard deviation for the remainder of the simulation period. The fact that the discharges in March and April 2016 are beyond one standard deviation of the average suggests more freshwater, and lower than normal salinity, in the SoG at the beginning of our simulation.
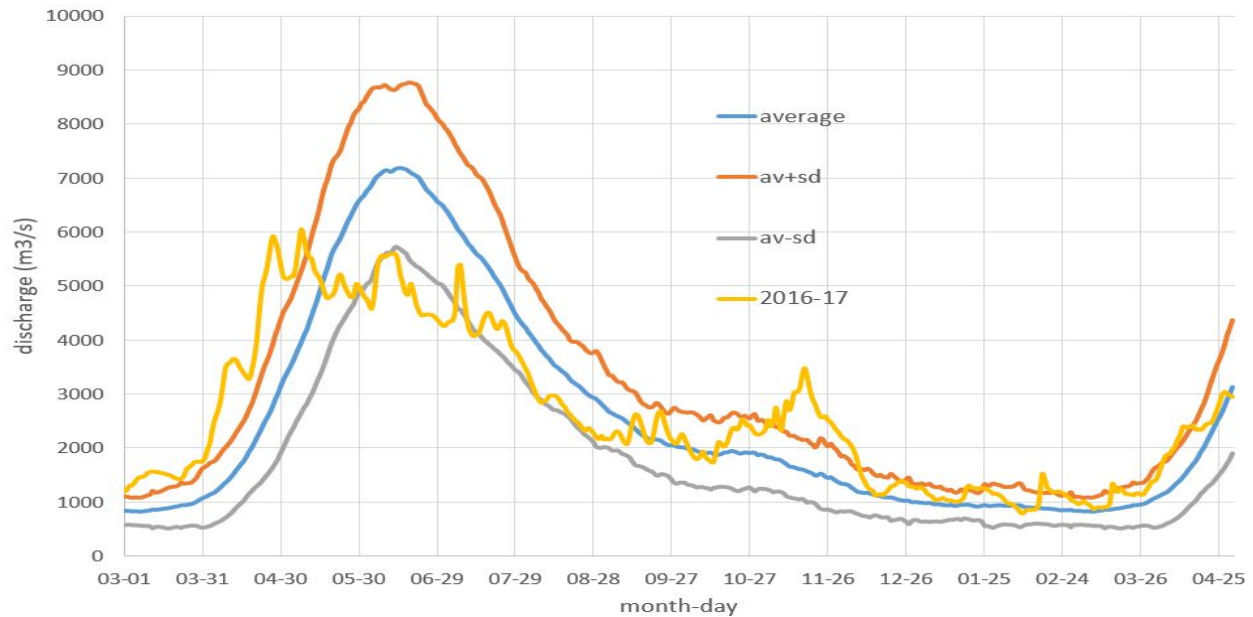
Figure A4: Average, average plus/minus one standard deviation, and March 1, 2016 to April 30, 2017 Fraser River discharges at Hope.

However, as the Fraser has a very large watershed, its discharge reflects both distant and local influences. A better indication of local freshwater influences is the Puntledge River which joins with the Tsolum River to become the Courtenay River just upstream of where it enters northern Baynes Sound. Its time series extends from 1914 to 2019 and in this case, the 2016-17 values (Figure A5) show average or considerably larger than normal discharges prior to beginning of the model simulation (consistent with the Fraser), less than normal discharge between May and September followed by five storm events in October and November that, in the middle three instances, resulted in discharges well above normal. As discharges for the Englishman River (not shown), fairly close to the southern Baynes entrance but still within the model domain, show similar peaks in March 2016 and October 2016 through February 2017, we can conclude there were similar runoff patterns all along the eastern Vancouver Island coastline. Puntledge discharge was below average in December/January but close to normal from February to April, with the exception of a small storm in late February. Though, as will be subsequently discussed, it is not expected that these discharges and the resultant lower than normal salinity will have much effect on the biological calculations in BiCEM; they may impact the Baynes ecosystem productivity through new nutrient inputs.
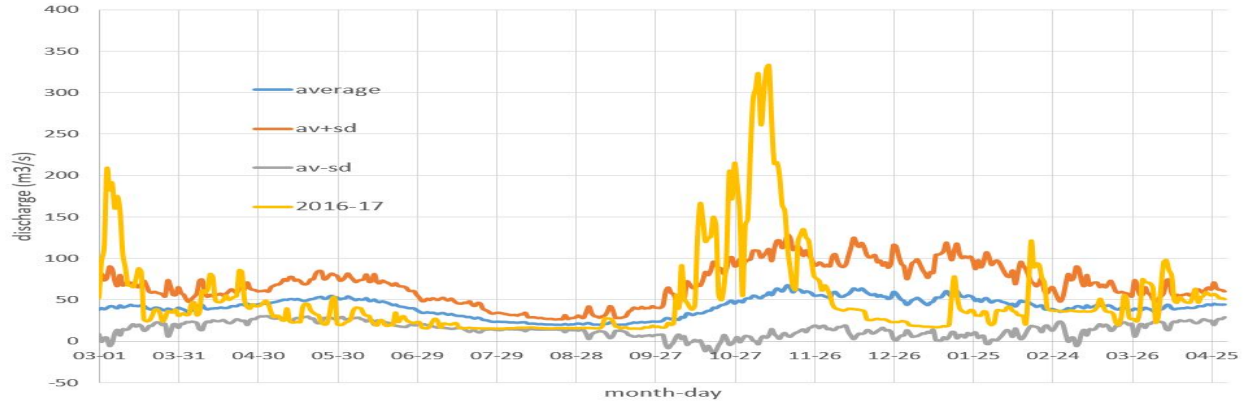
Figure A5: Average, average plus/minus one standard deviation, and 2016-17 Puntledge River discharges just above its confluence with the Tsolum River just north of Courtenay.

Temperature, salinity, and oxygen measurements have been taken over the entire water column at as many as forty stations in the Baynes Sound region since 2009 (Figure A1 shows some stations). Figures A6 and 7 show the temperature and salinity profiles for April and June, the most frequently visited months, at stations BS2 and BS17 (Figure A1), which are respectively located in the northern and southern ends of the Sound and represent two seasonally distinct water masses. As 2016 is seen to be the freshest and warmest April at both stations, it would seem that water properties at the beginning of our model simulation period were quite anomalous. Certainly, the low salinities are consistent with the discharges seen in Figure A5. The second freshest April is seen to be in 2017, at the end of our simulation, where the associated temperatures were "average".

A caveat should be noted in comparing these 2016-17 discharges with long-term statistics since the latter are not stationary due to climate change. For example, the Fraser River hydrograph has been shown to be flattening and have a peak that is arriving earlier in the year (Morrison et al. 2002). Analogous changes may be happening around Baynes Sound, as climate projections for coastal B.C. typically forecast wetter winters and dryer summers (e.g., Morrison et al. 2014). It is important to note that the summer of 2016 experienced record breaking drought (Stage 4) and forest-fire conditions across the Sunshine Coast, within the Baynes Sound watershed, and the B.C. southern mainland influencing the Fraser River outflows. Though this issue certainly warrants further research, it is beyond the scope of the present investigation.
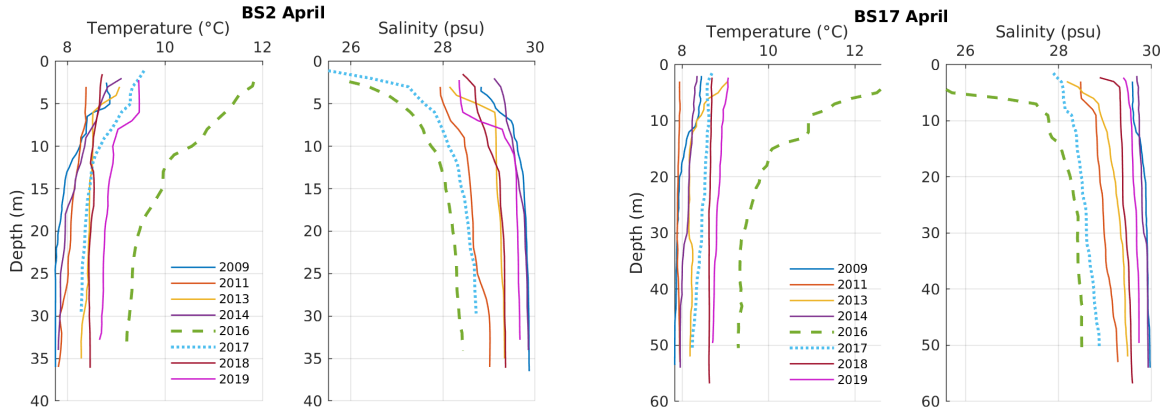
Figure A6: Salinity and temperature profiles at CTD stations BS2 (left panels) and BS17 (right panels) for April.

By June 2016, with the exception of the temperatures below 15m at BS17, all temperature and salinity profiles are seen (Figure A6) to be well within the envelope of profiles for other years. So within two months, the anomalous April water properties had reverted back to "normal", at least as determined by our limited observational set. However as indicated by the anomalously fresh salinity profiles noted previously for April 2017 (Figure A6), and perhaps as a lingering effect of the strong river discharges that arose in October and November 2016 (Figs A4 and A5), this normality did not persist. And though beyond the end of our simulation period, Figure A7 suggests that Baynes Sound remained anomalously fresh through to June 2017. In summary, over the duration of our model simulation period Baynes Sound was generally fresher than normal and had either normal, or warmer than normal, temperatures.
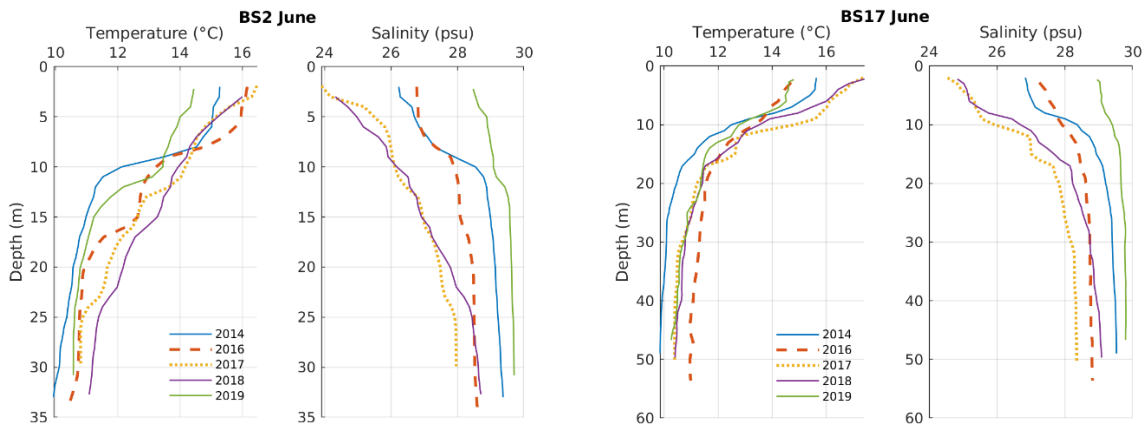
Figure A7: Salinity and temperature profiles at CTD stations BS2 (left panels) and BS17 (right panels) for June.

8.5. FVCOM EVALUATIONS

Comparisons between hydrodynamic model output and observations are typically used to evaluate model accuracy, with the understanding that though there can be errors in (or problems with) the observations (an example is given later), they are generally accepted to reflect the truth. Fortunately, there are considerable data that can be used to evaluate the

accuracy of our model simulation from May 1, 2016 to April 30, 2017. Those presented here will be restricted to comparisons of i) temperature and salinity, ii) currents; and iii) sea surface (predominantly tidal) elevation, as they will be the physical variables most affecting shellfish aquaculture.

8.5.1. Temperature and salinity comparisons

Figure A3 plotted observed and model sea surface salinities and temperatures at the Chrome Island lighthouse. Though there are only a few instances when the model temperatures missed observed warming or cooling events, relatively large salinity discrepancies are seen over the period of November to mid-December 2016, and to a lesser extent thereafter through to March 2017. Much of this can be attributed to the Englishman and Little and Big Qualicum Rivers not being included in our simulation and their freshwater discharges (analogous to those shown in Figure A5 for the Puntledge) not affecting the model salinities at Chrome Island. Average root mean square (RMS) differences over the entire yearly simulation were 1.46 psu and 1.01 °C, respectively, with the largest salinity discrepancies arising in November and the largest temperature discrepancies arising in July.

Figure A8 compares observed and model temperature and salinity profiles at standard CTD stations along the central axis (Figure A1) of Baynes Sound. Values from the June 2016 survey are shown here but similar plots are also available for April 2016 and April 2017, the only other months which had cruises during the model simulation period. As the April 2016 values were combined with other CTD observations to establish initial conditions for the model simulation, those model profiles are in close agreement with the observed. However with the exception of slightly cooler values at depth beyond the southern entrance (stations BS22, BS23, BS27 and BS29), the June 2016 model temperatures are seen to be slightly warmer than those observed. Note that BS22 is close to the Chrome Island lighthouse and Figure A3 showed the model sea surface temperatures (SSTs) to be too warm and the model sea surface salinities (SSSs) to be too fresh in late June. Though the near-surface model salinities are in reasonable agreement further to the north, they are slightly too salty at depth, especially beyond the southern entrance. Overall the salinity and temperature discrepancies are less than 1.0 psu and 1°C respectively, comparable to the RMS values at the Chrome Island lighthouse. We suspect they arise from a combination of i) inaccuracies in both the vertical and horizontal mixing and ii) the bathymetric smoothing that FVCOM requires to avoid instabilities and/or spurious currents.

(a) Observed temperatures
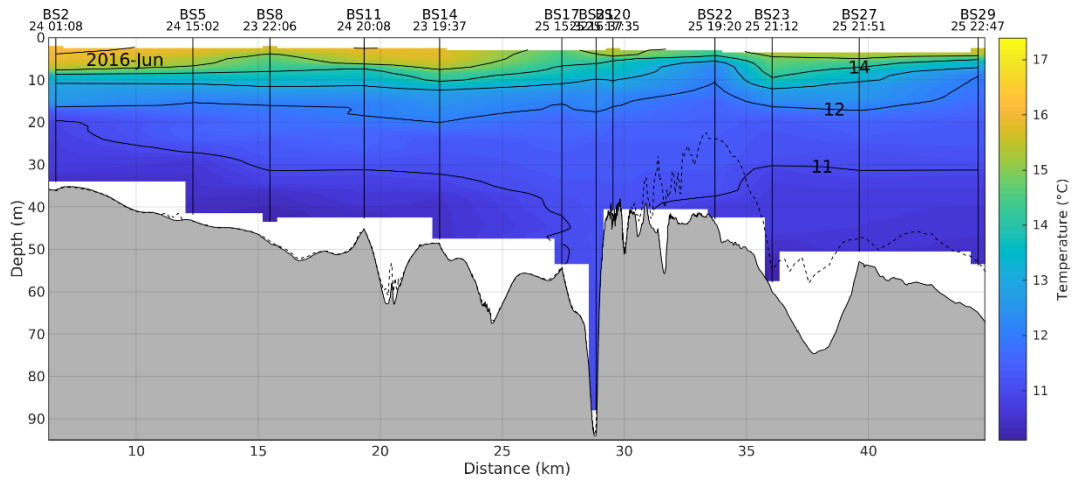
(b) Model temperatures
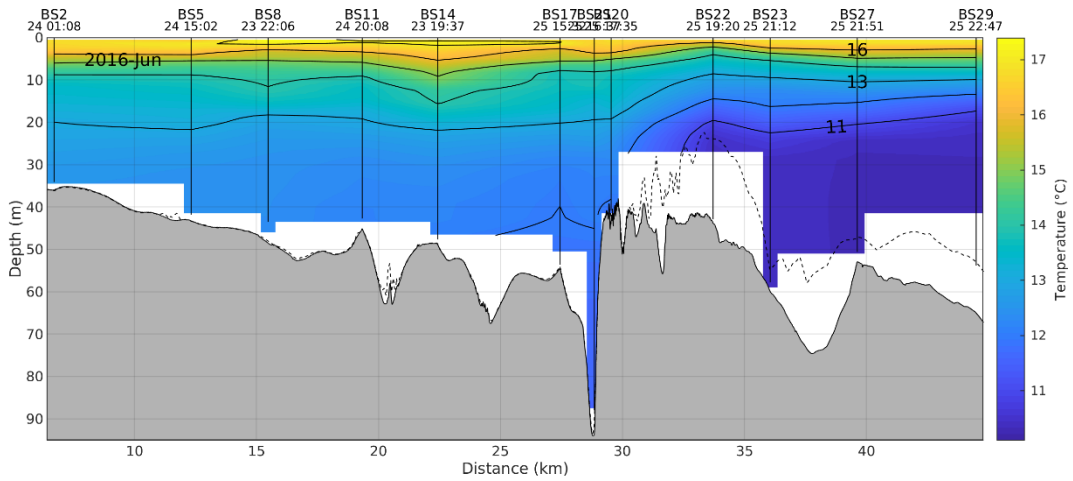
Figure A8: Temperatures (a) and salinities (c) observed at CTD stations along the Baynes Sound thalweg during the June 2016 survey and corresponding model values (b) and (d) at the same locations and time. Station names together with dates and times for each CTD cast are given at the top of each panel and model values were interpolated to coincide with these times. The dashed line is the bottom profile from the model bathymetry while the grey shaded region denotes the true bathymetry. Maps c and d appear on the following two pages.

(c) Observed salinities
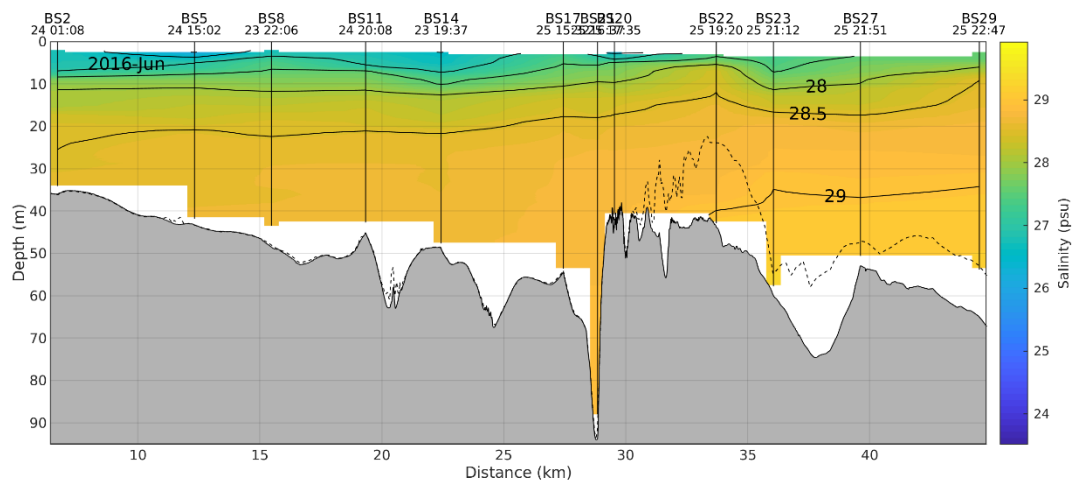
(d) Model salinities
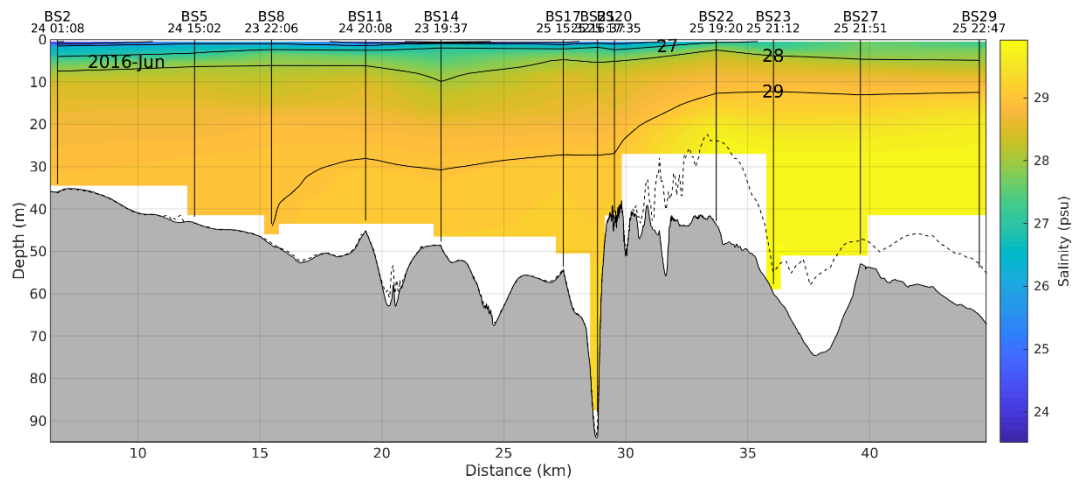
Figure A8 (continued).

Whereas the analogous thalweg plot for April 2017 (not shown) indicates that the model temperatures were generally too warm and the salinities too salty, Figure A9 allows a more precise indication of model versus observed discrepancies. It shows profiles at station BS17 in central Baynes Sound for April and June 2016, as well as April 2017. As mentioned above, the April 2016 agreement is quite good because the observations were used to establish initial conditions for the model simulation. The observed temperature profile is seen to lie within the model envelope of daily variations while the corresponding observed salinities fall below the envelope (i.e., the model is too salty) by a maximum of about 0.5 psu near the surface and below 20m depth. The June 2016 model temperatures are seen to be too warm by at most 1°C while the associated salinities are too salty by at most 0.4 psu. Finally, the April 2017 profiles show the model temperatures again being approximately 1°C too warm and the model salinities being approximately 0.6 psu too salty, both of which are consistent with the SST and SSS discrepancies seen for this time at Chrome Island (Figure A3).
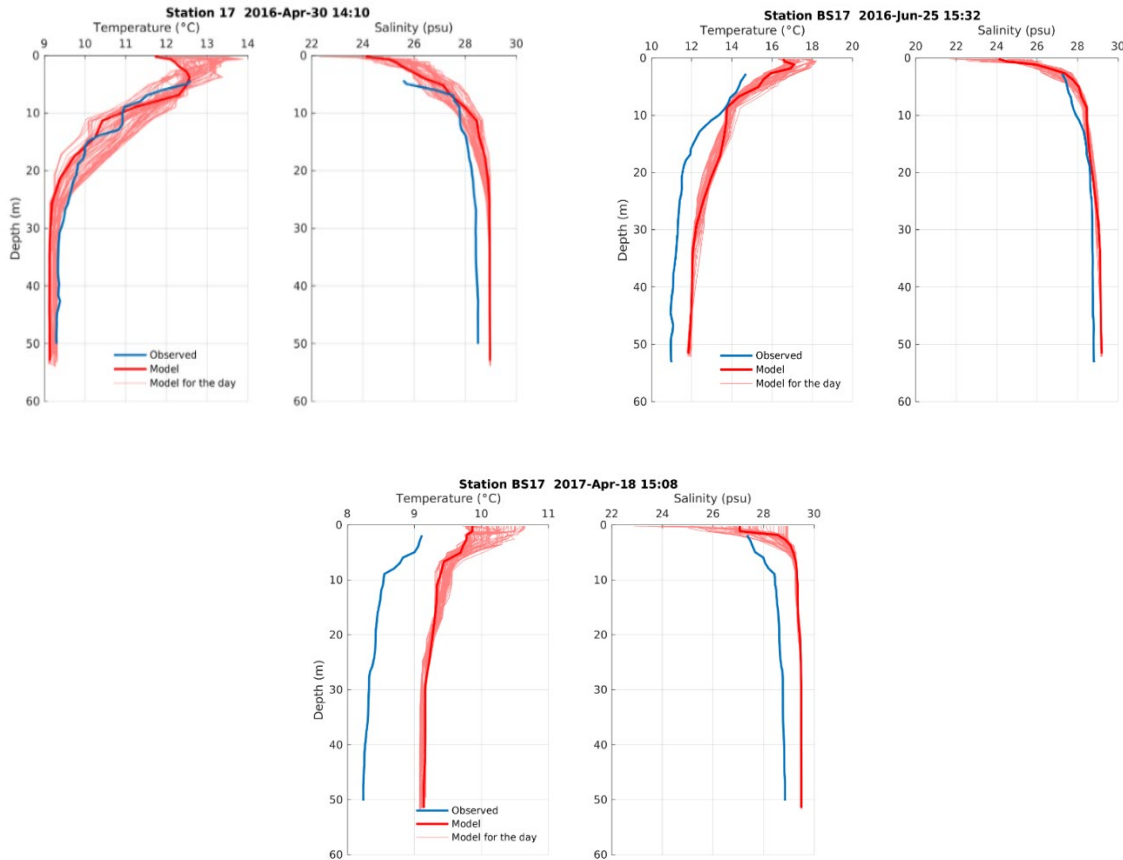
Figure A9: Observed and model temperature and salinity profiles at CTD station BS17 (see Figure A1) for April and June 2016 and April 2017. The thick red lines indicate model values at the time of observation while the thin red lines are at 20 minutes intervals over the day, thus providing an indication of variations over a tidal cycle. Note the different scaling on the x-axes.

Analogous to the daily SST and SSS observations taken at the Chrome Island lighthouse, temperatures and salinities were also observed (with 10 minute sampling and at approximately 5m depth) at five other sites within or near Baynes Sound (see the yellow triangles in Figure A1) for at least part of the model simulation period. As illustrated in Figure A10, there is generally good agreement between the model and observed temperatures, in terms of capturing both actual values and variations in time. However the agreement is uniformly much poorer for the associated salinities (not shown) and much of that can be attributed to bio-fouling of the measurement devices.
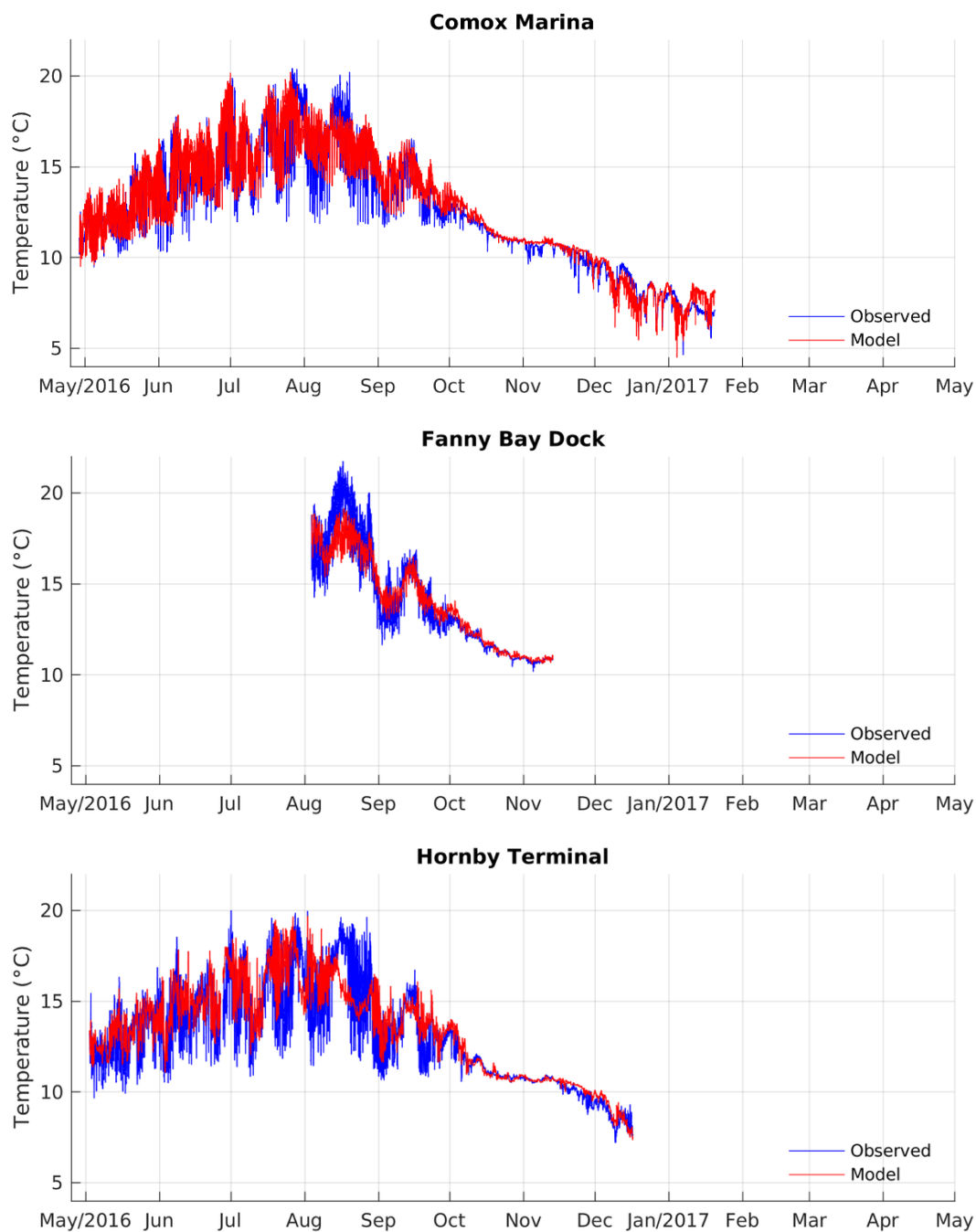
Figure A10: Observed and model temperatures at the five sites shown with yellow triangles in Figure A1. Lucky Seven and Mac's Oysters appear on the next page.
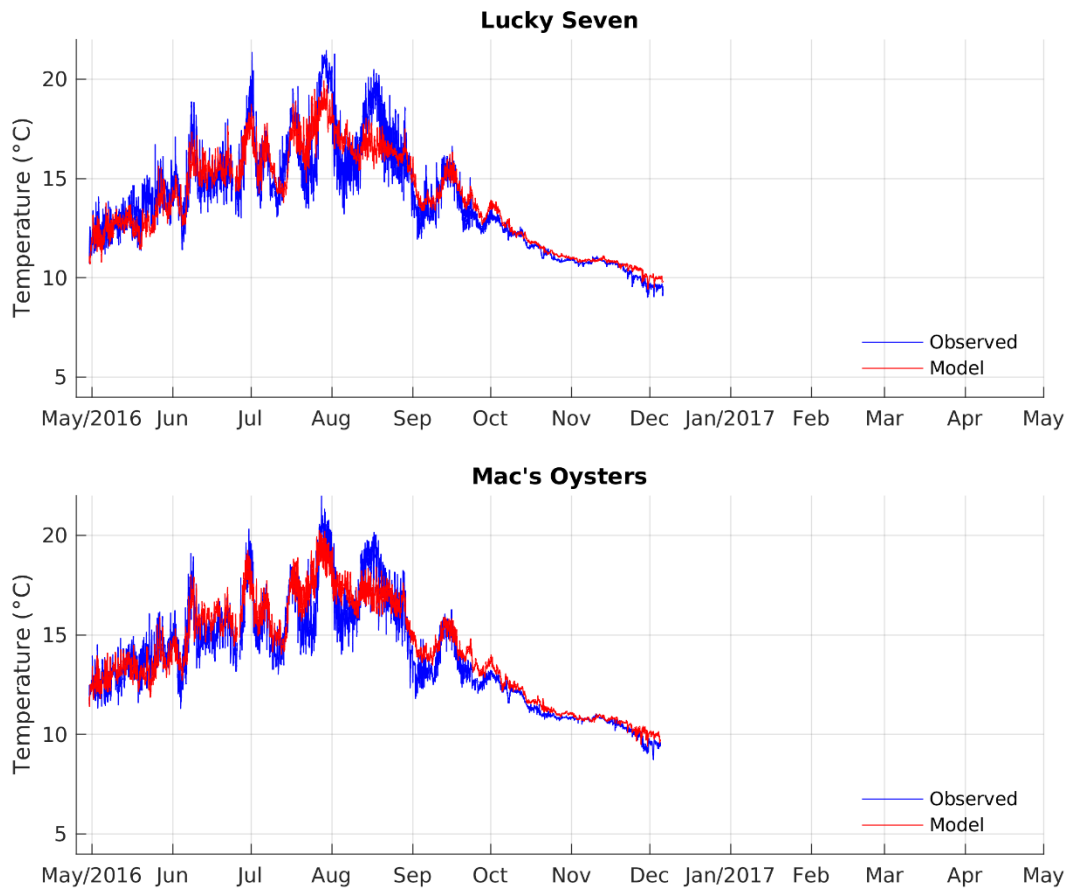
Figure A10 (continued)

Repeating the FVCOM simulation with the Englishman and Little and Big Qualicum Rivers included would have improved the model versus observation salinity comparisons in Figures A3, A8, A9, and perhaps to a lesser degree, the temperature comparisons in those same figures and A10. The salinity and temperature changes arising from this inclusion would also have had some impact of the horizontal and vertical mixing that partially depends on those variables. However incorporating these rivers would have been a significant undertaking, requiring not only refinements to the grid near the river mouths, but also re-aligning all the model forcing fields over the entire model domain. As this was not done, it is uncertain how much difference their addition would have improved (or degraded) aspects of the BiCEM simulations, such as the vertical distribution of phytoplankton. See Appendix C and the main document for further discussion.

8.5.2. Current comparisons

Unfortunately, there are not many current meter observations in Baynes Sound that can be used to evaluate the accuracy of our model currents. Though four ADCPs have been deployed at different times and locations, instrument failures at two made their data largely unusable. The two successful deployments were by Cascadia Coast Research (Clayton Hiles, personal communication, 2014) under contract to BC Ferries for the period of February 25 to April 12, 2012 and, by DFO (in support of this project) in Union Bay for the period of June 15 to August 30, 2016. See Figure A1 for all four locations. Both successful deployments were upward-looking bottom moorings with the first having hourly observations over the range of 38.5 to 1.5m

in 1m intervals, and the second having 5 minute sampling over the depth range of 11.1 to 2.1m in 1m intervals.

Though an ADCP typically measures currents in terms of orthogonal coordinates (e.g., east-west and north-south components), those currents can equivalently be expressed in terms of counter-rotating vectors, one rotating clockwise and the other counter-clockwise. Doing so can be beneficial in providing a better understanding of the underlying dynamics, such as the diurnal shelf waves that are found off the west coast of Vancouver Island (Foreman and Thomson, 1997). The left panel of Figure A11 adopts this convention in displaying the power spectra versus depth for the entire time series of the BC Ferries mooring. The clear vertical band at approximately two cycles per day is due to the semi-diurnal tides while the weaker band around one cycle per day arises from the diurnal tides. However, the most noteworthy feature in both rotary spectra is that most of their energy is in frequencies lower than daily, which would have been forced by variations in a combination of winds, river discharges, and inputs from the SoG. This low frequency energy is seen to be largest near the surface (predominantly from the winds and discharges) and smallest between 20 to 25m depth, which is the interface between the two layers of estuarine flow (outward toward the SoG near the surface and inward from the SoG below) that exist in Baynes Sound. (This estuarine feature will be described in more detail later.)
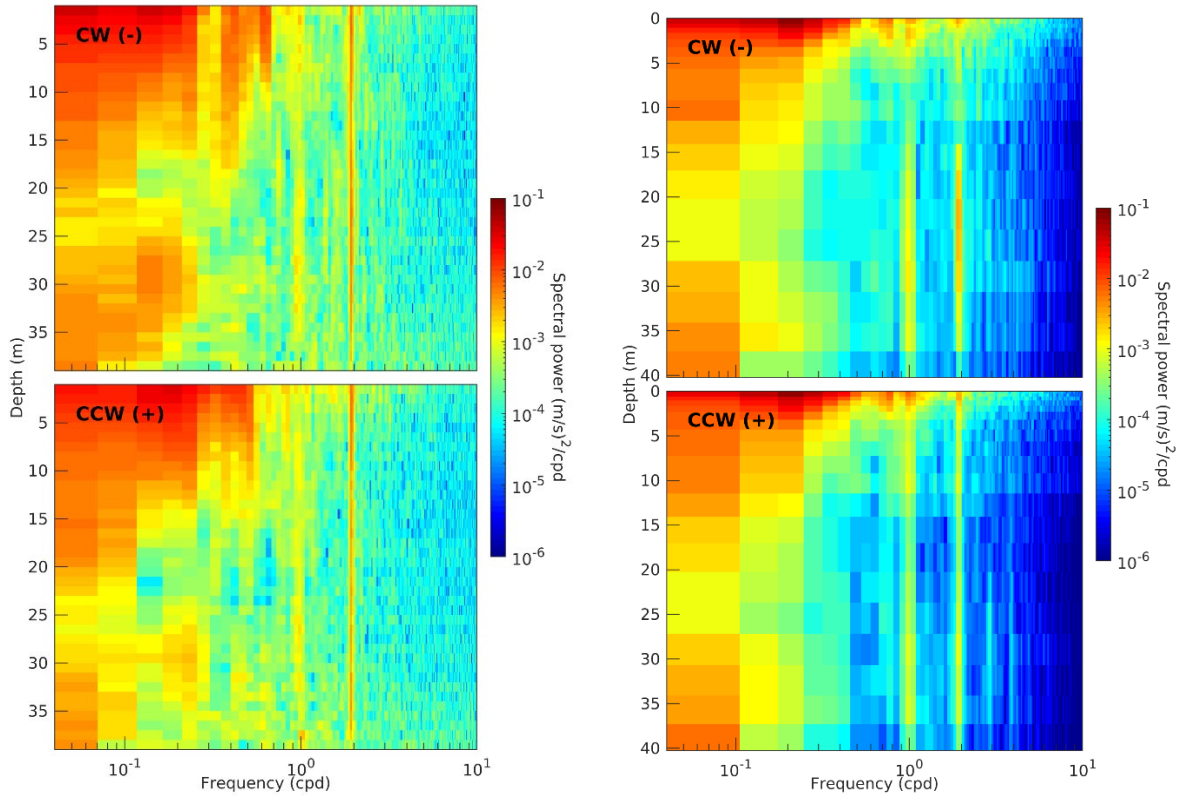
Figure A11: Rotary spectra versus depth at the BC Ferries ADCP mooring location over the period of February 25 to April 12. Left panel is for the observations in 2012 while the right panel is from the model simulation in 2017. CW and CCW denote clockwise and counter-clockwise components, respectively. Note the frequency axis and power colour legend have logarithmic scaling.

The right panel of Figure A11 also displays rotary spectra computed over the period of February 25 to April 12 but for the model simulation in 2017. Acknowledging that there will be differences solely because of the different years, the model spectra do show many of the same features as

those computed from the observations. The model has somewhat more energy near the surface and less energy at higher frequencies. But the relatively small energy in the tides, the much larger energy at low frequencies, and minimal energy in the 20 to 25m depth range indicate the model has done a reasonable job of capturing the current spectra at this location and for this time of the year.

Figure A12 presents a similar comparison for currents at the Union Bay site over the period of June 15 to August 30, 2016. In this case, tides in the left panel are seen to account for a relatively larger proportion of the power and to be larger near the surface. However significant energy still exists at frequencies below daily with more in the model currents than the observed. However because this site is so shallow there is not a two-layer estuarine flow. Mean flows over the observational period (not shown) are toward the north-northeast and range from a maximum of approximately 1.6 cm/s at 4m depth to 0.2 cm/s near the bottom.
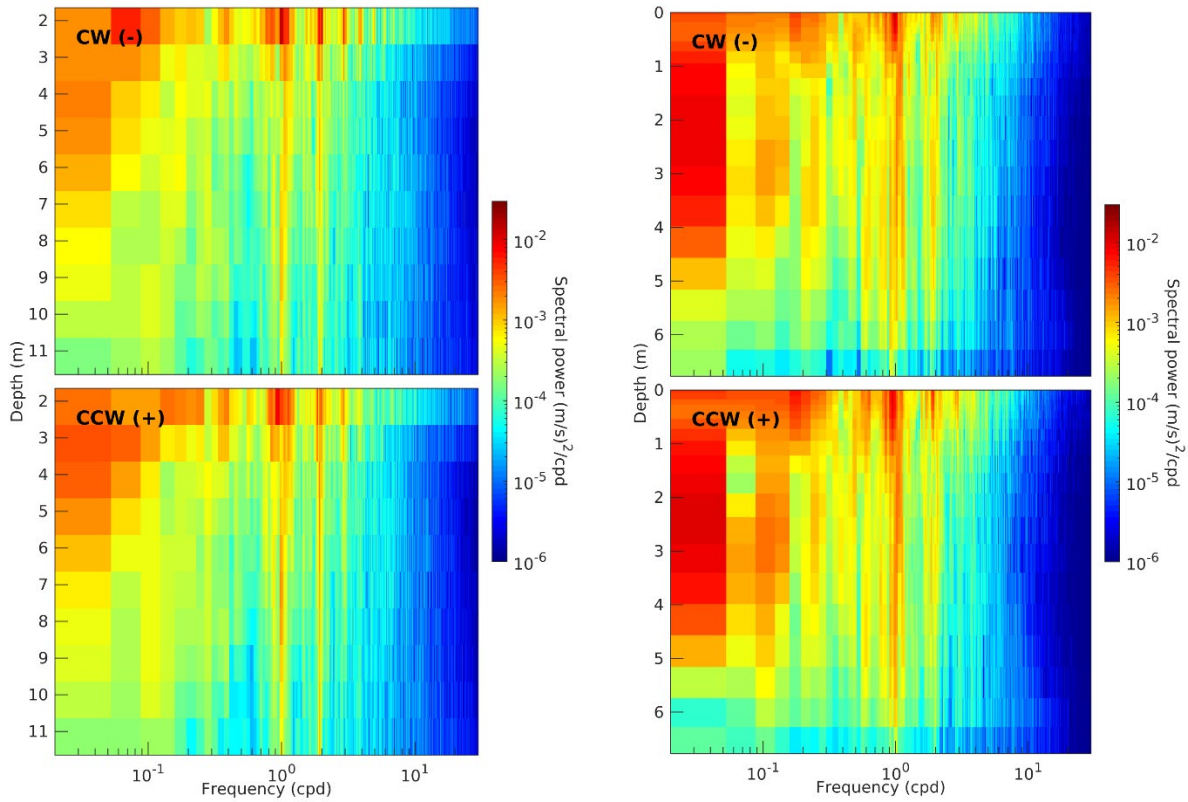
Figure A12: Rotary spectra versus depth at the Union Bay ADCP mooring location over the period of June 15 to August 30, 2016. Left panel, from observations; right panel, from the model simulation. CW and CCW denote clockwise and counter-clockwise components, respectively. Note the frequency axis and power colour legend have logarithmic scaling.

Even though the tides comprise a relatively small proportion of the total current energy at the BC Ferries site, traditional harmonic tidal analyses were performed to compute the observed and model current ellipses over the water column. (As the current vector for each tidal constituent traces out an elliptical pattern over its period, the ellipse parameters (major and minor axes lengths, orientation, and vector position at the time of maximum tidal potential forcing) provide a commonly used framework for characterizing tidal currents.) The left-most column of Figure A13 shows how the observed M2 (top) and K1 (bottom) ellipses vary with depth. (Note that due to acoustic contamination, observations are not reliable near the surface

so the uppermost values only go to 2m depth.) However as tidal currents can vary seasonally, the next four columns show analogous ellipses arising from harmonic analyses of the model currents, specifically for the periods of JFM 2017, MJ 2016, JAS 2016 and OND 2016.
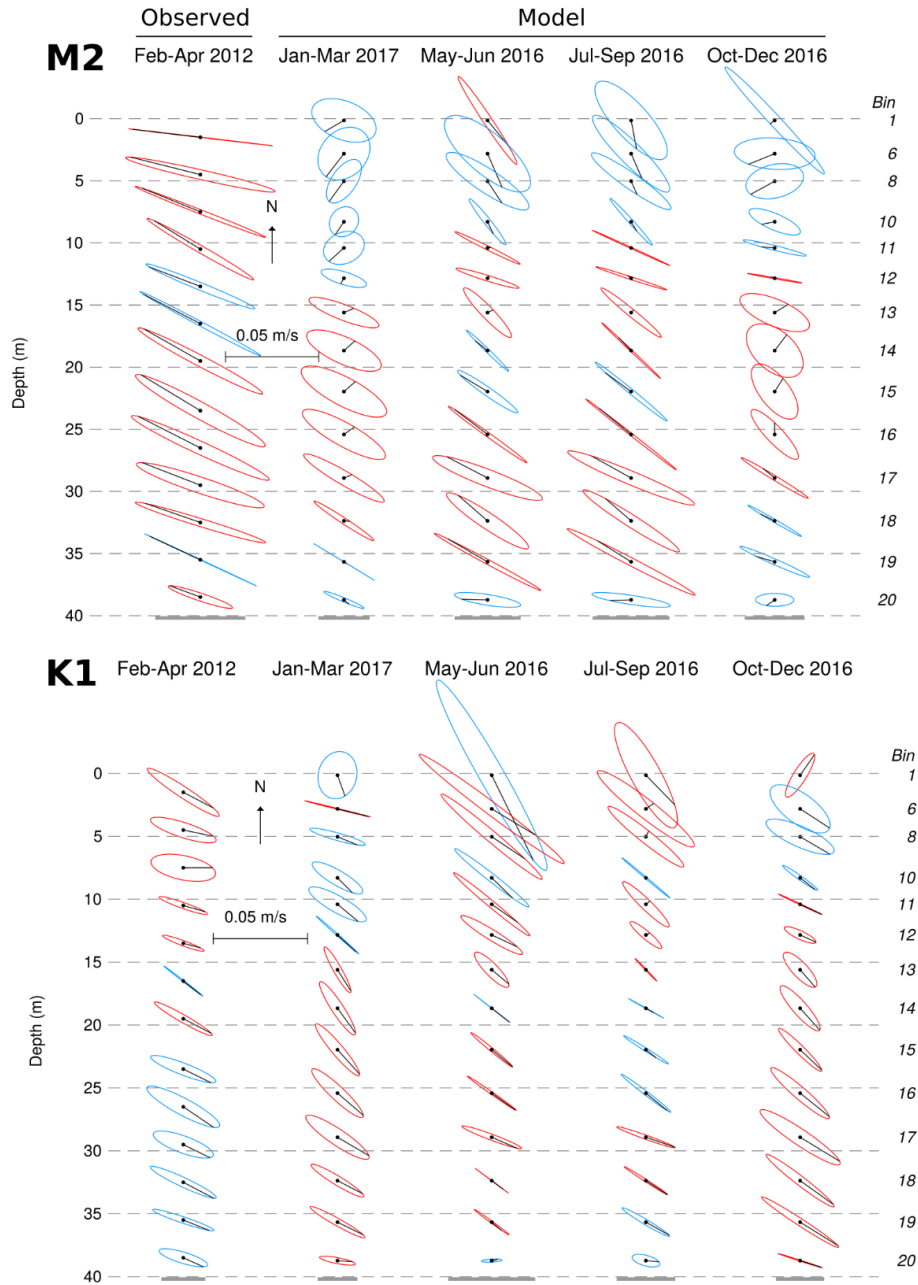
Figure A13: Ellipses versus depth at the BC Ferries ADCP location: upper panel for M2 and lower panel for K1. The left-most column was computed from the observations over the period of Feb 25 to Apr 12, 2012 while the next four columns were computed from the model currents for the respective periods of JFM2017, MJ2016, JAS2016, and OND2016. Blue ellipses denote vectors that are rotating counterclockwise while red ellipses denote clockwise rotation.

The K1 observed and model ellipses are generally seen to have similar eccentricity, orientation (both roughly aligned with the main axis of Baynes Sound), and magnitudes. Though the sense

of rotation of the current vector within each ellipse often differs, this is only an important issue when the minor axes are large relative to the major, which is generally not the case here. However, the considerable variation among the model phase lags (as designated by the black lines within each ellipse) is indicative of seasonal variations in ebb/flood timing associated with this constituent. The season with ellipses closest to those observed is JFM2017.

However, agreement between the model and observed M2 ellipses is not as good. The best agreement appears to be with the JAS2016 values when both sets of ellipses are reasonably consistent over the water column (i.e., barotropic). Considerable variations over the water column for the JFM model ellipses (i.e., baroclinic) suggest that horizontal and vertical gradients in water density (e.g., salinity and temperature) were different in 2012 than 2017. Unfortunately no CTD surveys were taken in April 2012 but Figure A6 does show that salinities in April 2017 (and presumably JFM 2017) were fresher than normal. Though the Puntledge River discharges were comparable for JFM in 2012 and 2017 (not shown), the Fraser River discharges for JFM 2012 (also not shown) were considerably smaller than those for 2017. So it is reasonable to conclude that near surface water entering Baynes Sound from the SoG in 2012 was more saline and thus more likely to produce the barotropic ellipses seen in the left-most column of Figure A13. A figure similar to A13 but for the ADCP at Union Bay has not been shown because model bathymetry has been significantly modified (smoothed) near the deployment location to ensure numerical stability of the simulation thus changing the local flow regime and preventing fair comparison between the model and observed currents.

8.5.3. Sea surface elevation comparisons

As a proxy for assessing the accuracy of the tidal elevations within the model, Table A2 compares observed and model amplitudes and phases (harmonics) for the five constituents specified in the model boundary forcing. The semi-diurnal and diurnal constituents have periods around twelve and twenty-four hours respectively, with the largest, M2 and K1, having periods of 12.42 and 23.93 hours respectively. This comparison is done at five tide gauge stations (Figure A2a) within the model domain and with the model values calculated from the simulation that included wetting-and-drying mudflats in the FVCOM dynamics (shorter simulation without wetting-and-drying showed little change to the model harmonics). The observed harmonics were taken from Canadian Hydrographic Services data bases and are based on analyses of historical data, as none of these sites were active during the model simulation period. The closest active sites are Campbell River and Point Atkinson, both of which are just outside our model domain. Though the model amplitudes are consistently within 2 cm of their observed counterparts, some of the associated phase differences are as large as 10.9°. (Note, for semi-diurnal constituents a 5° phase difference translates to high/low water being out by approximately 10 minutes while for the diurnals, a 5° difference translates to a 20 minute error). This is because boundary forcing for the M2 and K1 constituents were taken directly from Foreman et al. 2004, while analogous values for constituents S2, N2, and O1 were estimated using amplitude ratios and phase differences based on harmonic analysis results for the Comox tide gauge. Though further refinements could have been applied to improve their accuracy, this was not done as it was felt they would have only very minor impact on the subsequent BiCEM simulations. Though the results are not shown here, a sensitivity run with no wetting and drying of the mudflats (i.e., a minimum depth was set so that mudflats never became dry) made little difference to the model accuracy. This indicates that even though there are extensive mudflats in Baynes Sound, unlike the Bay of Fundy, they play a minor role in the overall regional tidal dynamics.

Table A2: Comparison of observed and model amplitudes (m) and phases (degrees) at five tide gauge locations (Figure A2a) within the model domain. RMS values were calculated using equation 3 in Cummins and Oey (1997).

Station	Consti-tuent	Observed		Model					
						Discrepancy with obs		RMS	
		Amp	Phase	Amp	Phase	Amp	Phase	Abs	Rel (%)
Comox	O1	0.489	264.6	0.484	272.8	0.005	-8.1	0.049	10.0
	K1	0.885	287.5	0.878	286.9	0.007	0.6	0.008	0.9
	N2	0.220	7.7	0.222	11.5	-0.002	-3.8	0.010	4.7
	M2	1.002	33.9	1.009	33.2	-0.008	0.7	0.010	1.0
	S2	0.253	62.6	0.256	53.8	-0.003	8.8	0.028	10.9
Little River	O1	0.496	263.6	0.484	272.6	0.012	-8.9	0.055	11.0
	K1	0.895	288.0	0.877	286.8	0.018	1.2	0.018	2.0
	N2	0.216	3.5	0.220	10.4	-0.004	-7.0	0.019	8.8
	M2	0.984	33.8	1.002	32.2	-0.018	1.6	0.023	2.4
	S2	0.250	63.8	0.254	52.9	-0.004	10.9	0.034	13.6
Hornby Island	O1	0.469	267.6	0.483	272.5	-0.014	-5.0	0.031	6.5
	K1	0.881	288.9	0.875	286.6	0.006	2.3	0.025	2.8
	N2	0.228	10.7	0.219	11.1	0.009	-0.4	0.007	2.9
	M2	0.982	36.5	0.994	32.8	-0.013	3.7	0.046	4.7
	S2	0.262	65.6	0.253	53.5	0.010	12.2	0.039	15.0
Irvines Landing	O1	0.483	263.8	0.484	271.9	0.000	-8.1	0.048	10.0
	K1	0.892	286.4	0.878	285.9	0.014	0.5	0.011	1.3
	N2	0.213	5.5	0.218	10.7	-0.005	-5.2	0.014	6.7
	M2	0.987	32.3	0.992	32.5	-0.005	-0.2	0.004	0.4
	S2	0.248	61.4	0.252	53.2	-0.004	8.2	0.026	10.3
Saltery Bay	O1	0.481	264.7	0.487	272.3	-0.006	-7.5	0.045	9.4
	K1	0.873	287.7	0.883	286.4	-0.011	1.3	0.016	1.8
	N2	0.226	5.7	0.223	11.4	0.003	-5.6	0.016	7.0
	M2	0.996	32.9	1.014	33.1	-0.018	-0.2	0.013	1.3
	S2	0.244	63.1	0.258	53.9	-0.014	9.2	0.030	12.4

8.6. VOLUME FLUXES IN/OUT OF BAYNES SOUND

The FVCOM currents produced over our yearly simulation can be used to estimate seasonal volume fluxes into and out of Baynes Sound. Figure A14 shows average velocity profiles along transects (Figure A2b) crossing the northern and southern entrances to the Sound for the four seasons: spring (April-May-June), summer (July-August-September), fall (October-November-December), and winter (January-February-March). Table A3 quantifies the associated volume fluxes (including a partition of outflow versus inflow along with the combination) and includes river input so that overall balances can be estimated. (Note that the incoming/outgoing fluxes do not perfectly add to the combined values because slightly different approaches were used in their respective calculations). Two layer estuarine flows (outflow at the surface, inflow at depth) are consistently seen at the southern entrance and in the northern (deeper) portion of the northern entrance. Note that the large outgoing volume flux at the northern entrance is generally

restricted to the top 5 m (approx.), while at the southern entrance it is between the top 5m and 35m. Sloping of the 2-layer system at the southern entrance is due to the Coriolis force wherein flows are pushed to their "right" in the northern hemisphere and to the "left" in the southern hemisphere. Similar slopes are also seen in the two layer flows in Juan de Fuca Strait and Queen Charlotte Strait.
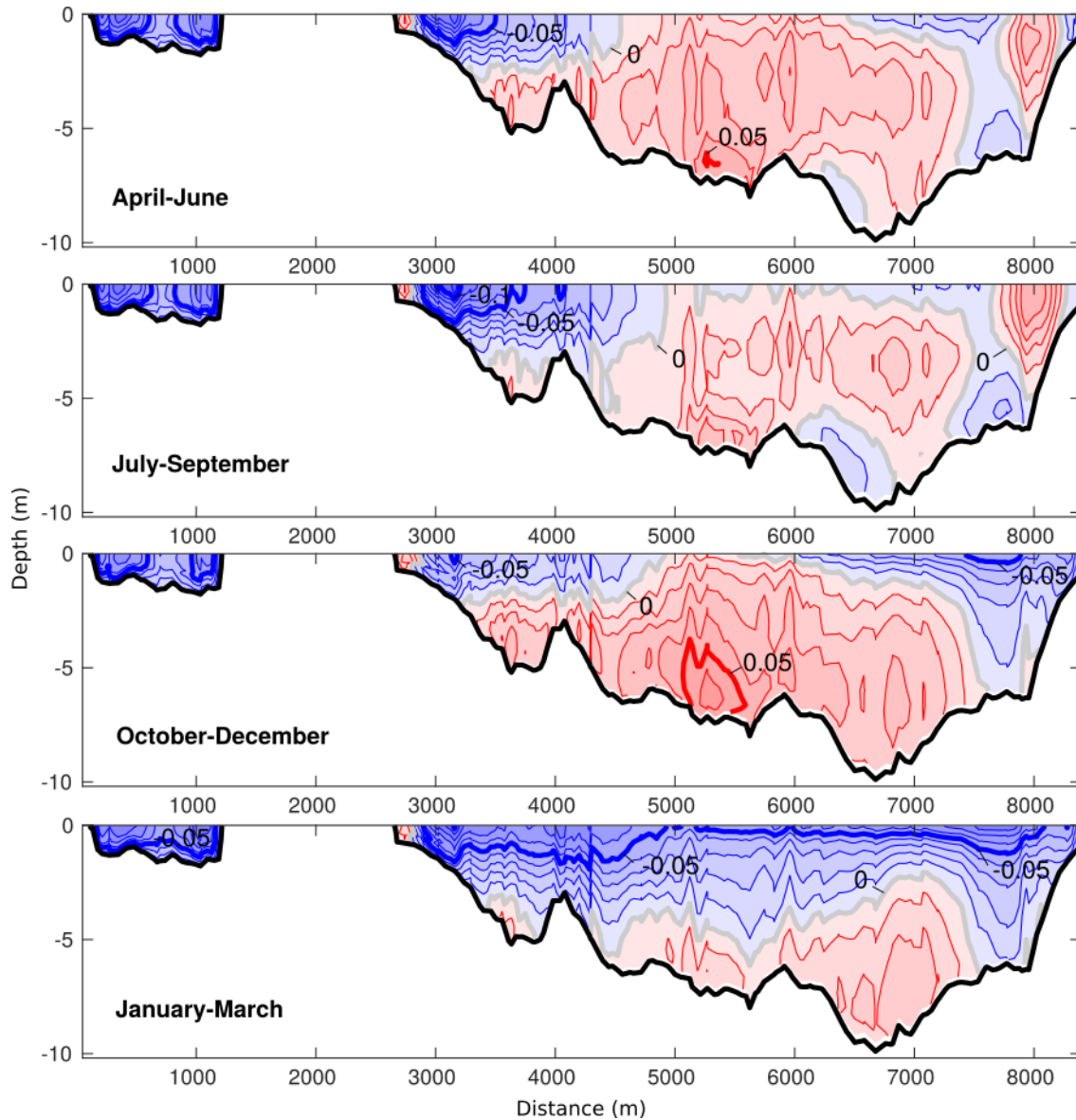
Figure A14: Average seasonal velocity profiles across transects at the northern (top four panels) and southern (bottom four panels) entrances to Baynes Sound (see Figure A2b for transect locations). Red= incoming, blue= outgoing, y-axis is depth (m), x-axis is transect distance (m), measured from Denman Island for the northern transect and from Vancouver Island for the southern transect.
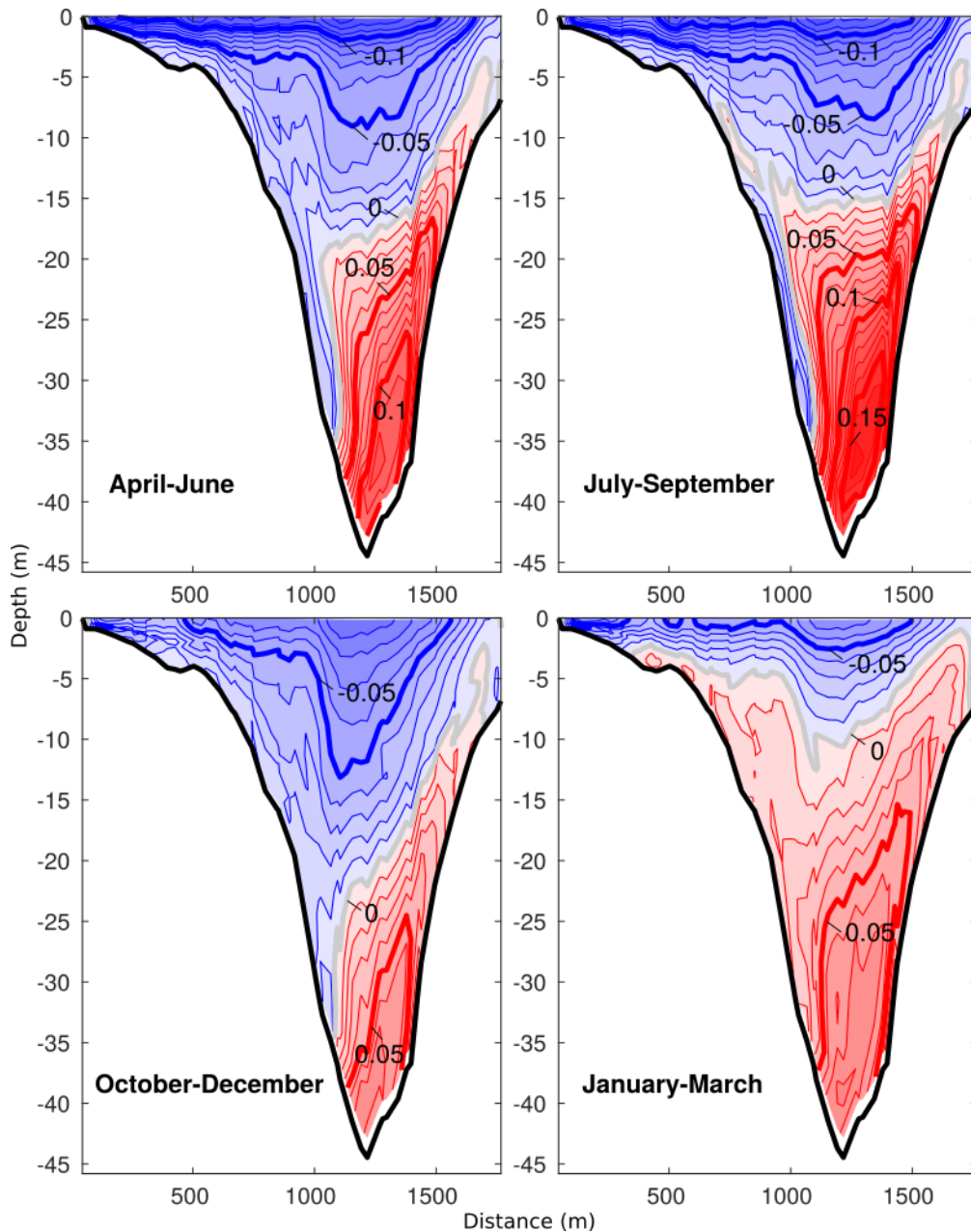
Figure A14 (continued)

The relative magnitude of outflow versus inflow is seen (Table A3) to not only fluctuate seasonally, but also between the two passages; i.e., one entrance is not consistently the conduit for inflow or outflow (Note that the volume transport estimates have been filtered to remove the tides). Except inflow in the fall and outflow in the winter, the larger fluxes are seen to be via the southern entrance. The relatively small, and consistently negative, seasonal imbalances can likely be attributed to a combination of i) model velocity output being 20-minute snapshots rather than averages over each time interval, ii) the FVCOM numerics not conserving volume perfectly, and iii) averaging errors arising when calculating the volume flux.

Table A3: Average seasonal volume transports (m³/s) crossing the northern and southern entrances to Baynes Sound, and estimated balances corresponding to the velocities shown in Figure A14. AMJ = April, May, June; JAS = July, August, September; OND = October, November, December; JFM = January, February, March.

Season	North			South			Rivers	Balance
	inflow	outflow	net	inflow	outflow	net		
AMJ	545	-321	224	566	-870	-304	67	-13
JAS	277	-393	-116	827	-757	70	33	-14
OND	646	-270	376	305	-778	-473	84	-13
JFM	177	-693	-516	690	-267	423	80	-12
Year	412	-418	-6	596	-670	-73	66	-13

8.7. WATER RENEWAL TIME

In the context of carrying capacity assessments for shellfish aquaculture, water renewal or flushing is a key feature of coastal ecosystems providing an indication of the hydrodynamic capacity of the system to renew shellfish food through exchange and mixing. FVCOM outputs were combined with a passive numerical tracer available through BiCEM's scheme to compute the spatial distribution of water renewal time (WRT) over BS following Koutitonsky et al. (2004). In brief, a passive tracer was introduced with an initial concentration C = 1 (arbitrary units) within BS, C = 0 everywhere else and forced to C = 0 at the river and open boundaries. This tracer was then transported and exchanged following the same advection-dispersion scheme as for temperature/salinity. Any location within BS was deemed renewed when the tracer concentration fell below 1/e (~ 37%) of its initial value (e-folding renewal time). Hence, the WRT corresponds to the time needed for the water initially located at a specific location within the Sound's 3D space to be renewed by water coming from the outside, i.e. either from the SOG or from river run-off. Figure A15 presents the WRT distribution in both the surface and bottom layers of the BS model. Overall WRT estimates in the 10 – 16 d range are consistent with the 15.8 d value reported by Hay and Co (2003) using a similar method but integrated through space. Although the WRT is influenced by the conditions prevailing at the time of the beginning of the simulation (1 May 2016), it can still provide insight in the main water circulation characteristics of BS. The surface layer results show the limited influence of the Courtenay river discharge and a fortiori of smaller rivers. Moreover, WRT tends to increase from south to north in both the surface and bottom layers, which is consistent with the southern entrance showing the largest net exchange on a yearly basis, although this situation fluctuates on a seasonal-scale (Table A3). This result and the generally shorter WRT in the bottom layer highlight the importance of the two-layered estuarine circulation mentioned in the previous section for the overall BS water circulation and renewal.
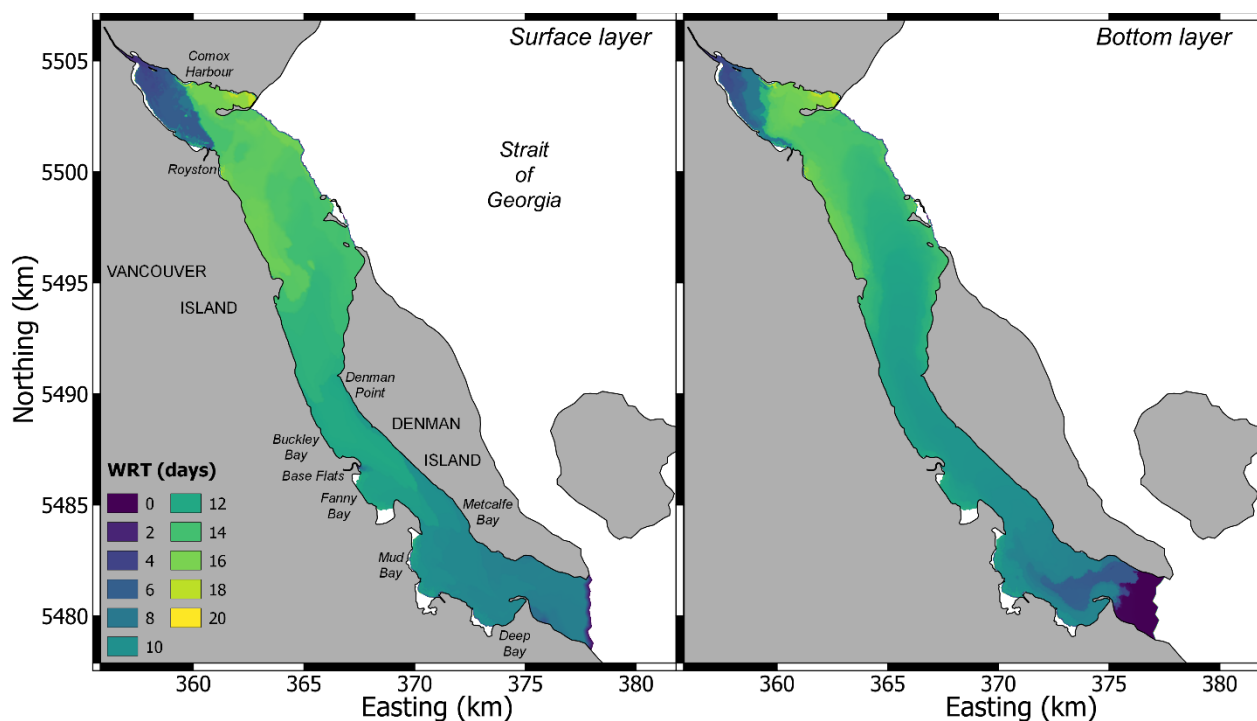
Figure A15: Spatial distribution of water renewal time (WRT) in the surface (left) and bottom (right) layers of Baynes Sound.

8.8. ACKNOWLEDGMENTS

8.9. REFERENCES

Barnes, P. 2007. Shellfish culture and particulate matter production and cycling: Field data report. Prepared for: B.C. Aquaculture Research and Development Committee. pp. 290.

Burchard, H. Bolding, K., and Villareal, M.R. 1999. GOTM—a general ocean turbulence model. Theory, applications and test cases. Technical Report EUR 18745 EN, European Commission. 101 p.

Chen, C., Liu, H., and Beardsley, R.C. 2003. An unstructured, finite-volume, three-dimensional, primitive equation ocean model: application to coastal ocean and estuaries. J. Atmos. Ocean. Technol. 20 (1): 159-186.

Chen, C., Cowles, G., and Beardsley, R.C. 2004. An unstructured grid, finite-volume coastal ocean model: FVCOM User Manual. SMAST/UMASSD Technical Report-04-0601.

Chen, C., Beardsley, R.C., and Cowles, G. 2006a. An unstructured grid, finite-volume coastal ocean model (FVCOM) system. Oceanogr. Spec. Iss. on Advanc. in Computat. Oceanogr. 19 (1): 78-89.

Chen, C., Beardsley, R.C., and Cowles, G. 2006b. An unstructured grid, finite-volume coastal ocean model. FVCOM user manual.

Chen, C., Xu, Q., Houghton, R., and Beardsley, R.C. 2008. A model-dye comparison experiment in the tidal mixing front zone on the southern flank of Georges Bank, J. Geophys. Res. 113, C02005. doi:10.1029/2007JC004106.

Cummins, P.F., and Oey, L.Y. 1997. Simulation of barotropic and baroclinic tides off northern British Columbia J. Phys. Oceanogr. 27 (5): 762-781.

DFO (Fisheries and Oceans Canada), 2019. Aquaculture Production Quantities and Values.

Foreman, M.G.G., and Thomson, R.E. 1997. Three-dimensional model simulations of tides and buoyancy currents along the west coast of Vancouver Island, J. Phys. Oceanogr. 27:1300-1325.

Foreman, M.G.G., Sutherland, G., and Cummins, P.F. 2004. M_2 tidal dissipation around Vancouver Island: An inverse approach. Cont. Shelf Res. 24 (18): 2167-2185.

Foreman, M.G.G., Stucchi, D.J., Garver, K.A., Tuele, D., Isaac, J., Grime, T., and Guo, M. 2012. A circulation model for the Discovery Islands, British Columbia. Atmosphere-, 50 (3): 301-316.

Foreman, M.G.G., Chandler, P.C., Stucchi, D.J., Garver, K.A., Guo, M., Morrison, J., and Tuele, D. 2015. The ability of hydrodynamic models to inform decisions on the siting and management of aquaculture facilities in British Columbia. DFO Can. Sci. Advis. Sec. Res. Doc. 2015/005. vii + 49 p.

Haney, R.L. 1991. On the pressure gradient force over steep topography in sigma coordinate ocean models. J. Phys. Oceanogr. 21 (4): 610-619.

Hannah, C.G., and Wright, D.G. 1995. Depth dependent analytical and numerical solutions for wind-driven flow in the coastal ocean. Lynch, D.R., Davies, A.M. (Eds.), In: Quantitative skill assessment for coastal ocean models, coastal and estuarine studies. Americ. Geophys. Union, Washington, pp. 125-152.

Hay and Company Consultants. 2001. Productive Capacity Study of Gorge Harbour, BCSC.001, British Columbia Science Council. 23 p.

Hay and Company Consultants. 2003. Baynes Sound Carrying Capacity Study Technical Report, MAFF.001, Ministry of Agriculture, Food and Fisheries, Ministry of Sustainable Resource Management and Environment Canada, Environmental Protection, Pacific and Yukon Region. vii + 24 p.

Koutitonsky V., Guyondet T., St-Hillaire A., Courtenay S.C., and Bohgen A.D. 2004. Water renewal estimates for aquaculture developments in the Richibucto Estuary, Canada. Estuaries, 27 (5): 339-350.

Madec, G., and the NEMO team. 2015: NEMO ocean engine, *Note du Pole de modélisation*, Institut Pierre-Simon Laplace (IPSL), France, No. 27, Ver 3.6, ISSN No 1288-1619.

Mellor, G.L., and Yamada, T. 1982. Development of a turbulent closure model for geophysical fluid problems. Rev. Geophys. Space Phys. 20: 857–875.

Mellor, G.L., Ezer, T., and Oey, L.-Y. 1994. The pressure gradient conundrum of sigma coordinate ocean models. J. Atmosph. Ocean. Technol. 11 (4 part 2): 1126-1134.

Morrison, J., Quick, M.C., and Foreman, M.G.G. 2002. Climate change in the Fraser watershed: Flow and temperature predictions. J. Hydrol. 263: 230-244.

Morrison,J., Callendar, W, Foreman, M.G.G., Masson, D., and Fine, I.V. 2014. A model simulation of future oceanic conditions along the British Columbia continental shelf. Part 1: Forcing fields and initial conditions. Atmosphere-Ocean. doi:10.1080/07055900.2013.868340.

Page, F., Chang, B.D., Beattie, M., Losier, R., McCurdy, P., Bakker, J., Haughn, K., Thorpe, B., Fife, J., Scouten, S., Bartlett, G., and Ernst, B. 2014. Transport and dispersal of sea lice bath therapeutants from salmon farm net-pens and well-boats operated in Southwest New Brunswick: a mid-project perspective and perspective for discussion. DFO Can. Sci. Advis. Sec. Res. Doc. 2014/102. v + 63 p.

Ratsimandresy, A.W., Donnet, S., and Goulet, P. 2020. Identification of geographic zones of influence associated with surface circulation for Aquaculture Bay Management Area application. J. Mar. Syst. 204: 103291.

Richardson, J,, and Newell, C. 2002. Building a model for sustainable west coast shellfish aquaculture production; Productive capacity study of Gorge Harbour, Cortes Island, B.C. Prepared for British Columbia Shellfish Growers Association. pp.38.

Smagorinsky, J. 1963. General circulation experiments with the primitive equations, I. The basic experiment, Mon. Weather Rev. 91: 99–164.

Stronach, J.A., Backhaus, J.O., and Murty, T.S. 1993. An update on the numerical simulations of oceanographic processes in the waters between Vancouver Island and the mainland: the GF8 model. Oceanogr. Mar. Biol. Ann. Rev. 31: 1-86.

Umlauf, L., and Burchard, H. 2003. A generic length-scale equation for geophysical turbulence models. J. Mar. Res. 61(2): 235-265.

Wu, Y., Chaffey, J., Law, B., Greenberg, D.A., Drozdowski, A., Page, F., and Haigh, S. 2014. A three-dimensional hydrodynamic model for aquaculture: a case study in the Bay of Fundy. Aquac. Env. Int. 5: 235-248. doi: 10.3354/aei00108.

9. APPENDIX B. DYNAMIC ENERGY BUDGET (DEB) PARAMETERIZATION FOR THE OYSTER, *CRASSOSTREA GIGAS*

9.1. INTRODUCTION

Over the last decade, Dynamic Energy Budget (DEB, Kooijman 2010) has become the most cutting-edge theory on the organization of metabolism of any individual organism, most extensively applied to the kingdom Animalia, and with *Mytilus edulis* being the most modelled species. Actually, most ecosystem models tackling bivalve aquaculture use DEB models to represent the bivalve component (e.g. Guyondet et al. 2010, Filgueira et al. 2014, Pete et al. 2020). DEB describes the flow of energy within the organism using three state variables: reserve(s), structure, and maturity/reproduction (Figure B1), and allows for the simulation of the whole life-cycle of the organism. A brief description of the model is presented in Table B1 and a more thorough presentation of the model and the equations are given in Pouvreau et al. (2006) and Rosland et al. (2009). Although the core structure of DEB is similar for all species, the parameters are species-specific. In addition, the forcing is also species-dependent. In the case of bivalves cultured in marine waters, forcing can be simplified to temperature and a proxy for food availability, commonly chlorophyll concentration. Although DEB is a mechanistic theory, local calibration of the model is usually required given the difficulty of defining a good proxy for food availability (Larsen et al. 2014). Accordingly, an oyster growth experiment has been carried out with the ultimate goal of parameterizing the juvenile-adult stages of the oyster DEB component of BiCEM for Baynes Sound.
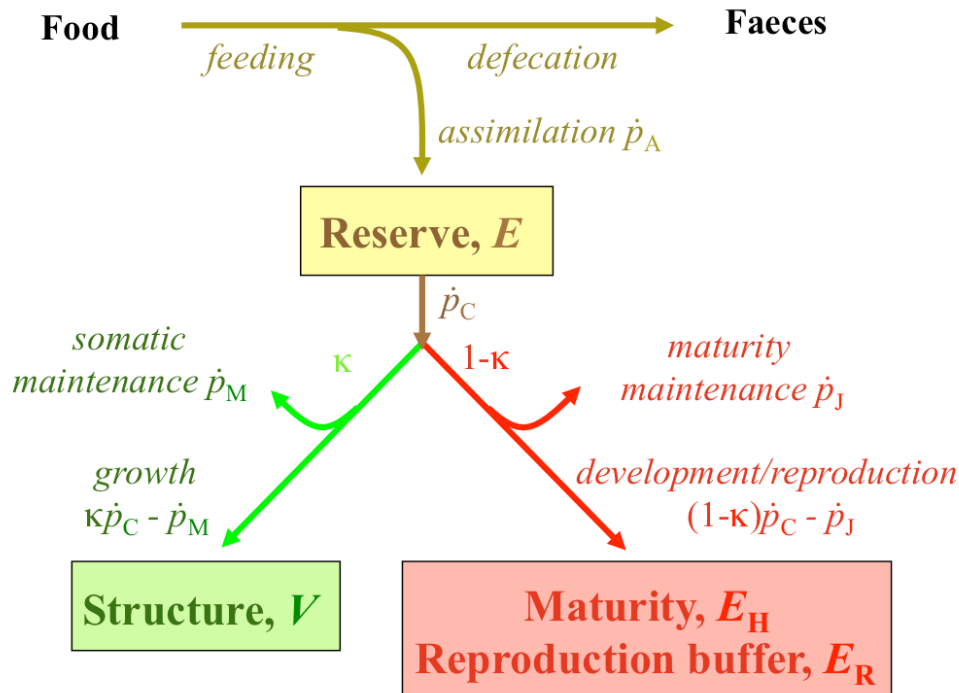
Figure B1: Dynamic Energy Budget (DEB) model scheme for juvenile (development/maturity) and adult (reproduction/reproduction buffer) life stages. See Table B1 for differential equations.

Table B1: Equations of the Dynamic Energy Budget (DEB) model. The description of the model follows the original notation by Kooijman (2010), in which [ ] denote quantities expressed as per unit structural volume, { } denote quantities expressed as per unit surface area of the structural volume and a dot over a symbol denotes a rate, or a dimension per time.

Equation	Terms and parameters	
$\dfrac{dE}{dt} = \dot{p}_A - \dot{p}_C$	E	Reserve (J)
	$\dot{p}_A$	Assimilation rate (J d^{-1})
	$\dot{p}_C$	Mobilization rate of reserve energy (J d^{-1})
$\dot{p}_A = \{\dot{p}_{Am}\} T_D f V^{2/3}$	$\{\dot{p}_{Am}\}$	Maximum surface-area-specific assimilation rate (J cm^{-2} d^{-1})
	f	Functional response
	V	Structural volume (cm^3)
	T_D	Arrhenius temperature function
$f = \dfrac{X}{X + X_K}$	X	Chlorophyll concentration (µg l^{-1})
	X_K	Half-saturation constant (µg l^{-1})
	κ	Fraction of utilized energy to somatic maintenance and growth
$\dot{p}_C = \dfrac{[E]}{[E_G]+\kappa[E]}\left(\dfrac{[E_G]\{\dot{p}_{Am}\}T_D V^{2/3}}{[E_m]}+\dot{p}_M\right)$	$[E_G]$	Volume-specific costs for structure (J cm^{-3})
	$[E_m]$	Maximum energy density (J cm^{-3})
$\dot{p}_M = [\dot{p}_M] T_D V$	$\dot{p}_M$	Maintenance rate (J d^{-1})
	$[\dot{p}_M]$	Volume-specific maintenance costs (J cm^{-3} d^{-1})
$\dfrac{dV}{dt} = \left(\kappa\,\dot{p}_C - \dot{p}_M\right)/[E_G]$	-	-
$\dfrac{dE_R}{dt} = (1-\kappa)\dot{p}_C - \left(\dfrac{1-\kappa}{\kappa}\right)\cdot V\cdot[\dot{p}_M]$	E_R	Energy allocated to reproduction buffer (J)
$\dfrac{dE_R}{dt} = \kappa\,\dot{p}_C - \dot{p}_M \mid \kappa\,\dot{p}_C - \dot{p}_M < 0$	-	Reproduction buffer dynamics when energy storage is too low

Equation	Terms and parameters	
$L = \dfrac{V^{1/3}}{\delta_M}$	L	Filter-feeder length (cm)
	δ_M	Dimensionless shape coefficient
	T_A	Arrhenius temperature (degrees Kelvin, K)
$T_D = \exp\left(\dfrac{T_A}{T_1} - \dfrac{T_A}{T}\right) \times s(T)/s(T_1)$	$T1$	Reference temperature (K)
	T	Absolute temperature (K)
$s(T) = \left(1 + \exp\left(\dfrac{T_{AL}}{T} - \dfrac{T_{AL}}{T_L}\right)\right.$	T_L	Lower tolerance range (K)
$\left. + \exp\left(\dfrac{T_{AH}}{T_H} - \dfrac{T_{AH}}{T}\right)\right)^{-1}$	T_H	Upper tolerance range (K)
	T_{AL}	Physiological rate decrease at T_L (K)
	T_{AH}	Physiological rate decrease at T_H (K)

9.2. METHODS

The parameterization of a model can be done by directly measuring the parameters with specific experiments, by using mathematical tools, or by a combination of both. In this study, the parameterization has been carried out using a mathematical tool based on the generation of 100,000 randomized sets of parameters followed by the analysis of the agreement between observations and simulations using those sets of parameters (e.g. Duarte et al. 2010, Sonier et al. 2016). The randomized sets of parameters were calculated from a pre-defined range of values from existing oyster DEB models, with the exception of kappa, whose range was extended to 0.35 based on preliminary runs of the model (Table B2). Spawning was parameterized to be triggered when temperature reached 20°C and the gonadosomatic index 39% (Pouvreau et al. 2006); however, these conditions were not met during the simulations. The set of parameters that produced the best fit was defined as the smallest deviation (D) between simulated and observed values calculated, following:

$$D = \frac{1}{N}\sum_{n=1}^{N}\left(\frac{1}{J}\sum_{j=1}^{J}\frac{|M_s(j) - M_o(j)|}{M_o(j)}\right)$$

where n is the dataset index, N the total number of datasets, j the observation index for a given dataset, J the total number of observations for a given dataset, and M_s and M_o are simulated and observed values, respectively. In this case, M_s and M_o include values of shell length and tissue dry weight.

Table B2: Crassostrea gigas *DEB parameters.*

Parameter	Data source		
	Bernard et al. 2011	Ren and Schiel 2008	Calibration (this study)
δ_M	0.175	0.21	0.190
$\{\dot{p}_{Xm}\}$	1027	894	995
$[\dot{p}_M]$	44	22.5	23.0
$[E_G]$	3900-7500[1]	2900	5259
$[E_m]$	4200	5900	5691
κ	0.45	0.65	0.61
X_K	calibration	1.9	0.22
T_A	5800	5900	5863
T_L	281	283	281
T_H	298	303	302
T_{AL}	75000	13000	72977
T_{AH}	30000	80000	73844
AE	0.75	0.75[3]	0.75
DW:WW	0.15-0.31[2]	0.2	0.165

[1]3900-7500 cost for structure and gonads, respectively

[2]0.15-0.31 for structure and gonads, respectively

[3]assumed

After calibration, a sensitivity test was carried out by increasing and decreasing by 10% each of the 14 parameters considered in the model. The impact of the change of each parameter on shell length (SL), dry weight (DW), dry weight minus gonads (DWmG), clearance rate (CR), respiration rate (RR) and excretion rate (ER) was analysed at the end of each simulation by comparing to the base scenario (calibrated parameters) and expressed as:

$$Impact \; (\%) = \frac{M_{calibrated} - M_{sensitivity}}{M_{calibrated}} \times 100$$

where *M* is the SL, DW, DWmG, CR, RR or ER value during the last day of simulation and *calibrated* and *sensitivity* stand for the value obtained with the calibrated set of parameters and the parameter considered in the sensitivity test, respectively. The maximum impact in the sensitivity test for each parameter was calculated following:

Maximum impact = Maximum [Absolute (Impact +10%), Absolute (Impact -10%)]

A total of 6 oyster growout datasets were used for calibration. Each oyster stack consisted of 14 vertically-stacked trays that were deployed at a depth of 5 metres. Oyster seed (individual size: ~1/2 inch) was placed in racks on June 13, 2016 (Denman Point) and June 14, 2016 at Metcalfe Bay. Starting concentration was 750 seed per rack. Ten oysters were collected from racks 2, 8, and 14 at a higher frequency at the beginning of the 1-year growout period and less frequently towards the end of the growout season.

9.2.1. Oyster condition index

Oyster tissue was dissected from its shell and placed into a labelled and pre-weighed aluminum pan. The tissue was then dried using a VWR 1370 GM Gravity Oven at 55°C for 48 hours or until a constant sample weight is achieved. Samples were desiccated for 2 hours prior to dry weight determinations to avoid potential condensation during the cooling process. Inorganic content was calculated using the differential weight values between dry and ashed measurements standardized by dry weight. Dried samples were ashed at 550°C for 2 hours in a Thermolyne 1400 furnace for this calculation.

9.2.2. Forcing

YSI-EXO2 Sondes were deployed at each site at the water depth of the oyster stacks (5m). Temperature and chlorophyll-a were logged every 10 minutes for varying periods between June, 2016 – July, 2017. These data were used in the preliminary stages of the DEB calibration but once available, the model was forced using temperature and chlorophyll concentration data extracted from a preliminary run of BiCEM (Figure B2) to facilitate the integration of the DEB component in the BiCEM structure (Appendix C).
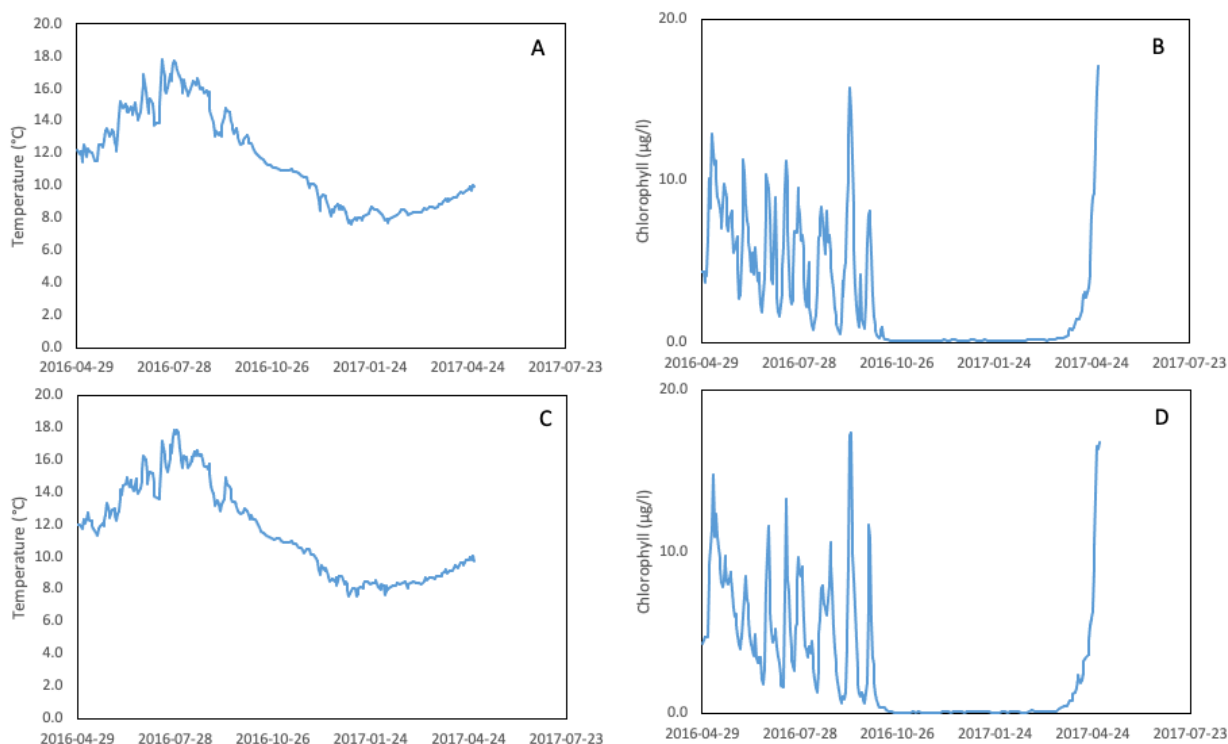
Figure B2: Temperature (°C) and chlorophyll (µg l⁻¹) in Lucky7 (A and B, respectively) and Mac's Oysters (C and D, respectively).

9.3. RESULTS AND DISCUSSION

The set of optimized parameters fits with the reported values from the literature with the exception of kappa (Table B2). The optimal value of kappa dropped to 0.4, which suggests a higher investment in reproduction than previously reported by Ren and Schiel (2008) and Bernard et al. (2011) for the same species. Despite this variation from previous models, the set of parameters seems to capture the temporal dynamics of oyster growth (Figure B3). In fact, when observations and simulations from the 6 datasets are represented together in a scatterplot (Figure B4), the values are close to the 1:1 line, which represents the perfect match between observations and simulations. The results could improve if Mac's Oysters Tray 2 would be removed from the analysis (Figure B3). The final tissue weight of this dataset is higher than the other datasets. The only plausible explanation of that high weight could be a mortality event affecting that tray by biasing its population towards larger individuals. Although some educated observations based on oyster counts support this hypothesis, there are no robust scientific data at the population level that could be used to test this hypothesis. Despite the poor agreement in Mac's Oysters Tray 2 dataset, the results highlight that the optimized set of parameters could be used in BiCEM to represent the observed growth pattern of *Crassostrea gigas*. The sensitivity test (Table B3) highlights the most sensitive parameters and consequently priority research lines that would improve model parameterization: feeding, $\{\dot{p}_{Xm}\}$, digestive processes, *AE*, and response to temperature T_L and T_H. Finally, additional datasets of oyster growth and environmental conditions would help to validate the model with independent datasets and improve the performance of the model as well as reduce uncertainties under different environmental conditions. However, the general good agreement of the model parameters with literature values suggests that the set of parameters is already robust and can be used to simulate physiology and growth of the Pacific oyster.
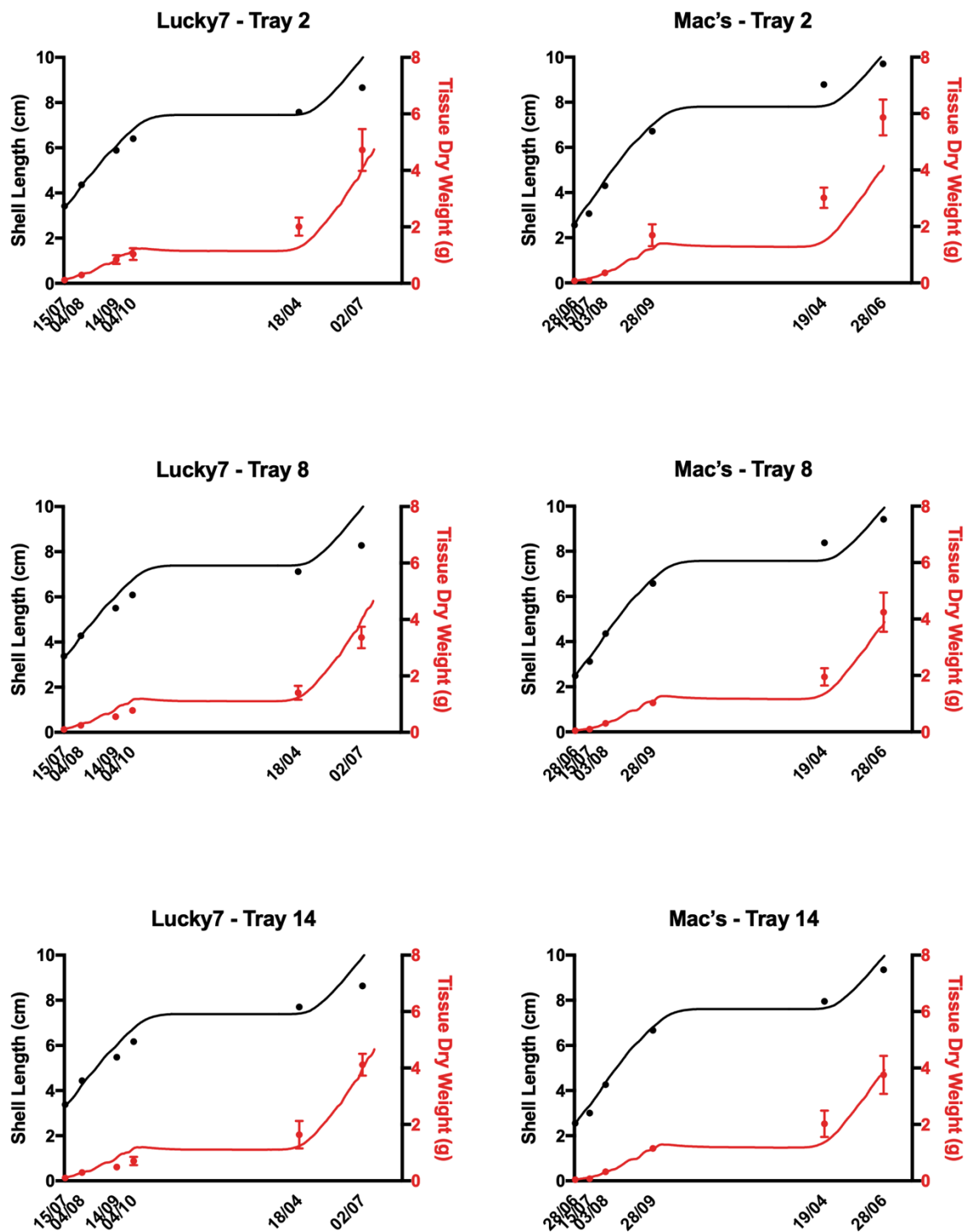
Figure B3: Observed shell length and tissue dry weight (black and red dots, respectively) and DEB-simulated shell length and tissue dry weight (red and orange continuous lines, respectively) for the two sampled sites, Lucky7 and Mac's Oysters at different depths (tray 2, 8 and 14).
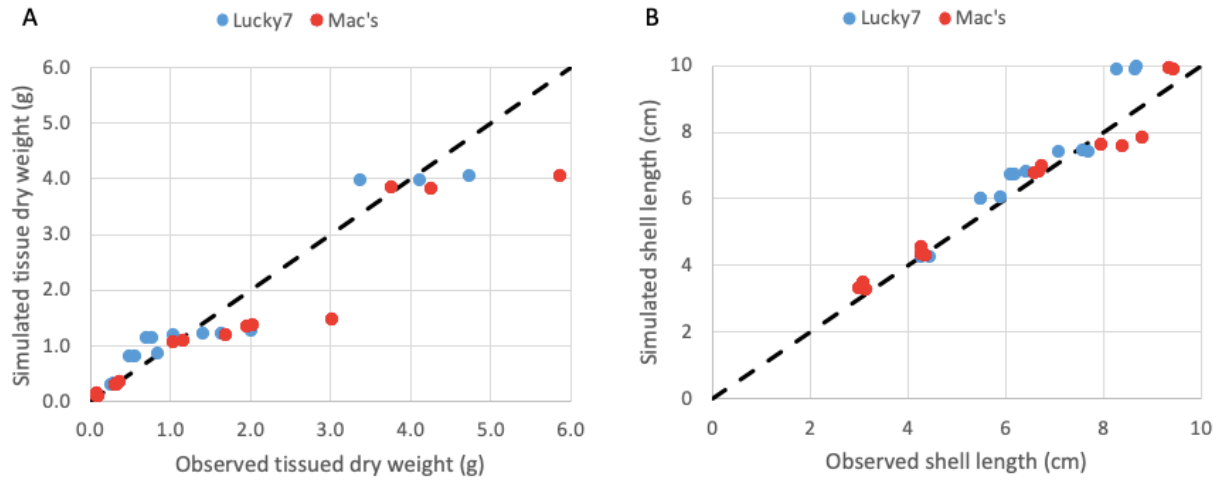
Figure B4: Observed vs simulated tissue dry weight and shell length (A and B, respectively) for all datasets.

Table B3: Maximum change in final SL, DW, DWmG, CR, RR or ER of Crassostrea gigas *after a ±10% in parameter.*

Parameter	Maximum change (%) after a ±10% in parameter					
	SL	DW	DWmG	CR	RR	ER
δ_M	9.8	3.8	3.6	2.5	2.2	3.6
$\{\dot{p}_{Xm}\}$	8.4	27.3	27.7	29.3	29.8	23.2
$[\dot{p}_M]$	1.7	4.1	4.8	3.3	2.2	27.4
$[E_G]$	5.6	13.1	16.8	11.5	9.2	17.8
$[E_m]$	1.7	3.0	3.0	3.4	7.9	14.0
κ	7.0	7.5	20.5	13.9	10.6	19.5
X_K	2.7	9.4	9.4	6.9	8.9	21.6
T_A	2.6	8.6	8.9	13.2	15.4	16.1
T_L	1.4	5.2	6.6	21.3	26.3	15.2
T_H	0.3	1.1	1.1	1.2	1.3	22.3
T_{AL}	0.4	1.3	1.5	3.6	4.6	3.9
T_{AH}	0.0	0.1	0.1	0.1	0.2	3.5
AE	8.4	27.3	27.7	17.5	29.8	23.2
DW:WW	0.0	3.1	6.5	0.1	0.1	27.4

9.4. ACKNOWLEDGMENTS

9.5. REFERENCES

Bernard, I., de Kermoysan, and G., and Pouvreau, S. 2011. Effect of phytoplankton and temperature on the reproduction of the Pacific oyster *Crassostrea gigas*: Investigation through DEB theory. J. Sea Res. 66: 349-360.

Duarte, P., Fernández-Reiriz, M.J., Filgueira, R., and Labarta, U. 2010. Modelling mussel growth in ecosystems with low suspended matter loads. J. Sea Res. 64: 273-286.

Filgueira, R., Guyondet, T., Comeau, L.A., and Grant, J. 2014. A fully-spatial ecosystem-DEB model of oyster (*Crassostrea virginica*) carrying capacity in the Richibucto Estuary, Eastern Canada. J. Mar. Syst. 136: 42-54.

Guyondet, T., Roy, S., Koutitonsky, V.G., Grant, J., and Tita, G. 2010. Integrating multiple spatial scales in the carrying capacity assessment of a coastal ecosystem for bivalve aquaculture. J. Sea Res. 64: 341-359.

Kooijman, S.A.L.M. 2010. Dynamic energy budget theory for metabolic organization. Cambridge University Press. 419 pp.

Larsen, P.S., Filgueira, R., and Riisgård, H.U. 2014. Somatic growth of mussels *Mytilus edulis* in field studies compared to predictions using BEG, DEB, and SFG models. J. Sea Res. 88: 100-108.

Pete, R., Guyondet, T., Bec, B., Derolez, V., Cesmat, L., Lagarde, F., Pouvreau, S., Fiandrino, A., and Richard, M. 2020. A box-model of carrying capacity of the Thau lagoon in the context of ecological status regulations and sustainable shellfish cultures. Ecol. Model. 426 C, 109049.

Pouvreau, S., Bourlès, Y., Lefebvre, S., Gangnery, A., and Alunno-Bruscia, M. 2006. Application of a dynamic energy budget to the Pacific oyster, *Crassostrea gigas*, under various environmental conditions. J. Sea Res. 56: 156-167.

Ren, J.S., and Schiel, D.R. 2008. A dynamic energy budget model: parameterisation and application to the Pacific oyster *Crassostrea gigas* in New Zealand waters. J. Exp. Mar. Biol. Ecol. 361: 42-48.

Rosland, R., Strand, Ø., Alunno-Bruscia, M., Bacher, C., and Strohmeier, T. 2009. Applying dynamic energy budget (DEB) theory to simulate growth and bio-energetics of blue mussels under low seston conditions. J. Sea Res. 62: 49−61.

Sonier, R., Filgueira, R., Guyondet, T., Tremblay, R., Olivier, F., Meziane, T., Starr, M., LeBlanc, and A.R., Comeau, L.A. 2016. Picophytoplankton contribution to *Mytilus edulis* growth in an intensive culture environment. Mar. Biol. 163: 73. doi:10.1007/s00227-016-2845-7.

10. APPENDIX C: EVALUATION OF THE COUPLING BETWEEN FVCOM AND A BIVALVE CULTURE ECOSYSTEM MODEL (BICEM) FOR BAYNES SOUND CARRYING CAPACITY ASSESSMENT

10.1. INTRODUCTION

Coupled Hydrodynamic-Biogeochemical modelling is commonly used to address questions related to shellfish aquaculture carrying capacity (Filgueira et al. 2015) and was identified as the method of choice based on a recommendation from a Canadian Science Advisory Secretariat (CSAS) process in the Gulf Region reviewing available carrying capacity modelling approaches (DFO, 2015). The spatially-explicit and dynamic nature of these models as well as their integration of the main processes driving the lower trophic levels of a marine food web are critical to capture the often non-linear interactions between cultured bivalves and the receiving ecosystem. In addition to the classic Nutrient-Phytoplankton-Zooplankton-Detritus (NPZD) model structure, carrying capacity studies generally require the inclusion of a shellfish physiology module dynamically coupled to the other components and that can predict the growth/production of the cultured species.

For the present study, the choice of the biogeochemical modelling framework was driven by 1) the compatibility with the Finite Volume Community Ocean Model (FVCOM) as the hydrodynamic engine, 2) the fulfillment of the above-stated constraints requiring as little code development as possible and 3) the availability of models already successfully applied in the region of interest. These criteria considerably narrowed down the list of potential candidates and the FVCOM-ICM (Integrated-Compartment Model) previously known as UBM (Unstructured Biogeochemical Model) model coupled by the US-Pacific Northwest National Laboratory (Khangaonkar et al. 2012; Kim and Khangaonkar, 2012) was chosen.

In-house code development was mostly limited to the inclusion of the shellfish physiology module based on the Dynamic Energy Budget (DEB, Kooijman, 2010) and its coupling with other biogeochemical components. The complete biogeochemical-shellfish model was renamed BiCEM (Bivalve Culture Ecosystem Model) in the context of the present study. The initial set of biogeochemical parameters extracted from the Puget Sound application of FVCOM-ICM by Khangaonkar et al. (2012) was further refined for the present Baynes Sound application as described in the following sections.

The objectives of the present Appendix are to answer questions related to the first objective in the Terms of Reference of this CSAS process as copied below:

10.2. TERM OF REFERENCE OBJECTIVE #1:

Evaluate the hydrodynamic accuracy of the FVCOM model component and discuss the biological applicability of the biogeochemical (BiCEM) component in the coupled Baynes Sound model.

a. Compare modelled and observed water properties

b. Identify uncertainties and consequences associated with data availability and modelling parameterization through sensitivity analysis for this Pacific region application of FVCOM-BiCEM.

10.3. METHODS

10.3.1. Field sampling

Ecosystem variables supporting bivalve ecological carrying capacity assessments were collected with varying frequency and spatial resolution depending on modelling requirements and resources available. Sampling and data collection can be divided into the following components:

- **Oceanographic attributes:** Temperature, salinity, oxygen, turbidity, in vivo fluorescence, photosynthetically active radiation (PAR),

- **Plankton-nutrient variables**: Phytoplankton (primary production and productivity), seston (suspended particulate matter: organic/inorganic fractions); dissolved nutrients (nitrate/nitrite (NO_3/NO_2), phosphate (PO_4), silicate (SiO_3)); zooplankton (abundance/biomass).

- **Oyster growth characterization:** *in situ* grow-out trials took place at two suspended oyster-rafts, where each trial was located in the upper reach (Denman Point) and lower reach (Metcalfe Bay) of Baynes Sound. These two locations present different water and planktonic attributes between the spring-summer season. The oyster growth attributes and environmental data were used to develop a Dynamic Energetic Budget model (Filgueira et al. 2016; Appendix B) required for the FVCOM-BiCEM carrying capacity model.

- **Intertidal bivalve diversity across cultured and non-cultured substrates:** Clam biomass data were provided by industry, academia, and Fisheries and Oceans Canada shellfish data base sources.

- **Aquaculture lease properties:** Existing, new, and amended License information were provided through a secure channel to support scenario-building modelling.

Vertical profiles of oceanographic attributes: Vertical profiles of temperature, salinity, oxygen, turbidity, *in vivo* fluorescence, and PAR (photosynthetically active radiation) were collected using a Seabird911 profiling CTD (conductivity, temperature, depth) equipped with a 24 Niskin-bottle Rosette. Physical oceanographic data (temperature, salinity, and dissolved oxygen) collected from these deployments are the same as those described in Appendix-A (FVCOM). In general, CTD profiles were carried out in the spring and summer periods between 2009 and 2019, with an increase in station coverage within the boundary zone of the SoG (including north and south entrances). Central-axis stations were surveyed annually with the exception of 2010, 2015, and 2017 (reduced stations). Additional CTD data was available from local DFO monitoring programs that provided increased spatial and temporal coverage within the entire modelling domain. This long time-series of CTD data addresses ecosystem variation with respect to the TOR Objective 1a&b examining data availability and sensitivity analysis of BiCEM.

Vertical profiles of plankton and nutrient variables: Congruent water samples were collected during the CTD Niskin-Rosette deployments, where an individual bottle was triggered at a certain standard oceanographic depth in a vertical series to capture a profile of both physical and biological analyses. These standardized sampling depths (0, 5, 10, 15, 25, 50, 75, 100, 150, 200, 250, 300, 350 m) were established by the Water Properties Section at the Institute of Ocean Sciences (Fisheries and Oceans Canada). Each water sample was analyzed for seston (suspended particulate matter), particulate carbon and nitrogen, phytoplankton production (chlorophyll) and dissolved nutrients [nitrate/nitrite (NO_3/NO_2), phosphate (PO_4), silicate (SiO_3)] concentrations.

In addition to vertical profiles of CTD and biological properties across Baynes Sound and the boundary zone (northern SoG), three other deployment strategies were established to collect both physical and biological oceanographic variables (Table C1):

- ***Hourly tidal-series of vertical CTD profiles (Seabird-911-Rosette):*** Three fixed stations (ST2-upper, ST17-lower, ST23-outer Baynes Sound) in both April and June of 2017.

- Time-series CTD data at fixed depth (5m) on oyster rafts (YSI-EXO2 Sondes):

  o Deployment at 5 m depth (oyster-rack height) at each oyster grow-out site in the upper (Denman Point) and lower (Metcalfe Bay) reaches of Baynes Sound. Other non-grow-out deployment locations included Comox Marina, Fanny Bay, and Lambert Channel (Figure 1).

  o Water samples were collected in 1-L Nalgene bottles from a portable Niskin bottle deployed at the depth of the oyster rafts (5m) during the oyster growout trials. These water samples were collected to support the CTD time-series data and both DEB and BiCEM modelling.

- ***Time-series temperature data at 3 fixed rack on oyster stack (HOBO pendants):*** HOBOs attached to the top, middle, and bottom oyster racks within each replicate oyster stack deployed at both Denman Point and Metcalfe Bay. This data supported the oyster DEB modelling outlined in Appendix B.

Table C1: Physical and biological oceanographic variables collected from CTD vertical profiles and fixed-depth time-series deployments. PAR = photosynthetically active radiation.

Deployment	Vertical Profiles		Time-series 5m depth		Time-series 5m depth oyster racks: 2, 8, 14
Instrument/ Samples	CTD Seabird-911	Water samples	YSI-EXO-CTD	Water samples	HOBO Temp probe
Time period	2009-2019	2009-2019	2016-2017	2016-2017	2016-2017
Temperature	X	X	X	-	X
Salinity	X	X	X	-	-
Oxygen	X	X	X	-	-
Fluorescence	X	-	X	-	-
Turbidity	X	Seston	X	Seston	-
PAR	X	-	-	-	X
Chlorophyll extraction	-	X	-	X	-
Dissolved nutrients	-	X	-	-	-
Locations	Selected stations (see Appendix Table A1)	Selected stations (see Appendix Table A1)	Comox Harbour	Comox Harbour	-
			Denman Point	Denman Point	Denman Point
			Fanny Bay	Fanny Bay	-
			Metcalfe Bay	Metcalfe Bay	Metcalfe Bay
			Lambert Channel	Lambert Channel	-

10.3.2. Laboratory analyses of water samples

10.3.2.1. Organic and inorganic seston concentration

Pre-weighed Advantec filters GF75 (25 mm diameter, 0.3 µm pore size) were placed in labelled Petri dishes. Each water sample (800 – 1000 mL) was filtered on to a pre-weighed Advantec filters GF75 and then placed in a labelled Petri dish, stored in a freezer, and transported back to the laboratory in a cooler. Seston concentration was determined by the weight of dry material on the filter standardized by the water volume filtered. Total seston was derived by placing each filter dish in a drying oven at 55 °C for 24 hours or until a constant weight is achieved. The samples were desiccated for 2 hours to remove moisture during the cool-down process. Inorganic seston was determined by combusting dried seston samples at 500 °C for 2 hours or a constant weight. Organic seston was calculated as the difference between dried and ashed weights, standardized by the dried weight for each sample.

10.3.2.2. Seston carbon and nitrogen concentration

Pre-burnt Advantec filters GF75 (25 mm diameter, 0.3 µm pore size) were used to filter the water samples (300 mL to 1 L) and then placed in a labelled Petri dish, stored in a freezer, and transported back to the laboratory in a cooler. The filters were dried at a 55 °C oven temperature. The filters were desiccated for 2 hours to remove moisture during the cool-down process. The filters were treated with 0.5M HCl to remove inorganic carbon and sent to the Université du Québec à Rimouski (UQAR) for analysis through a Carlo-Erba NA-1500 analyser for the determination of organic carbon and nitrogen content. Samples were washed with distilled water, centrifuged, dried, homogenized and weighed prior to analysis.

10.3.2.3. Chlorophyll abundance (Total phytoplankton and picoplankton)

Samples were size fractionated into 2 size categories: 1) total phytoplankton (> 0.3 µm); and 2) picoplankton (0.3 – 2.0 µm). The Advantec GF75 25-mm filter (0.3 µm pore-size) was used to determine total plankton, while the GE polycarbonate 25-mm filters (2.0 um pore-size) was used along with the 0.3 µm filter to estimate picoplankton. 180 ml of seawater was filtered through the GF75 filter (0.3 µm), while 60 ml of seawater was filtered through the GE filter (2.0 µm). After filtration, each filter was folded inward and placed in a 10-ml scintillation file and stored in a freezer or cooler for transportation back to the laboratory. Chlorophyll filters were placed in 90 % acetone and extracted in the dark for 24 h at 5 °C. The acetone solution was analyzed for chlorophyll a (Chl-a) using a Turner Designs Model 10 fluorometer according to Parsons et al. (1984).

10.3.2.4. Dissolved nutrient concentrations (nitrate/nitrite (NO_3^-/NO_2^-), phosphate (PO_4^{3-}), silicate (SiO_3^{2-}))

Dissolved nutrients were collected after filtration through a Whatman GF/F 2.5-cm glass-fibre filter. The filtrate was captured in a falcon tube for the CTD-Rosette samples and a 30-ml Nalgene bottle for oyster raft samples. The samples were frozen and placed in a cooler for transport back to the laboratory. Dissolved nutrients were analyzed using an Astoria analyser following methods described in IOS Nutrient Methods (Barwell-Clarke and Whitney, 1996).

10.3.2.5. Phytoplankton primary productivity

In order to establish a rate of primary productivity for each distinct water mass in Baynes Sound, phytoplankton incubations took place in the upper, lower, and outer Sound using single moorings with C13-spiked light/dark incubations at 1m, 5m, and 10m below the surface. The CTD-rosette was deployed and water samples were collected from Niskin bottles triggered at 1m, 5m, and 10m at each Sound water mass. Seawater remained in the Niskin bottles for a minimum of 20 minutes for dark adaptation before samples were collected. Each deployment

site had 12 x 500ml polycarbonate incubations with each depth interval equipped with 2 clear and 2 darkened bottles. 650 ml of seawater was transferred from the 1-m Niskin bottle into each of the 4 polycarbonate bottle designated for the 1-m depth incubation. The bottles were filled to the top and 600 μL of the ^{13}C solution [6g of NaH$_{13}$CO$_3$ (99% ^{13}C) in 250ml of de-ionized water] was spiked into each bottle. The sample was secured with the bottle screw cap and labels on the bottles. This procedure was repeated for the other deployment depths and sites. A pipe clamp was placed at mid-height of a bottle and thread through the mooring polypropylene rope to fix a bottle at a specific depth in the water column. Black tape was used to reduce chafing of rope with the movement of the bottles. The deployments at the upper and lower regions of Baynes Sound were suspended from Denman Point and Metcalfe Bay rafts respectively, while the outer Sound deployment required a bottom-up weighted mooring. All moorings were built such that the depths of the incubations were standardized. HOBO temperature/light pendants were attached to each incubation depth at each mooring. The moorings were retrieved after a 24 hour incubation period. Each bottle was filtered for size fractionation: total phytoplankton (>0.3 μm) and picoplankton (0.3 – 2.0 μm). The filters were placed in labelled scintillation vials and placed in a freezer. Prior to shipping to UQAR for analysis, a 100 μL of 0.5 N HCl was added to each vial to remove any residue of carbonates through evaporation overnight.

10.3.2.6. Stable carbon and nitrogen isotopes

The primary productivity filters were sent to UQAR for analysis. Stable isotope values were obtained using a Thermo Finnigan Flash 1112 EA coupled to a Thermo Finnigan Delta Plus XL through a Conflo III. Data were blank corrected. Carbon isotope ratios were corrected for contribution using the Craig correction and reported in per mil notation relative to the VPDB scale. Nitrogen isotope ratios are reported in per mil notation relative to AIR. Precision of data were monitored through routine analyses of in-house standards which are stringently calibrated against the IAEA standards. Precision of d13C and d15N measurements were 0.12‰ and 0.22‰, respectively (n = 18, 2s). Percent C and N measurements have a precision of ±10% of the reported percentage which is based on mass. The 13C data was used to derive phytoplankton assimilation over the incubation period as primary productivity rates.

10.3.2.7. Satellite-based chlorophyll estimates

Chlorophyll-a concentrations were retrieved from European Space Agency (ESA) Sentinel-3 imagery (Morel et al. 2007a,b) using a OC4Me standard Maximum Band Ratio semi-analytical algorithm. The two ESA Sentinel-3 Ocean and Land Colour Instruments (OLCI) were launched in February 2016 and April 2018, now enabling a revisit time of less than two days. Data spanning the period April 25, 2016 through June 30, 2017 were processed, covering the "Baynes Sound" model domain by sub-setting the full Sentinel-3 scenes provided to the area of interest. Data have been provided as a time series of 10-day Chl means for the full period described above, as a single netcdf file (total of 43 time-steps from April 2016 through June 2017).

10.3.2.8. Zooplankton abundance and biomass

Vertical net hauls were carried out in April and June, 2016, for zooplankton abundance and biomass. The SCOR VNH net was 2m in length with a mesh size of 236 μm and a mouth diameter of 0.56 m. A TSK flowmeter was installed in an offset position at the net mouth to record volume filtered. A 5 kg weight was used to stabilize the net during the vertical haul. The net was lowered into the water at a speed of 0.5 ms^{-1} and retrieved at a speed of 1 ms^{-1}. Samples were preserved in Formalin (37.5% formaldehyde in filtered seawater buffered with borax). Each sample jar (250 ml) had a ratio of 1 part sample to 2 parts preservative. Zooplankton taxa were analysed using a dissecting microscope to provide abundance estimates which were then converted to biomass. Zooplankton were sampled at up to 40 stations across

BS and the northern SoG during the 2016-2017 sampling period. Since the depths in the northern SoG were sometimes deeper than those in BS, the former net hauls captured larger deeper-dwelling zooplankton. Following the advice of the DFO Pacific Water-Properties plankton group, the authors limited the zooplankton community used in the model based on seasonal depth-preference, which coincided with a size and age spectrum (e.g. Euphausids), to standardize zooplankton between Baynes Sound and the northern SoG. These deeper larger species were removed from the data used to build the model inputs as well as the larger species feeding predominantly on other zooplankton to adhere more closely to the model Zooplankton variable that only feeds on phytoplankton and organic detritus.

10.3.2.9. Shellfish Growth Rates

Oyster seed (~1/2 inch) was placed in racks on June 13, 2016 (Denman Point) and June 14, 2016 at Metcalf Bay. Starting concentration was 750 seed per rack. Ten oysters were collected from each rack at a higher frequency at the beginning of the 1-year growout period and less frequently towards the end of the growout season.

10.3.2.10. Oyster condition index

Oyster tissue was dissected from its shell and placed into a labelled and pre-weighed aluminum pan. The tissue was then dried using a VWR 1370 GM Gravity Oven at 55°C for 48 hours or until a constant sample weight is achieved. Samples were desiccated for 2 hours prior to dry weight determinations to avoid potential condensation during the cooling process. Inorganic content was calculated using the differential weight values between dry and ashed measurements standardized by dry weight. Dried samples were ashed at 550°C for 2 hours in a Thermolyne 1400 furnace for this calculation.

10.3.2.11. Intertidal bivalve inventory

Data on wild bivalves in Baynes Sound was acquired from the DFO Shellfish Data Unit that is curated by the Stock Assessment section located at the Pacific Biological Station (PBS). These data were obtained following a standardized sampling protocol as described by Gillespie and Kronlund (1999) and Biggs (2015). All samples were collected in non-aquaculture beach areas, consisting of Mud Bay, Base Flats, Seal Island (Comox Sandbar), Gartley Beach, Royston, and Comox Harbour. Daphne Munroe provided clam data collected from North Denman Beach B and Fillongley Park Beach A (Munroe, 2000). Rob Marshall (Mac's Oysters) provided clam data collected in leases within and beside netted areas on Base Flats and Mud Bay (Figure C1).
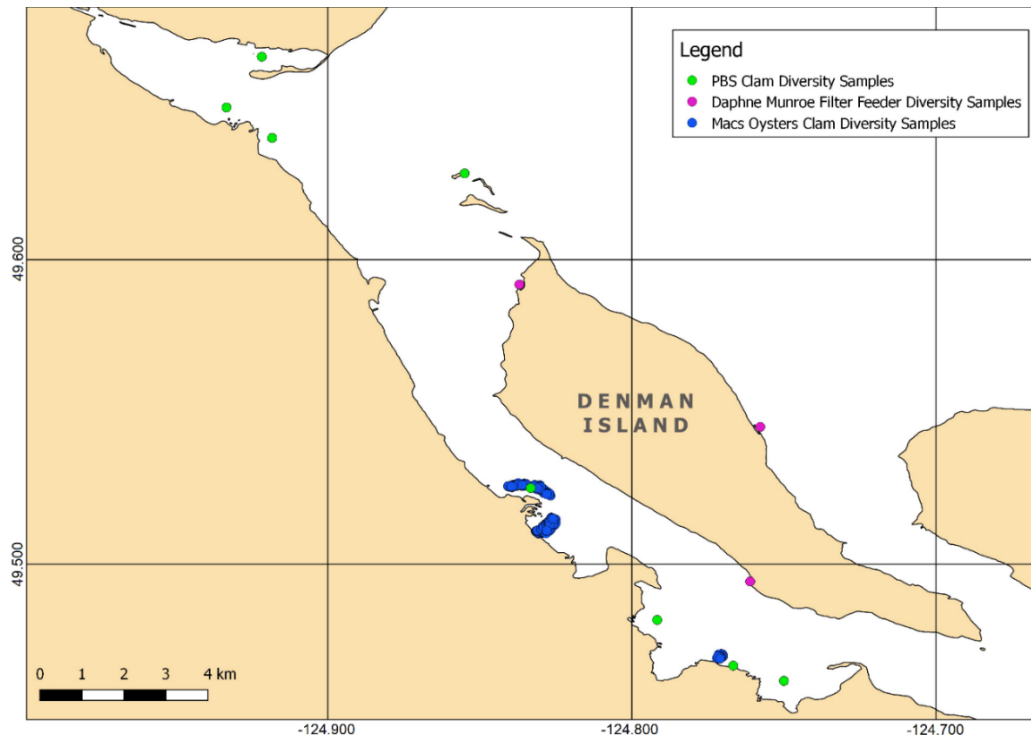
Figure C1: Map of intertidal bivalve inventory sites used to derive the size and abundance of clams included in the Baynes Sound ecosystem model.

10.3.3. Application to the Strait of Georgia - Baynes sound domain

The annual cycle from May 2016 to April 2017 is the focus of the present coupled modelling application. This period was identified as the most suitable in terms of data availability, in particular with respect to cultured bivalve growth, to support the model calibration effort.

10.3.3.1. Coupling with FVCOM Model

The biogeochemical model uses the exact same grid and advection-dispersion transport of variables as FVCOM such that it can directly use the fluxes and scalars (temperature, salinity) generated by the hydrodynamic model in an off-line coupling. The off-line coupling, where hydrodynamics results are generated first and stored, to then be used by the biogeochemical model, provides flexibility and time efficiency during the cumbersome biogeochemical calibration phase. In the present application a 20-min frequency for FVCOM output storage was used as a compromise between detailed hydrodynamic processes and practicality (availability of storage space and duration of network file transfers).

FVCOM also provides information on wetting and drying in inter-tidal areas. In these regions, when a model grid cell became dry according to the hydrodynamic results, all biogeochemical processes stopped, including wild and cultured bivalve feeding until that area was flooded again on the next incoming tide.

10.3.3.2. Biogeochemical Structure

The original biogeochemical model is based on CE-QUAL-ICM (Cerco and Cole, 1993) that was initially developed to address questions related to coastal-nearshore biogeochemistry such as eutrophication. This model can simulate up to 32 state variables, including three phytoplankton classes and two zooplankton classes, as well as distinct cycles for Carbon, Nitrogen, Phosphorus and Silica. Throughout this document the acronyms used refer to the variable

names rather than the corresponding chemical constituents. Dissolved oxygen (here noted as O2) is also accounted for and the model may incorporate a detailed diagenetic sediment module. The choice of the final biogeochemical structure for the Baynes Sound application (Figure C2) was driven by 1) including the minimum complexity required to adequately simulate the main features of the pelagic ecosystem and address the carrying capacity question and 2) data availability to constrain and validate the included variables. Consequently, assuming Nitrogen limitation, only the N cycle was considered and limited to nitrate-NO_3 + nitrite-NO_2 (noted as NO3), ammonium (noted as NH4), one class of phytoplankton (Phyto), one class of zooplankton (Zoo) and non-living organic material split over dissolved and particulate organic nitrogen (DON and PON). The ICM default formulation and parameters of light attenuation through the water column were used in this application, accounting for contributions of phytoplankton Chlorophyll *a*, total suspended particles and dissolved organic matter. The general validity of attenuation values was checked against observations made through the CTD vertical profiles (detailed in section 10.3.1) equipped with a Photosynthetically Active Radiation (PAR) sensor. Both simulated and observed values were seen to slightly fluctuate around a typical attenuation of 0.3 m^{-1}. The benthic compartment was kept to a minimum complexity level with prescribed, spatially uniform and temperature dependent NO3, NH4 and O2 exchange fluxes based on *in situ* measurements (Lavoie et al. 2016). Additional variables related to the shellfish components are described in the next section.
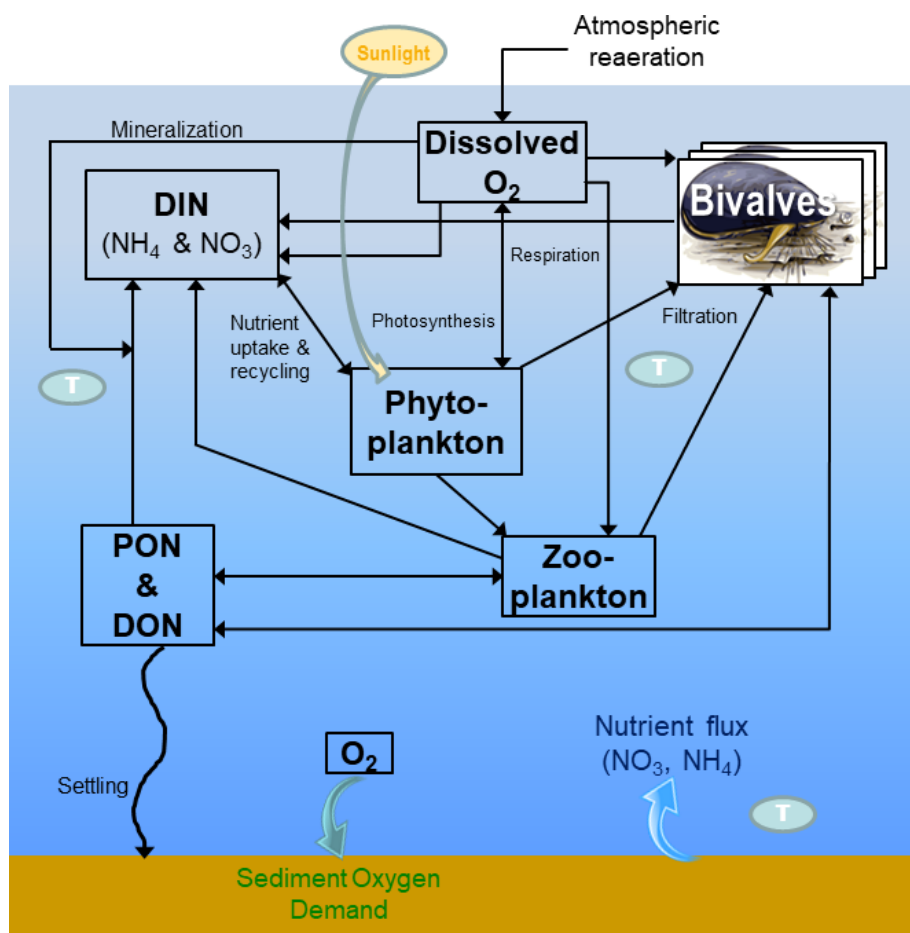
Figure C2: BiCEM biogeochemical structure as implemented for the present study. T: water temperature, which regulates most model biochemical processes, see text for other acronyms.

10.3.3.3. Integration of Wild and Cultured Bivalves

The Bivalve model component requires both spatial and biochemical integration. First, geo-localizations were derived from farm and wild bed layouts provided by the DFO Aquaculture Management Directorate (AMD, Figure 2) and the B.C. provincial government Coastal Resource Information Management System (Figure C3), respectively. This distribution of wild bivalves is limited to the intertidal and high subtidal areas and excludes species inhabiting deeper parts of the Sound. This limitation prevents BiCEM from explicitly accounting for the dynamics of these populations. However, their contribution to the ecosystem dynamics are implicitly accounted for in the Current scenario (2016-17 reference) as this contribution was reflected by the observations collected and used to calibrate BiCEM over this period. Moreover, not explicitly including this component in the carrying capacity assessment, which is conducted by comparison of different modelling scenarios, results in making the assumption that the influence of this component on the ecosystem dynamics does not change between scenarios.

Figure C3: Map of wild clam beds distribution in the Baynes Sound area, (source: iMapBC).

For cultured bivalves, annual production reports also provided by DFO AMD for 2015-2016 were used to determine which species were produced on each farm. For modelling purposes this information was compiled into five different bivalve categories as follows:

- Wild clam beds

- Clam bottom culture

- Oyster bottom culture

- Mixed clam and oyster bottom culture

- Oyster suspended raft culture

In the case of oyster suspended culture, rafts were positioned at 5 m below the water surface and extended for 1.5 m, except in areas with depths shallower than 9.5 m where they were brought up to 2 m below surface to accommodate for the tidal range.

Biofouling on the suspension culture equipment (stack-tray) was not significant and consisted of a light layering of a Caprellid population and the occasional juvenile sea urchin (1-2 cm). While the urchin grazes on biofilms on substrates, Caprellids are facultative filter and scraping feeding types from the water-column and substrate, respectively. It was rare to find a clubbed tunicate or an encrusting sponge attached to an oyster shell. The oysters were seeded in new stack-trays in mid-June and transferred to a different size of clean stack-trays in October. The closely-spaced oyster stack-trays may have reduced biofouling due to 1) permanent movement from wave action and tidal currents and 2) the vertical movement associated with culture operations. In terms of the relative biomass between biofouling organisms and cultured oysters, biofouling competition for food resources would result in noise in the system, thereby not influencing potential phytoplankton depletion detected by oyster feeding. As such, biofouling's influence was not explicitly included in BiCEM's structure.

In addition, all clams (wild and cultured) included in the model were considered to be Manila clams. According to wild bed surveys in Baynes Sound, Manila clams are by far the most abundant clam species (72.5% mean relative abundance, DFO-PBS Shellfish Data Unit). From the annual production reports they also appear as the species most commonly cultured in the Sound, representing more than 88% of all clam production in weight for years 2011 to 2016. Moreover, the current lack of data suitable to build dedicated physiological models for other species (Filgueira et al. 2016) prevented the inclusion of a larger diversity. The resulting compromise of all clam culture farms being included but as Manila clam farms was deemed representative enough for the present carrying capacity assessment.

Finally, the Dynamic Energy Budget for wild and cultured bivalve species (Manila clam, *Venerupis philippinarum* (Filgueira et al. 2016) and Pacific oyster, *Crassostrea gigas* (Appendix B)) were connected to the biogeochemical structure of BiCEM through their feeding on suspended particles (Phyto, PON and marginally Zoo), respiration, and excretion of both dissolved, as ammonium, and particulate (feces) forms. Feeding on the different particle types was scaled using different factors (0 – 1) accounting for the preference/catchability of each prey type by the bivalves. For simplicity the same preference factors were used for clams and oysters and were set to 0.9, 0.7 and 0.5 for Phyto, PON and Zoo, respectively. A lower value was used for Zoo to reflect that this variable includes species either too big or too mobile to be considered as bivalve food. Feces were accounted for through a specific detritus variable (BDPN) subject to the exact same dynamics as PON but with its own specific settling speed.

10.3.4. Supporting data for model development

10.3.4.1. Pelagic variables

All supporting data for open boundary and initial conditions of BiCEM pelagic variables (except zooplankton, see below for details on this specific variable) were provided by CTD and rosette vertical profiles collected through various DFO cruises in the SoG and Baynes Sound areas (see Figure C4 for the location of profile stations). Northern and southern stations (16 and 27) were used to build seasonal cycles (from sampling in April, June, September and November) at the corresponding open boundary as shown on Figure C5 and detailed below.

For phytoplankton, as the last observation available in 2016 was in November and the first of 2017 in April, no data were available to constrain the 2017 Spring bloom. A Spring bloom forcing (timing, duration and amplitude) was reconstructed from satellite observations and model outputs in the SoG (Allen and Wolfe, 2013; Gower et al. 2013; Gower and King, 2012) and imposed only to the southern boundary.

Zooplankton biomass information was available from vertical net tows collected in April and June 2016. All these data were pooled together and screened for larger deeper species as described in Section 10.3.2 to derive a single uniform biomass that was then used to adjust a seasonal cycle based on observed biomass time series in the SOG (Mackas et al. 2013). Following common practices Zooplankton biomass is reported in Carbon equivalent units and a carbon to nitrogen ratio Znc = 0.2 was used for conversions in BiCEM. Both for initial and boundary conditions the zooplankton biomass was uniformly distributed over the top layers of the water column and down to 100-m depth. Below this depth a constant and uniform biomass of 0 mgN L^{-1} was imposed. The aggregation of all zooplankton diversity into a single variable strongly limits the ability of the model to detail the dynamics of this trophic level. The intent is to provide a realistic overall biomass for this variable and consequent grazing pressure on prey items. On the other hand, the response of this bulk variable to changes in food availability should be considered a very crude depiction of changes in mass/energy utilization from lower trophic levels. Further interpretation about the consequences at higher trophic levels was out of the scope of the present assessment and should not be attempted given the aforementioned model limitations.
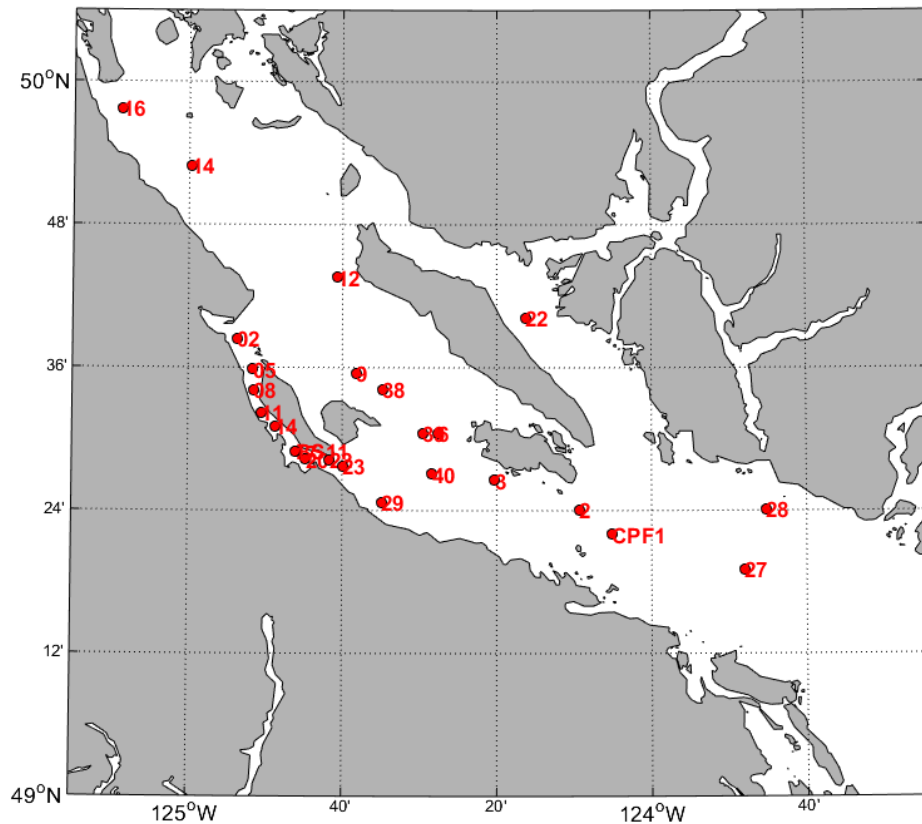
Figure C4: Map of stations used to create BiCEM input. Station 27 (south) and 16 (north) were used for boundary conditions; data from all stations in Spring 2016 were included in the set of initial conditions.

All stations from the Spring 2016 cruises served in building the model initial conditions. Data profiles were first individually interpolated in the vertical on a regular depth grid. The regular profiles were then further interpolated in space using the Data-Interpolating Variational Analysis (DIVA) to cover the whole 3D model domain for initial conditions or the grid sections corresponding to the open boundaries.

PON observations include both detritic and non-detritic (mostly phytoplankton) material while the PON model variable only accounts for dead material. The non-detritic portion was then removed from total PON using observed phytoplankton concentration (measured in µg Chl-a L^{-1}) in the corresponding sample and a conversion factor based on the Redfield Carbon to Nitrogen ratio and a fixed C/Chl-a ratio of 55 gC gChl-a^{-1}. Available data were insufficient to provide a detailed seasonal cycle at the boundaries, which were then forced with a constant and uniform very low value (0.001 mgN L^{-1}).

No data were available to construct inputs for the DON and NH4 variables. Consequently, both initial and boundary conditions of these two variables were kept to a uniform and constant zero value.
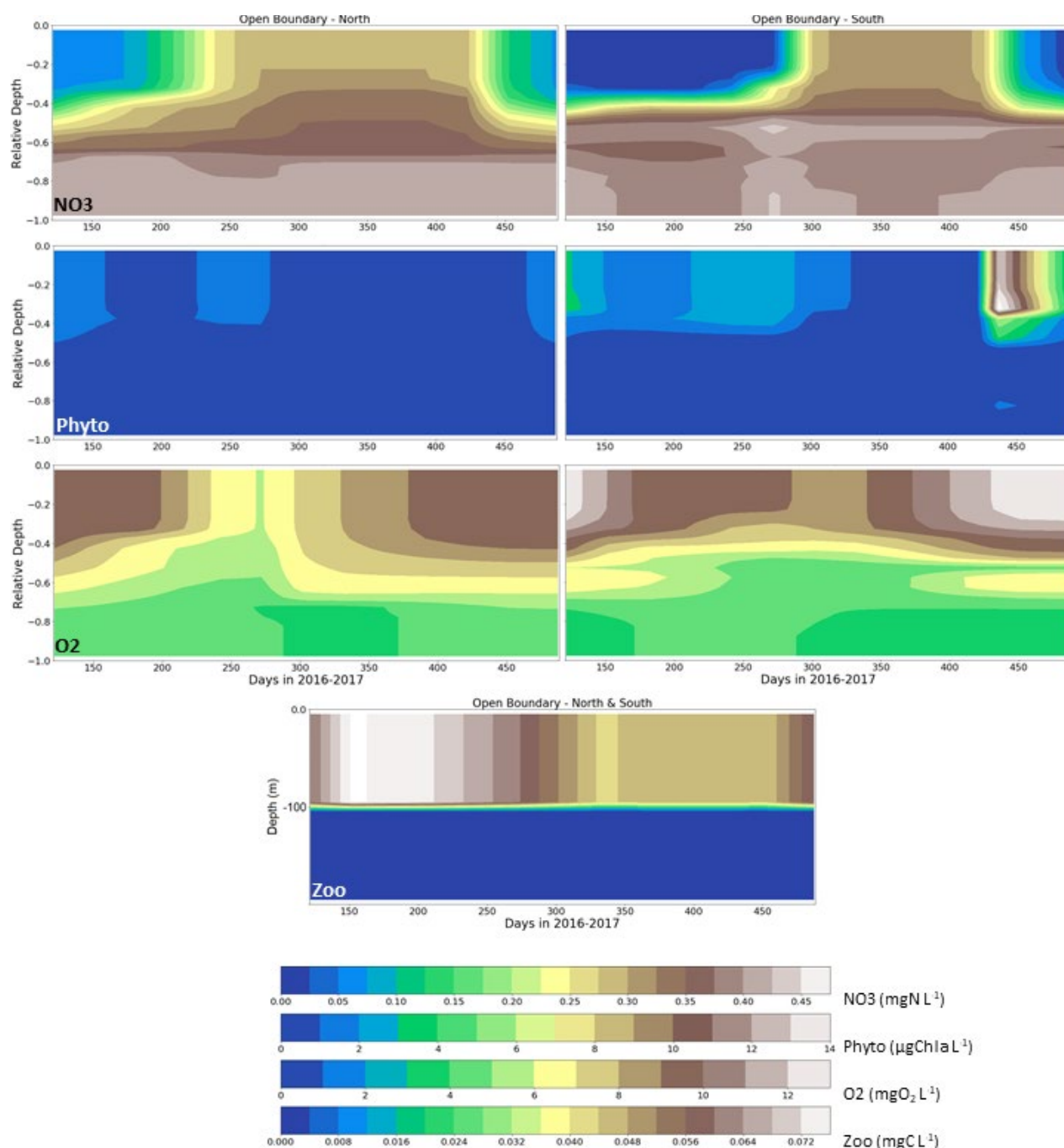
Figure C5: BiCEM open boundary forcing for variables with sufficient supporting data to build time-varying conditions. These profiles were constructed from data collected at stations 16 (north) and 27 (south) leading to horizontally uniform conditions at each boundary. The x time axis extends from 1 May 2016 to 30 April 2017.

10.3.4.2. Bivalves

In addition to the spatial distribution of wild and cultured bivalves BiCEM requires inputs of abundance or density (ind. m^{-2}) and initial size (shell length and tissue dry weight) for the various combinations of species and culture/habitat. Table C2 summarizes all the information

necessary to the BiCEM simulations and the following sections describe the data and methods used to derive these inputs.

Clams

The DFO Shellfish Data Unit survey data and industry data were used to estimate clam densities on wild (146 ind. m^{-2}, n = 3126 spanning over 1980 to 2016) and cultivated beds (400 ind. m^{-2}, n = 2033 spanning over 1999 to 2004), respectively. The culture density estimate accounted for potential differences between areas with and without cargo nets and was used in all leases reporting clam production. Only subsets of these data also provided information about the shell length and age of the sampled clams (n = 53 and 1035 for wild and cultured clams, respectively). This data was further used to derive a mean shell length representative of the whole population. Mean shell length for each age group was weighted by the relative frequency of that group in the population to derive the overall mean. Separate estimates for wild and cultured clams were very similar (within 3 mm) such that a single initial shell length of 31.3 mm was used for all model clams. A corresponding initial clam tissue weight (163.6 mg dry weight) was estimated from published data (Flye-Sainte-Marie et al. 2007; Robert et al. 1993) that also served for the estimation of the clam DEB parameters used in BiCEM (Filgueira et al. 2016).

Oysters

Very limited well-documented information was available to build the model inputs for bottom oyster culture. We considered that the density could vary from 25 to 60 oysters m^{-2}, when reported to the whole lease area. The shell length at seeding is between 40–50 mm and the growing period extends from 2 to 4 years depending on the density and targeted shell length at harvest. Based on this information a mean density of 40 oysters m^{-2} was used throughout Baynes Sound farms. The initial shell length (56 mm) was chosen so that the mean annual shell length would be representative of oysters in the middle of the production cycle. The initial tissue weight (630 mg dry weight) was estimated from suspended oysters of the same shell length. The influence of the bottom oyster component was tested through the model sensitivity analysis in the context of the present carrying capacity assessment.

Inputs for oyster culture in suspension from rafts were established from the information provided by the industry collaborators of this project and from the oyster growth monitoring carried out at their sites in 2016-2017. Broken down to the culture units, the mean oyster density used corresponds to 100 to 150 dozens of oysters per stack of trays and assumes that a 7 m by 7 m raft holds between 80 and 100 stacks. For input into BiCEM, this culture unit density was further distributed over the lease area using a lease relative occupancy (i.e. the ratio of area covered by rafts to total area of the lease) estimated from satellite images of Baynes Sound available through Google Earth. The first sampling time of our oyster growth monitoring in late June 2016 provided a reference oyster size both in terms of shell length and tissue weight. This reference was extrapolated back in time to the May simulation starting time using the first observed growth rate to produce a preliminary estimate of initial size. Finally, the preliminary initial size was finely adjusted so model and observations would match at the time of the first sampling.

Further information is required about the stage of bivalve species in their respective reproduction cycle at the start of the simulation to constrain the initial values of the three DEB variables from the initial shell lengths and tissue weights. Assumptions made in this regard are summarized in Table C2. Finally, we assumed that leases reporting mixed clam and oyster production were using half the available area for each species cultivation.

Table C2: Inputs used for the bivalve components of BiCEM.

Habitat/Culture type	Species	Density (ind. m^{-2})	Initial size Shell length (mm)	Initial size Tissue weight (mg d.w.)	Reproductive cycle assumption
Wild bottom	Manila Clam	146.0	31.3	163.6	Early - 20%*
Cultured bottom	Manila Clam	400.0	31.3	163.6	Early - 20%*
Cultured bottom	Pacific Oyster	40.0	56.0	630.0	Early - 10%**
Cultured suspension	Pacific Oyster	258.7	6.0	0.3	Juvenile - 0%

* Spawning usually starts in June (Gillespie et al. 2012); ** Industry partners reported partial spawning late June 2016 and 2017.

10.3.4.3. Benthic fluxes

A literature review did not provide sufficient data to estimate truly representative sediment-water exchange fluxes at the Baynes Sound scale. Fluxes reported in a recent study conducted within the Sound in intertidal and upper-subtidal areas (Lavoie et al. 2016) and summarized in Table C3 were considered the best data available to constrain this component of BiCEM and were used throughout the model domain. Given the uncertainty associated with this approach, a specific attention was paid to these fluxes in our sensitivity analysis.

Table C3: Sediment-water exchange fluxes of dissolved inorganic components used in BiCEM and range found in a literature review targeted to the Salish Sea and western Vancouver Island coastal areas. Positive fluxes are out of the sediment.

Variable	Specified benthic flux (g m^{-2} d^{-1})	Literature range* (g m^{-2} d^{-1})
NO3	0.0017	-0.027 – 0.016
NH4	0.1616	-0.006 – 0.211
O2	-0.0438	-1.710– -0.100

* essentially from Belley et al. 2016; Ingall et al. 2005; Khangaonkar et al. 2012; Rigby, 2019

10.3.4.4. River inputs

Environment and Climate Change Canada (ECCC) water quality data from the Tsolum and Englishman rivers (closest stations to Baynes Sound, 08HB0018 and 08HB0019) were combined to build monthly time series of NO3, DON and O2 concentrations over 2016-2017 (Figure C6). A constant value of river PON concentration was derived from observations in the Oyster and Englishman rivers (PON = 0.652 mgN L^{-1}, Sutton et al. 2013). Given the environmental difference compared to the rest of the model domain (i.e. freshwater vs seawater), river inputs of phytoplankton and zooplankton were kept to zero as well as for NH4 whose concentration was assumed much lower than NO3. Concentrations of all components were combined with the river discharges included in the FVCOM simulation (see Appendix A) to provide the final time-varying inputs into the model domain.
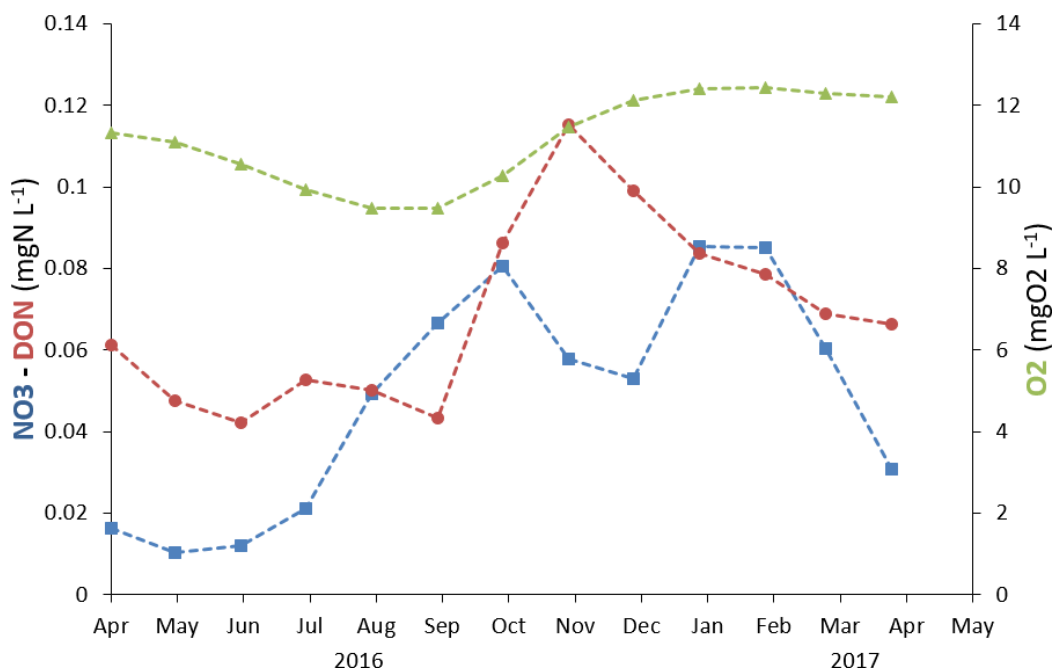
Figure C6: Freshwater discharge concentrations for variables with sufficient supporting data to build time-varying conditions.

10.3.5. Calibration procedure

The BiCEM calibration started from the parameter set used in the FVCOM-ICM application to Puget Sound and proceeded with tuning some of the parameter values to reach the best match between BiCEM results and observations. Data available for this comparison consisted of vertical profiles of pelagic variables (mainly NO3 and Phyto) collected during DFO cruises in June 2016 and April 2017, complemented by time series of Phyto and PON samples from the two suspended oyster farms used in our growth monitoring. These sites were also equipped with multi-parameter probes that provided 10-min time series of phytoplankton concentration (measured by fluorometry and converted into Chl-a units) at the depth of oyster rafts from late April to early December 2016. Noise was removed from these probe series using a moving average operator before they were subsampled at a hourly time step. The hourly series were further daily averaged to remove higher frequency fluctuations. Such data were considered indicative of the relative abundance of phytoplankton given the difficulty in calibrating *in situ* fluorescence measurements and were used to explore the high frequency variability in BiCEM results. For an easier visual comparison, the final probe series were adjusted using a scaling factor calculated as the ratio of model results to probe observations over the first two weeks of the series, when probe data were less prone to biofouling bias. Phytoplankton concentration time series were also built from Sentinel-3 satellite imagery (European Space Agency, freely available data retrieved from the [EUMETSAT earth observation portal](#), and processed using the standard OC4Me algorithm to derive Chl-a concentrations (Morel et al. 2007a,b). A 10-day composite time series was compiled from this imagery, that helped further assess the seasonal cycle simulated by BiCEM and in particular the onset of production in the Spring of 2017.

The oyster growth data sets from the two suspended oyster farms were also compared to the growth predicted by the oyster DEB component at each site and both in terms of shell length and tissue weight in order to fine tune the DEB parameter set initially derived by Filgueira et al. (2016).

The fit of BiCEM results with observations was focused only within Baynes Sound locations and assessed through qualitative visual comparisons for the most part. Quantitative assessments, as root mean square deviations (RMSD), were also provided when possible. The simulation with the set of parameters providing the best fit was selected as the Reference simulation, which included a shellfish aquaculture component representative of the 2016-2017 conditions as described for the Current scenario (section 3.3).

10.3.6. Sensitivity analysis

The very large number of parameters involved in the BiCEM dynamics prevented a systematic sensitivity analysis. The choice of the subset of parameters/processes to be included in this analysis was driven by 1) the relevance of the information generated with respect to the functioning of Baynes Sound in general and its carrying capacity for shellfish aquaculture in particular, 2) the scarcity of data to constrain a given parameter value as mentioned in previous sections and 3) any particular sensitivity observed during the calibration phase. As much as possible a systematic approach was followed by changing each selected parameter or process value by +10% and -10%. The changes in BiCEM results corresponding to each sensitivity run were compared to the Reference simulation for one or more relevant response variables. Scenarios specifically designed to explore the carrying capacity questions and reported in the main document also contributed to assessing BiCEM's sensitivity. The sensitivity (subscript s) and reference (subscript r) scenarios were compared based on a sensitivity index (SI, %) representing the relative change in the response variable X as follows:

$$SI = 100 \times \frac{X_s - X_r}{X_r}$$

This sensitivity index can vary both in time and space such that averaging procedures had to be used to facilitate the comparison between scenarios. First, for pelagic variables, including suspended oysters that can be distributed over several model vertical layers, a vertical integration was used prior to the SI calculation. At each location and time, the variable concentration was summed (or averaged in the case of oyster shell length and tissue weight) over the water column and these depth-integrated values were compared through the sensitivity index. The resulting SI still presented both horizontal and temporal dimensions that were illustrated as maps of SI temporal mean and standard deviation and compilations of SI spatial and temporal mean and other basic spatial statistics (absolute mean, minimum, maximum and standard deviation) of time-averaged SI over the whole Baynes Sound area.

10.4. RESULTS AND DISCUSSION

10.4.1. FVCOM-BiCEM coupling

A major limitation of offline or one-way coupling of hydrodynamics and biogeochemistry is the inability for biogeochemical variables to influence back on the hydrodynamics. However, this limitation is not seen as a significant issue for the present application, which focuses on pelagic variables that for the most part could only interact with hydrodynamics through very limited changes in water density. The influence of shellfish farming structures on local flow conditions is another interaction between hydrodynamics and a biological component that was not accounted for in the present model application. Given the low density of suspended structures relative to Baynes Sound dimensions the consequences of not including this feedback mechanism in a carrying capacity assessment were thought to be minimal. The very small differences to the tidal characteristics simulated by FVCOM when the extensive Baynes Sound intertidal areas were incorporated in the model tend to corroborate this assumption (see Appendix A).

Another consequence of the offline coupling is the use of a somewhat coarse temporal scale for hydrodynamic forcing (i.e. 20 min in the present study), which may impact model accuracy, especially in locations with sharp temporal and/or spatial variability such as vertical and horizontal fronts or places with stronger flow conditions. Model output interpretation needs to account for this caveat, which could at least partially be evaluated through comparisons with field observations in the following sections.

10.4.2. BiCEM calibration for application to Baynes Sound

The calibration based on the comparison of BiCEM outputs with observations collected in Baynes Sound in 2016-2017 yielded the main set of parameters reported in Table C4. Although the uncertainty in field measurements cannot be excluded, they are the reference against which model performance is assessed and other sources of uncertainty/discrepancy in model results are discussed in the following sections. The larger the pool of observations and the more diverse the available data are, the more robust the model performance assessment will be. Here we could rely on a diversity of observations related to nutrients, phytoplankton, particulate non-living material and bivalve growth. An evaluation of model skills covering both time and space is also critical for such spatially explicit dynamic models. Here, we relied on time-series to better assess the consistency of the model result quality and its ability to capture important temporal patterns such as seasonal cycles. Vertical profiles at various locations and transects regrouping several sampling stations were used to assess the model validity through the three dimensional space.

Starting with time series, our main focus was on phytoplankton as it represents the main source of food for bivalves. These time series also constitute the best available data to assess the model performance in simulating the bivalve food availability corresponding to our suspended oyster growth monitoring as they were collected at the farm monitoring sites and cover a large part of the 2016 oyster growing period. Looking at individual data points from water sampling, the model seems in general agreement with the observed phytoplankton biomass levels at both the Lucky7 and Mac's Oysters monitoring sites (Figure C7). Daily YSI probe data show series of peak-trough cycles in the phytoplankton biomass that are also present in BiCEM output although the timing of these extremes is not always captured by the model. Assuming the relative signal provided by the probes is accurate, higher phytoplankton concentrations seemed to occur in spring (May and early June) and late summer (September) 2016 with lower values in between, in accordance with typical seasonal cycles in temperate waters. This pattern is not as clear from the BiCEM results with only slightly higher peaks in September 2016 compared to summer values. The reasons for the absence of a proper late summer – fall bloom in the model output are difficult to pinpoint. These late season blooms are usually attributed to an increase in wind intensity that starts disrupting the summer stratification and increases mixing of nutrients into the euphotic zone and can be dominated by other phytoplankton species than the ones most abundant during the summer months. The BiCEM structure relying on a single phytoplankton variable might not be flexible enough to allow for an accurate simulation of these refined dynamics. Inclusion of a second phytoplankton variable could be considered in future iterations of the model as this late season bloom could constitute an important resource for cultured bivalves as they rebuild their energy reserves before the winter months. However, no mismatch between observed and simulated oyster growth was reported during that specific period (see Figure C11). This result tends to eliminate the possibility of food limitation in the model bivalves during fall and limits the impact of the bloom underestimation on the present carrying capacity assessment.

Finally, the satellite-derived data tend to confirm the seasonal cycle observed with the probes. The source of the relatively strong values shown by these remote-sensing data during the winter

period is questionable and BiCEM could not match these concentrations when low light and water temperature limit primary productivity to extremely low rates. Partly due to these high winter values, the satellite data does not show a clear spring bloom in 2017 compared to BiCEM output. Still time series from these two sources agree reasonably well at the time of the production onset in spring 2017.

PON time series (Figure C8) also provide insight into bivalve food availability. BiCEM appears in general agreement with PON concentrations at the northern monitoring site (Lucky 7). However, higher values in June, July and September at the southern site (Mac's Oysters) were not simulated by the model. These peak values were not observed at the northern site and could result from localized events related or not to the presence and activity of the oyster farm (e.g. plume of suspended material from farm structures).

Table C4: Main BiCEM parameters adjusted during the calibration process of the present Baynes Sound application.

Variable	Symbol	Value	Unit	Literature range	Definition
Phytoplankton	Pm	300	gC gChl-a^{-1} day^{-1}	200-350	Maximum photosynthetic rate of Phytoplankton
	Topt	12	°C	up to 35	Optimal temperature for growth of Phytoplankton
	BMRp	0.1	day^{-1}	0.01-0.1	Basal metabolic rate of Phytoplankton
	Wp	0	m day^{-1}	0-30	Settling velocity of Phytoplankton
	Presp	0.2	-	0-1	Photo-respiration fraction of Phytoplankton
	BPRp	0.05	day^{-1}	0.05-1.0	Mortality rate of Phytoplankton (other than predation by Zoo)
	KHNp	0.014	mgN L^{-1}	0.003-0.923	Half-saturation concentration for DIN uptake by Phytoplankton
	CChl	55	gC gChl-a^{-1}	30-143	Carbon-to-chlorophyll ratio Phytoplankton
	Anc	0.175	gN gC^{-1}	-	Nitrogen-to-Carbon ratio Phytoplankton (Redfield ratio)
	Kd	0.3	m^{-1}	-	Light attenuation coefficient (based on PAR measurements from 2016 CTD profiles)
NH4-NO3	NTm	0.2	mgN L^{-1} day^{-1}	0.01-0.7	Reference nitrification rate (reference T = 20°C)
DON-PON	Kdn	0.2	day^{-1}	0.005-0.25	Reference Respiration rate of DON (reference T = 20°C)
	Kpn	0.15	day^{-1}	0.005-1.5	Reference Dissolution rate of PON (reference T = 20°C)
	Wd	4	m day^{-1}	0.0-6.0	Settling velocity of detritus particles
Bivalves	Wbdp	846	m day^{-1}	-	Settling velocity of bivalve feces (Callier et al. 2006)
	KHNc	0.004	mgN L^{-1}	-	Half-saturation concentration for clam ingestion
	KHNbo	0.05	mgN L^{-1}	-	Half-saturation concentration for bottom oyster ingestion
	KHNso	0.04	mgN L^{-1}	-	Half-saturation concentration for suspended oyster ingestion
Zooplankton	Im	1	day^{-1}	-	Maximum ingestion rate of Zooplankton
	Ez	0.3	-	-	Assimilation efficiency of Zooplankton
	BMRz	0.05	day^{-1}	-	Basal metabolic rate of Zooplankton
	BPRz	0.05	day^{-1}	-	Mortality rate of Zooplankton
	RFz	0.05	day^{-1}	-	Cost of growth for Zooplankton
	Znc	0.2	gN gC^{-1}	-	Nitrogen-to-Carbon ratio Zooplankton
	KHNz	0.03	mgN L^{-1}	-	Half-saturation concentration for Zooplankton ingestion
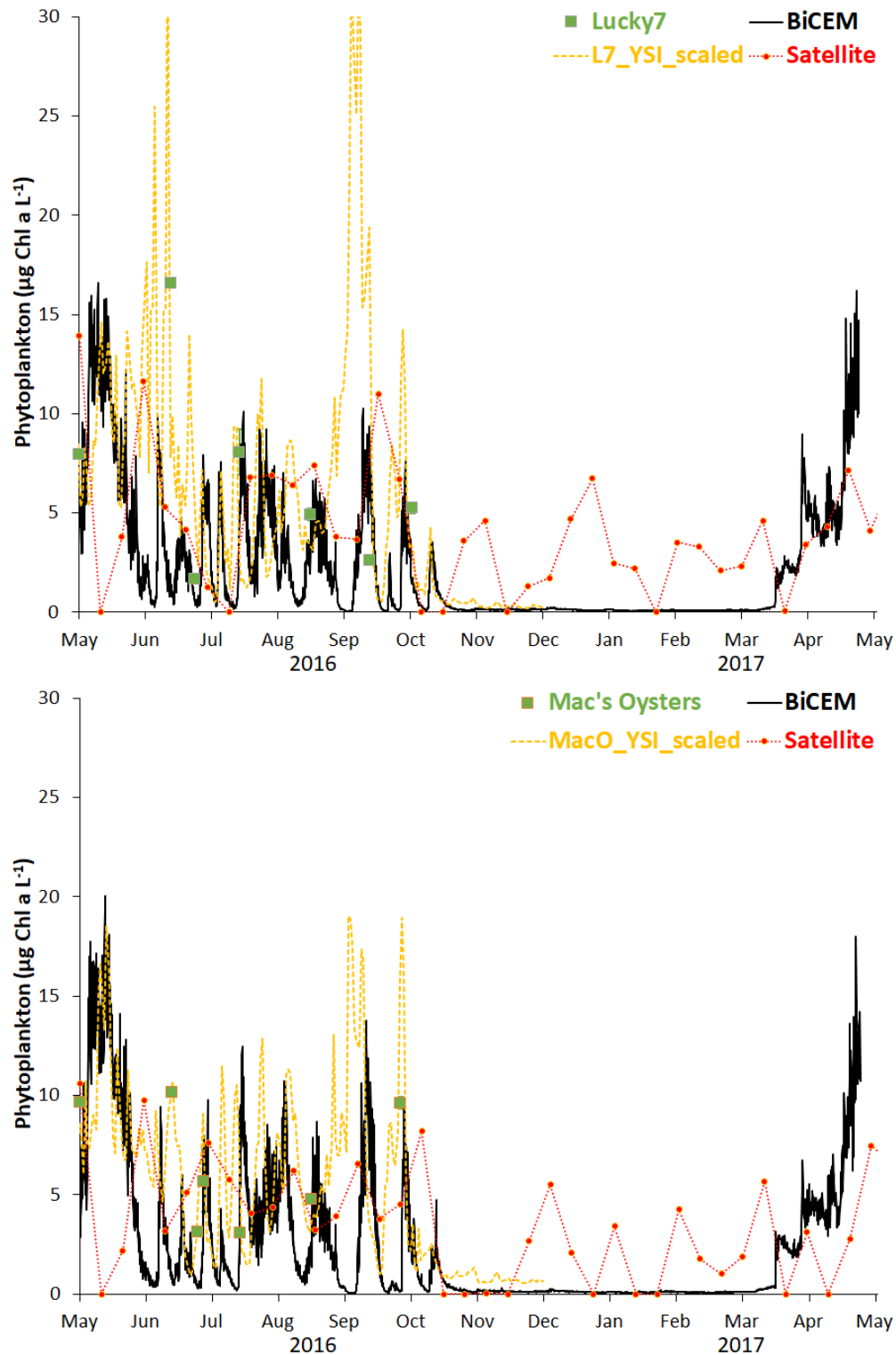
Figure C7: BiCEM – Observation comparison for phytoplankton time series at the Denman Point Lucky7 (top) and Metcalfe Bay Mac's Oysters (bottom) farms (see Figure 1 for locations). Individual water sampling, moored YSI probe and model data were all collected at the depth of cultured oysters (5 m). Satellite-derived data consist in a 10-day composite time series, are representative of surface waters and are included as reference for seasonality and in particular, the spring 2017 production onset.
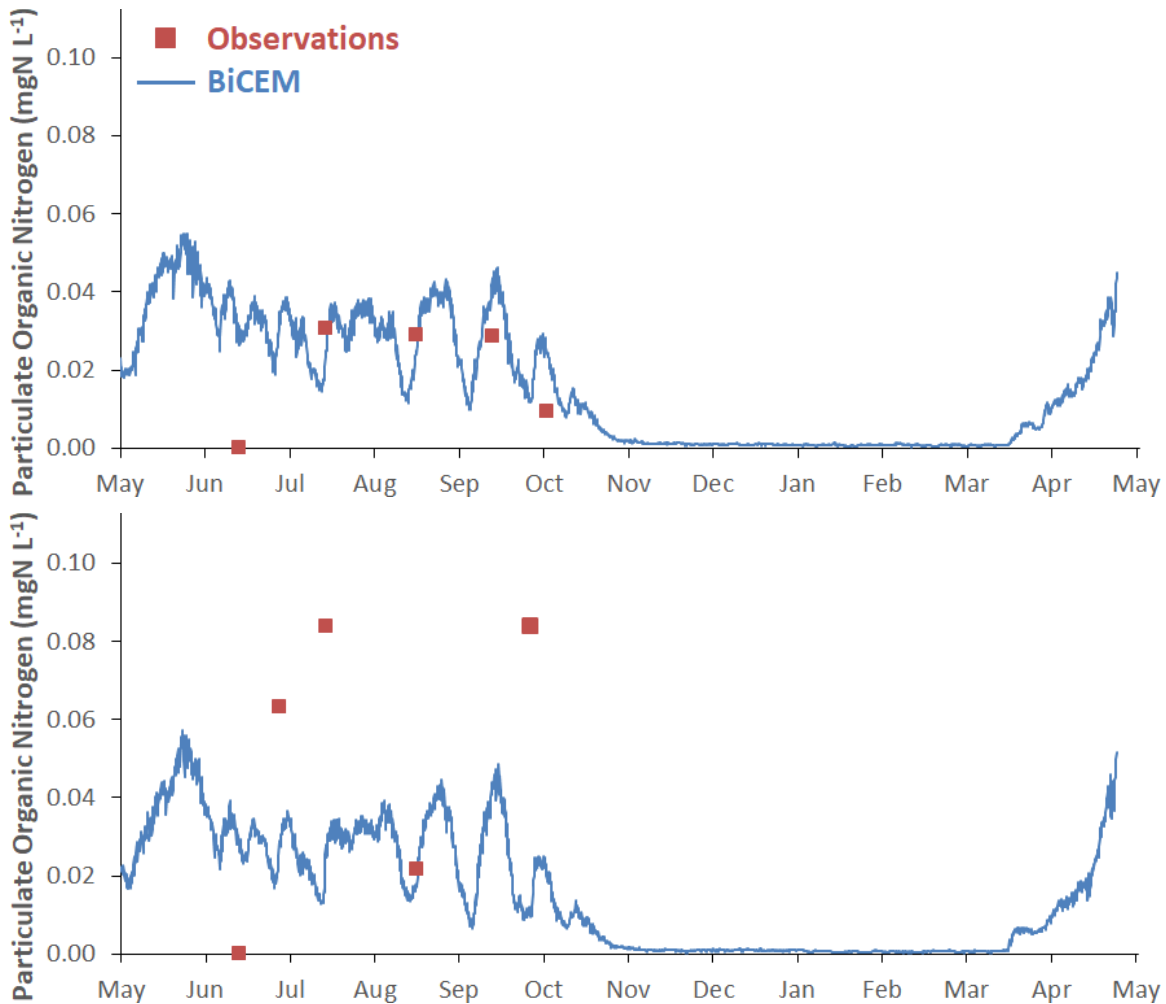
Figure C8: BiCEM-Observation comparison for particulate organic nitrogen concentrations at both oyster growth monitoring stations (Lucky7: top, Mac's Oysters: bottom).

Vertical profiles collected in late June 2016 at stations 2, 5, 8, 11, 14, 17, 20, 22 and corresponding BiCEM grid nodes along the main longitudinal axis of the Sound were gathered and plotted as 2D-contour thalwegs to assess the model performance in simulating the spatial structure of the pelagic variables. Two days (24-25 June) were necessary to survey the whole Sound while model outputs from 24 June early morning were used in the comparison presented in Figure C9. Some general spatial patterns, such as the aggregation of phytoplankton biomass in surface layers and corresponding reduced nitrate concentrations, the relatively lower phytoplankton biomass in the center part of the Sound compared to both the northern and southern ends and the intrusion of nutrient rich SOG bottom waters at the southern entrance, are well captured by BiCEM. Nevertheless, vertical gradients of both Phyto and NO3 are not as sharp in the model results with the phytoplankton biomass distributed over a slightly deeper surface layer, which also translates in a surface nitrate depletion not as severe as in the observed profiles. Considering that these results were obtained with a nil phytoplankton settling speed, Wp = 0 m d^{-1}, other factors spanning from bottom-up (i.e. nutrient availability from loading and hydrodynamics control) to top-down (i.e. zooplankton grazing pressure) processes have to be considered to explain this discrepancy.

Figure C9: BiCEM-Observation comparison along Baynes Sound main axis transect (stations 2, 5, 8, 11, 14, 17, 20, 22) for nitrate (top) and phytoplankton (bottom) in late June 2016. BiCEM output was extracted at grid nodes close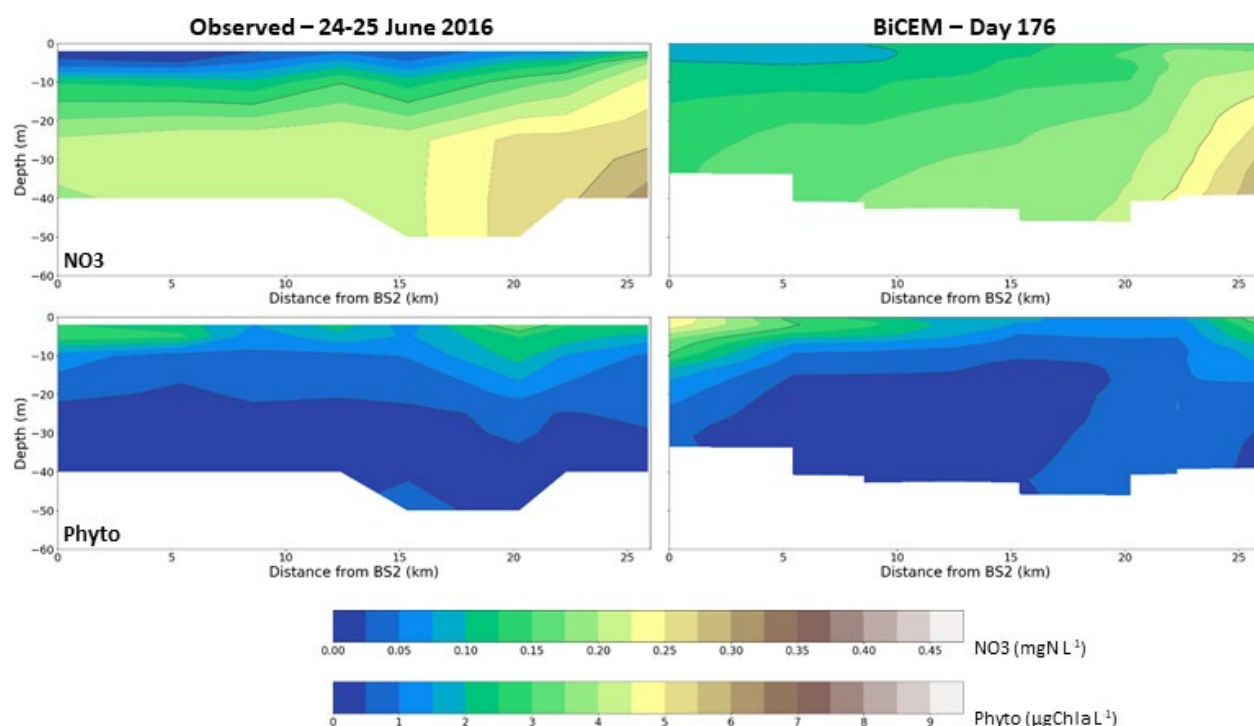st to each sampling station and the contours plotted represent a snapshot of day 176 early morning (24 June 2016), while observations were collected over two days (24-25 June 2016).

First, the light limitation of phytoplankton production could be at play here although it was tested during the calibration procedure and the model productivity is actually limited to a thinner surface layer (~10 m) than suggested by the biomass distribution. Some phytoplankton species are capable of adjusting their buoyancy to try and optimize their vertical position in the water column in terms of light and nutrient availability (Lännergren, 1979; Moore and Villareal, 1996). Such a behaviour, not accounted for in the model, could explain the aggregation of phytoplankton into a thinner layer. The zooplankton model variable also lacks any behaviour, in particular in terms of vertical migration, which could also explain part of the discrepancy in the vertical distribution of its main prey. Finally, overmixing, an issue commonly present in numerical models could also explain part of the discrepancy in the vertical distribution of variables between model results and observations. This vertical overmixing could originate from the FVCOM outputs and/or the BiCEM off-line coupling procedure.

Only three stations (2 in the north, 17 in the south and 23 just outside Baynes Sound southern entrance) were sampled during the spring 2017 survey. Sampling was however repeated through time to cover a full tidal cycle at each station. The observed vertical profiles of nitrate and phytoplankton were compared with model results over the same periods (Figure C10). This comparison confirms the previous outcome that BiCEM cannot simulate sharp enough vertical gradients as it tends to overestimate phytoplankton in the lower layers and nitrate in the surface waters. However, these only direct observations of 2017 show that the model is still in general agreement with the concentrations of both these variables towards the end of the simulation.

Observed primary productivity rates at Lucky7 and Mac's Oysters stations both in spring (29 April and 1 May 2016, respectively) and summer (24 and 26 June 2016, respectively) appear low compared to typical rates in temperate waters and the BiCEM simulated rates. When

reported to phytoplankton biomass, using the same Carbon to Chlorophyll a conversion ratio as in BiCEM, observed turnover rates ranged from 0.03 to 0.48 times per day in the surface waters (sampling at 1 and 5m depth), while the corresponding simulated ones ranged from 0.26 to 1.56 d^{-1} and reported rates typically range from 0.25 to 1.2 d^{-1} (Chen and Liu, 2010; Fox et al. 2020). These punctual measurements are subject to temporary adverse conditions in terms of light and nutrient availability that the model might not have captured. On a longer time scale, more relevant for the present carrying capacity assessment, the model simulated a mean productivity rate of 328.6 gC m^{-2} yr^{-1} over Baynes Sound, which is well within the range of 120 – 465 gC m^{-2} yr^{-1} reported in the SoG region (Harrison et al. 1983; Parsons et al. 1970; Winter et al. 1975).

Ultimately, disentangling the main causes for the mismatch in nitrate and phytoplankton vertical distributions would require additional observations, in particular of the temporal evolution of the nutrient profiles to evaluate the hydrodynamic control on nutrient availability (transport and mixing). Animations of the vertical viscosity (vertical mixing for velocity) and vertical diffusivity (vertical mixing for temperature, salinity and BiCEM pelagic variables) along a thalweg starting at the northern entrance, continuing along central Baynes, and ending beyond the southern entrance over day 190 (a random choice) of the FVCOM simulation indicate that most mixing is occurring near the sharp bathymetric changes just inside the southern entrance. However the strong mixing cells are not continuous in time, rather fluctuating with the tides and wind. Furthermore, they do not appear to be focused neither near the bottom nor surface. Either there are no mixing observations to evaluate the accuracy of these model values, or their location and magnitudes do seem reasonable. Although these results point towards a limited discrepancy in hydrodynamic control, even a slight deviation could combine with slight inaccuracies in the purely biological processes to lead to the observed mismatch. The overestimation of nitrate concentrations in surface layers could lead to an overestimation of primary productivity but some of this overestimation would be curtailed by light limitation on productivity below ~10 m.

Moreover, as mentioned above annual values of depth-integrated primary productivity simulated by BiCEM are not unrealistic and the comparison of depth-integrated phytoplankton biomass shows mixed results. When integrating the June 2016 data (shown on Figure C9) over the whole water column and averaging over all stations, the model actually underestimates the overall phytoplankton biomass by 2.5%. On the other hand, in April 2017 (profiles of Figure C10) the model does overestimate the depth-integrated phytoplankton biomass during this period of stronger primary productivity by 32 – 65% depending on the station.

Finally, although the general performance of the model is difficult to assess with these limited snapshots, most of the discrepancy in phytoplankton is occurring at depths deeper than the water layers occupied by bivalve farms (0 – 7 m), which would also limit its impact on the present carrying capacity assessment conducted through the relative comparison of scenarios.
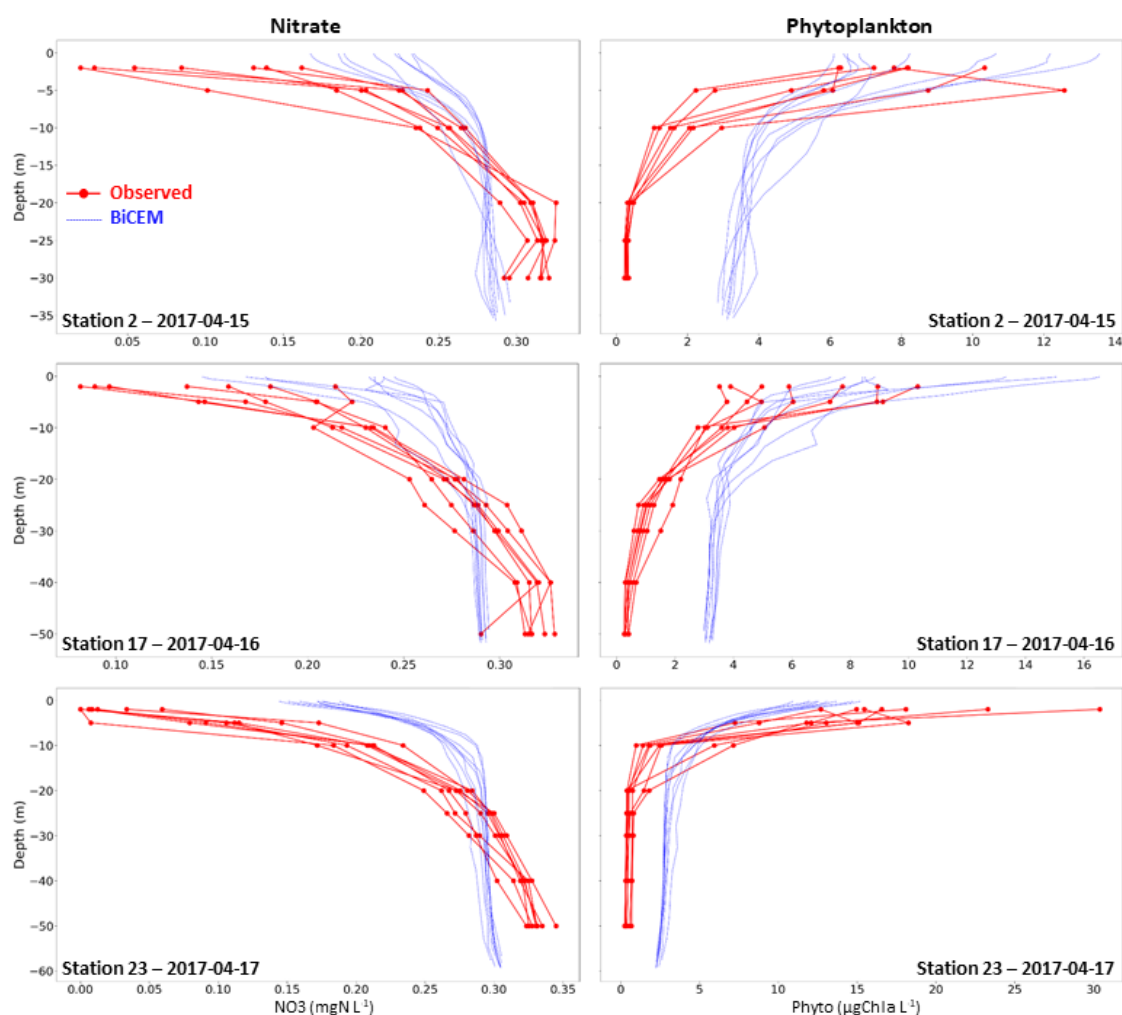
Figure C10: BiCEM-Observation comparison for vertical profiles of nitrate (left) and phytoplankton (right) at the 3 stations (2: top, 17: middle, 23: bottom) sampled in April 15-17 2017.

Bivalve growth constitutes another critical aspect of the model performance assessment. For the present study a dedicated growth monitoring was carried out for Pacific oysters reared in suspension at two partner farms located off the Denman Island coast, Lucky7 just south of Denman Point in the northern part of the Sound and Mac's Oysters in the Metcalfe Bay area in the south. The monitoring covered a full year from June 2016 to June 2017, which constitutes the majority of the production cycle for oysters reared in suspension. A new set of the main DEB parameters was calibrated using BiCEM outputs of food and temperature as forcing and observed growth at both monitoring sites to assess the model performance. Contrary to the calibration performed in Appendix B, the limited vertical resolution of BiCEM prevented a tray by tray comparison, hence observations from all trays were combined to build the growth data used here. Figure C11 presents the observation – BiCEM-DEB comparison at both monitoring sites and both in terms of oyster shell length and tissue weight. A difference was observed between the two sites with growth of Lucky7 oysters slowing down in late summer early fall 2016 (August-October) while Mac's Oysters maintained a fast growth until the last 2016 sampling date (28 September). The model outputs do not show this difference as simulated growth is similar at both sites and matches better with the observations at the Mac's Oysters raft.
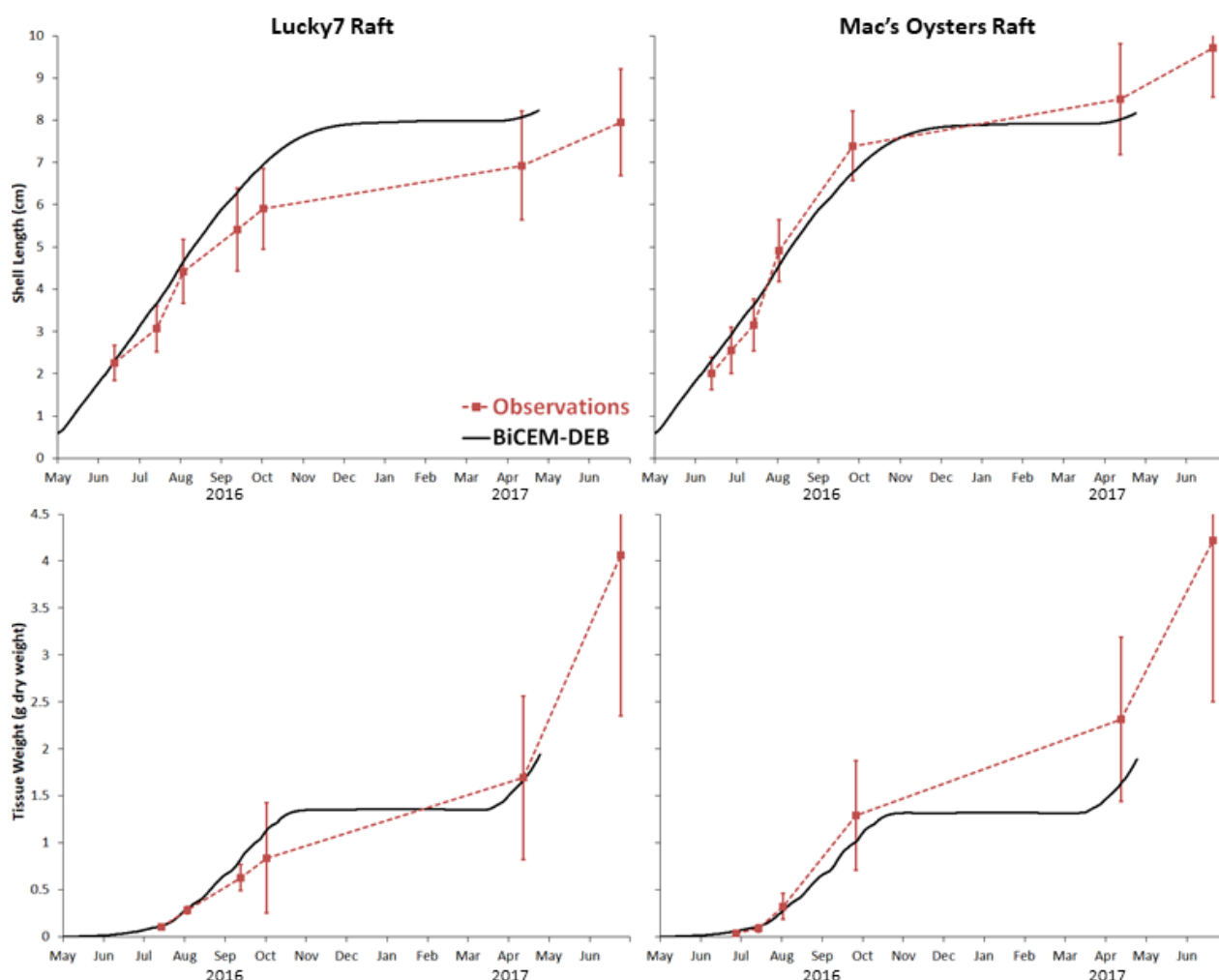
Figure C11: BiCEM-DEB – Observation comparison for the growth of oysters cultivated in suspension at both our monitoring sites (Lucky7 raft, Denman Point: left and Mac's Oysters raft, Metcalfe Bay: right see Figure 1 for exact locations) and both in terms of shell length (top) and tissue weight (bottom).

Several factors could contribute to this growth mismatch. First, any discrepancy between observed and simulated food levels and their potential differences between the two sites would also translate into oyster growth discrepancies. Such site differences in food levels are not obvious from the available phytoplankton observations (Figure C7), although Mac's Oysters did present higher PON concentrations on a few occasions that were not captured by BiCEM (Figure C8). In any case, food differences would have to be sustained over an extended period of time to cause the observed growth dissimilarity. Any differences in husbandry practices between the two farms during the monitored production cycle could potentially lead to growth differences that cannot be accounted for by the model. Finally, the same DEB parameter set was used for all oysters reared in Baynes Sound, which prevents the model from representing any potential differences in the stock reared by the different producers (seed origin, genetics, etc.).

Considering the above-mentioned limitations and in particular the use of a single DEB parameter set, including the feeding half-saturation coefficient usually adjusted to local conditions, an overall good agreement was reached with model results staying within ±1 SD of the observed inter-individual growth variability and achieving RMSD of 0.66 cm and 0.24 g dry

weight respectively for oyster shell length and tissue weight, when both sites are pooled together.

No growth data were available to assess the model performance for Pacific oysters reared on the bottom. Compared to suspension oysters only the feeding half saturation coefficient was slightly increased (0.05 vs 0.04 mgN L^{-1}) to account for a potential reduction in food accessibility in the 2D benthic set-up as opposed to the 3D pelagic environment provided to suspended oysters.

For Manila clams the set of DEB parameters derived by Filgueira et al. (2016) was adopted in the present BiCEM-DEB application and only the feeding half-saturation was adjusted to fit simulated growth with observations. Survey data reporting clam size at age (using shell rings) was used to derive annual growth rates for each age class. Simulated growth was compared to the observed growth for the age classes whose mean size corresponded to the shell length of model clams and at the grid nodes closest to the survey locations (n = 7). A good agreement was reached between simulated (5.55 ± 1.51 mm yr^{-1}) and observed (5.73 ± 0.23 mm yr^{-1}) mean shell growth rates (mean ± SD between sites) for a half-saturation coefficient KNHNc = 0.004 mgN L^{-1}.

10.4.3. Sensitivity analysis

An overall comparison of the +10% and -10% scenario results shows a symmetrical response of BiCEM to changes in all parameters tested except the optimal temperature for phytoplankton production (Table C5). This symmetry indicates a somewhat linear response of the model, a sign that BiCEM is in a rather stable state that eliminates the risk of extreme sensitivity and unpredictable behaviour.

On the other hand, the asymmetrical and strongest sensitivity of model results to the phytoplankton parameters tested and not only for Phyto itself but NO3 and PON as well, highlight both the importance of phytoplankton for the overall dynamics of the Baynes Sound model ecosystem and the capacity of these two parameters (optimal temperature and settling speed) to affect the model predictions. The statistics reporting spatial variability in the induced change (maximum, minimum and standard deviation) indicate a spatial heterogeneity within the Sound confirmed when the temporal mean is mapped out (Figure C12). Although Figure C12 summarizes the response of the Phyto variable to its optimal production temperature, it also illustrates features that were present in the response of other variable-parameter combinations. In particular, a stronger change is generally observed in the northern part of the Sound designating this area as more vulnerable to perturbations. Another prominent feature is the higher temporal variability encountered in the shallower and inter-tidal areas resulting from the more dynamic environment as opposed to the slower changing deeper and more open waters of the Sound. An exception to this general result can be seen in the vicinity of rivers (most visible in the Comox Harbour area) where external forcing tends to minimize change intensity and variability.

Table C5: Sensitivity analysis results. Mean and Absolute mean (mean of absolute values) represent both time (over 1 year) and space (over Baynes Sound) averages, while other statistics account for the spatial variability (over BS) of time-averaged change. SD: standard deviation, SL: shell length, TDW: tissue dry weight, ne: not evaluated.

| | | Sensitivity Index - Response Variable Change (%) | | | | | | | | | |
| | | NO3 | | | | | Phyto | | | | |
Parameter/Process	Degree of Change	Mean	Abs. Mean	Max.	Min.	SD	Mean	Abs. Mean	Max.	Min.	SD
River N (DIN&PON-DON) inputs	+10%	0.09	0.10	8.76	-0.04	0.57	0.03	0.04	0.51	-0.05	0.03
	-10%	-0.07	0.11	0.00	-7.83	0.48	-0.03	0.04	0.01	-0.54	0.03
Sediment DIN inputs	+10%	1.92	1.92	4.53	0.00	0.53	0.30	0.74	1.83	-0.16	0.20
	-10%	-1.92	1.93	0.00	-4.21	0.52	-0.30	0.75	0.18	-1.83	0.22
Phytoplankton settling speed	0.6 m d⁻¹	8.72	8.74	249.51	0.00	12.92	-20.04	21.02	0.00	-33.82	3.90
Phytoplankton optimal temperature	+10%	10.80	18.88	2056.6	-14.81	71.89	-7.24	23.75	60.75	-15.43	16.91
	-10%	3.98	10.08	99.37	-0.05	5.91	17.62	28.54	27.36	-8.09	5.59
Bottom oysters (feeding half-saturation)	+10%	ne	ne	ne	ne	ne	0.06	0.12	1.67	-0.08	0.14
	-10%	ne	ne	ne	ne	ne	-0.06	0.14	0.09	-1.86	0.16
Zooplankton (feeding half-saturation)	+10%	ne	ne	ne	ne	ne	13.79	14.14	21.38	0.00	3.80
	-10%	ne	ne	ne	ne	ne	-12.14	12.53	0.00	-14.92	3.00

| | | Sensitivity Index - Response Variable Change (%) | | | | | | | | | |
| | | PON | | | | | Zoo | | | | |
Parameter/Process	Degree of Change	Mean	Abs. Mean	Max.	Min.	SD	Mean	Abs. Mean	Max.	Min.	SD
River N (DIN&PON-DON) inputs	+10%	2.11	2.11	10.00	0.00	1.46	ne	ne	ne	ne	ne
	-10%	-2.11	2.11	0.01	-10.00	1.46	ne	ne	ne	ne	ne
Sediment DIN inputs	+10%	ne	ne	ne	ne	ne	ne	ne	ne	ne	ne
	-10%	ne	ne	ne	ne	ne	ne	ne	ne	ne	ne
Phytoplankton settling speed	0.6 m d⁻¹	-13.09	13.21	0.00	-28.06	4.92	-10.73	10.75	0.00	-19.33	2.74
Phytoplankton optimal temperature	+10%	ne	ne	ne	ne	ne	3.70	9.21	6.59	-5.31	1.55
	-10%	ne	ne	ne	ne	ne	4.60	12.58	7.12	-8.07	1.92
Bottom oysters (feeding half-saturation)	+10%	0.11	0.11	1.06	-0.02	0.11	0.16	0.16	1.33	0.00	0.13
	-10%	-0.13	0.13	0.00	-1.19	0.13	-0.18	0.18	0.00	-1.52	0.15
Zooplankton (feeding half-saturation)	+10%	2.61	3.30	5.06	-0.13	1.08	0.23	2.03	2.44	-0.89	0.44
	-10%	-2.67	3.48	0.13	-4.61	0.99	-0.43	2.31	0.73	-2.73	0.41

Sensitivity Index - Response Variable Change (%)

| Parameter/Process	Degree of Change	Bottom Oysters									
		Mean		Abs. Mean		Max.		Min.		SD	
		SL	TDW	SL	TDW	SL	TDW	SL	TDW	SL	TDW
River N (DIN&PON-DON) inputs	+10%	ne	ne	ne	ne	ne	ne	ne	ne	ne	ne
	-10%	ne	ne	ne	ne	ne	ne	ne	ne	ne	ne
Sediment DIN inputs	+10%	ne	ne	ne	ne	ne	ne	ne	ne	ne	ne
	-10%	ne	ne	ne	ne	ne	ne	ne	ne	ne	ne
Phytoplankton settling speed	0.6 m d^{-1}	ne	ne	ne	ne	ne	ne	ne	ne	ne	ne
Phytoplankton optimal temperature	+10%	ne	ne	ne	ne	ne	ne	ne	ne	ne	ne
	-10%	ne	ne	ne	ne	ne	ne	ne	ne	ne	ne
Bottom oysters (feeding half-saturation)	+10%	-1.80	-5.14	1.80	5.14	0.00	0.00	-2.04	-27.98	0.18	2.41
	-10%	1.97	6.01	1.97	6.01	2.32	39.90	0.00	0.00	0.21	3.92
Zooplankton (feeding half-saturation)	+10%	1.62	5.32	1.62	5.32	2.40	41.83	0.00	0.00	0.32	5.64
	-10%	-1.77	-5.25	1.77	5.25	0.00	0.00	-2.61	-29.38	0.33	3.83
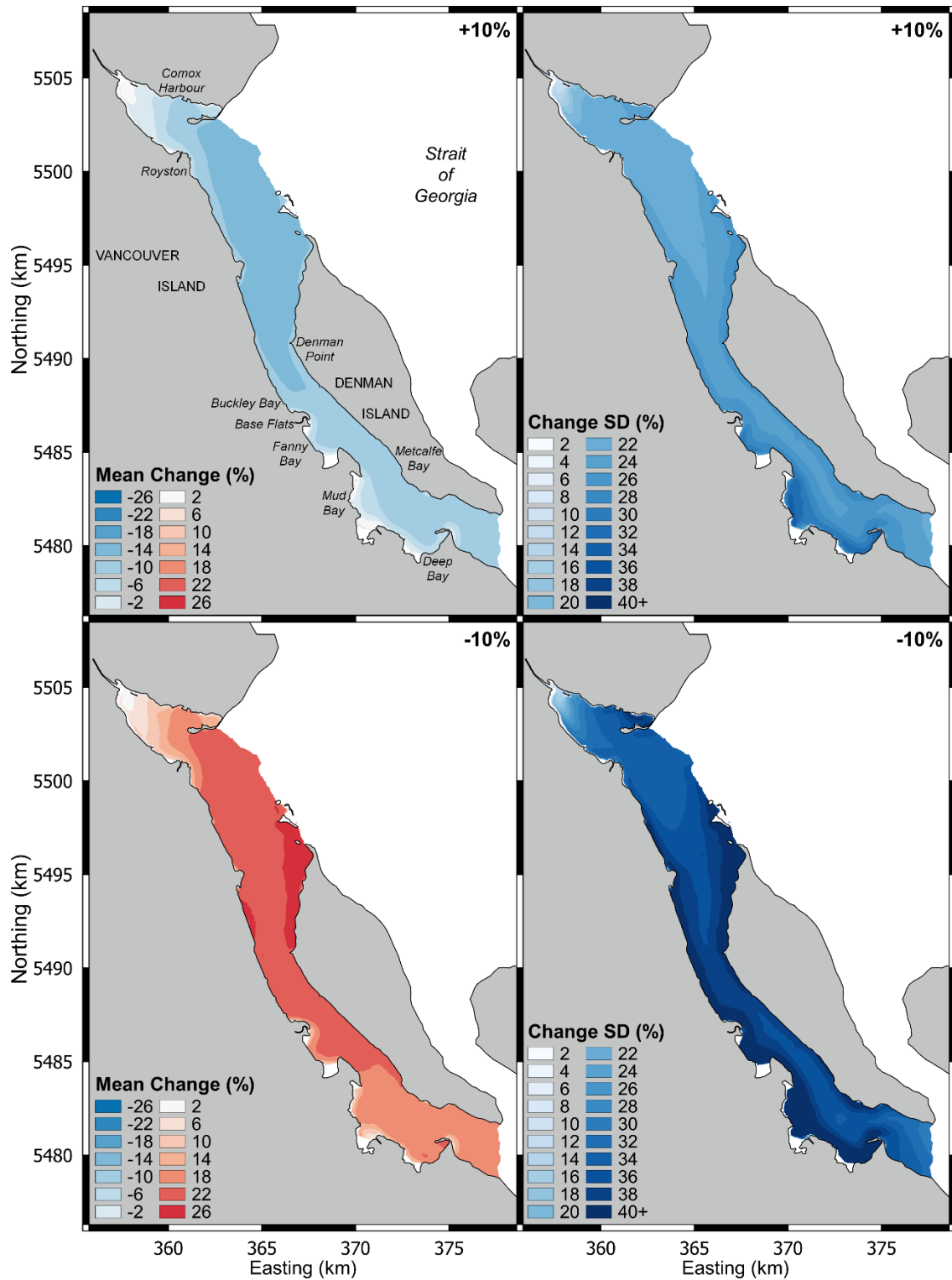
Figure C12: Maps of Sensitivity Index (SI) statistics over Baynes Sound for the response of the Phyto variable to a change in the Phyto production optimal temperature parameter (top: +10%, bottom: -10%). Left panels show the distribution of the SI time average and right panels correspond to the SI temporal variability expressed as the standard deviation (SD).

Further attention should be paid to the model sensitivity to this phytoplankton parameters, in particular the optimal temperature which could limit the model applicability, for example in the context of climate change scenarios. Phytoplankton settling speed is difficult to parametrize given the potential influence of both external (nutrient and light availability) and internal (algae cell condition) factors, in addition to inter-specific differences (Gemmell et al. 2016; Lännergren, 1979; Moore and Villareal, 1996; Richardson and Cullen, 1995).

Following the phytoplankton parameters, in order of strongest sensitivity comes the zooplankton feeding half-saturation (Table C5). This parameter had its largest influence on zooplankton food items, especially phytoplankton, rather than on its own biomass, showing the tight top-down control exerted by this primary consumer. The response of bottom oysters to this zooplankton parameter was also stronger than the response of Zoo biomass, which illustrates the competition between these two secondary producers and probably results, at least in part, from the poor food assimilation efficiency (Ez = 0.3) characterizing zooplankton. As is the case for most marine biogeochemical modelling applications, BiCEM would benefit from additional data that could help further constrain the zooplankton parameter values.

Overall, the model showed little sensitivity to bottom oyster feeding half-saturation, except for oyster themselves that responded moderately both in terms of shell length (~1.9%) and tissue weight (5 - 6%). The weak response of oyster food items illustrates the very limited influence the bottom culture of these bivalves exerts on the overall Baynes Sound model ecosystem dynamics, which tends to mitigate the lack of specific information available to validate this component of the present model application.

Finally, the scenarios testing the sensitivity of the system to nitrogen inputs from rivers and sediments show a fairly limited response (Table C5). A particularly weak response of NO3 and Phyto to river inputs can be noted (< 0.1% mean SI), while PON concentration responds a bit more to the direct discharge of PON from the rivers. Overall these river inputs seem to play a minor role in the model ecosystem, which could be expected considering the low river DIN and DON loading of 0.97 and 1.41 gN m^{-2} yr^{-1}, when scaled to the whole BS surface area. Sediment DIN inputs tend to trigger a slightly stronger response of the system, directly as a change in NO3 concentration (~1.9% mean SI), which also translates into a change in Phyto biomass (0.3% mean SI to 0.75% absolute mean SI). This result indicates that sediment inputs can alleviate some of the bottom-up control exerted by nutrient availability on the system's productivity. This benthic-pelagic coupling effect seems however restricted to the shallower areas of the Sound as shown by the spatial distribution of the mean SI (Figure C13). Additional data to inform the potential heterogeneity of these sediment fluxes over BS could help improve the simulation of the benthic-pelagic coupling effect by the model. However, the gain in accuracy at the scale of the ecosystem productivity seems limited according to the present results.

As previously stated, the general level of sensitivity revealed by this analysis seem limited enough to allow for further interpretation of the model results in the context of the present carrying capacity study. These results also highlighted some features of the BS model ecosystem functioning relevant in this context and that are further discussed in the main section of this document.
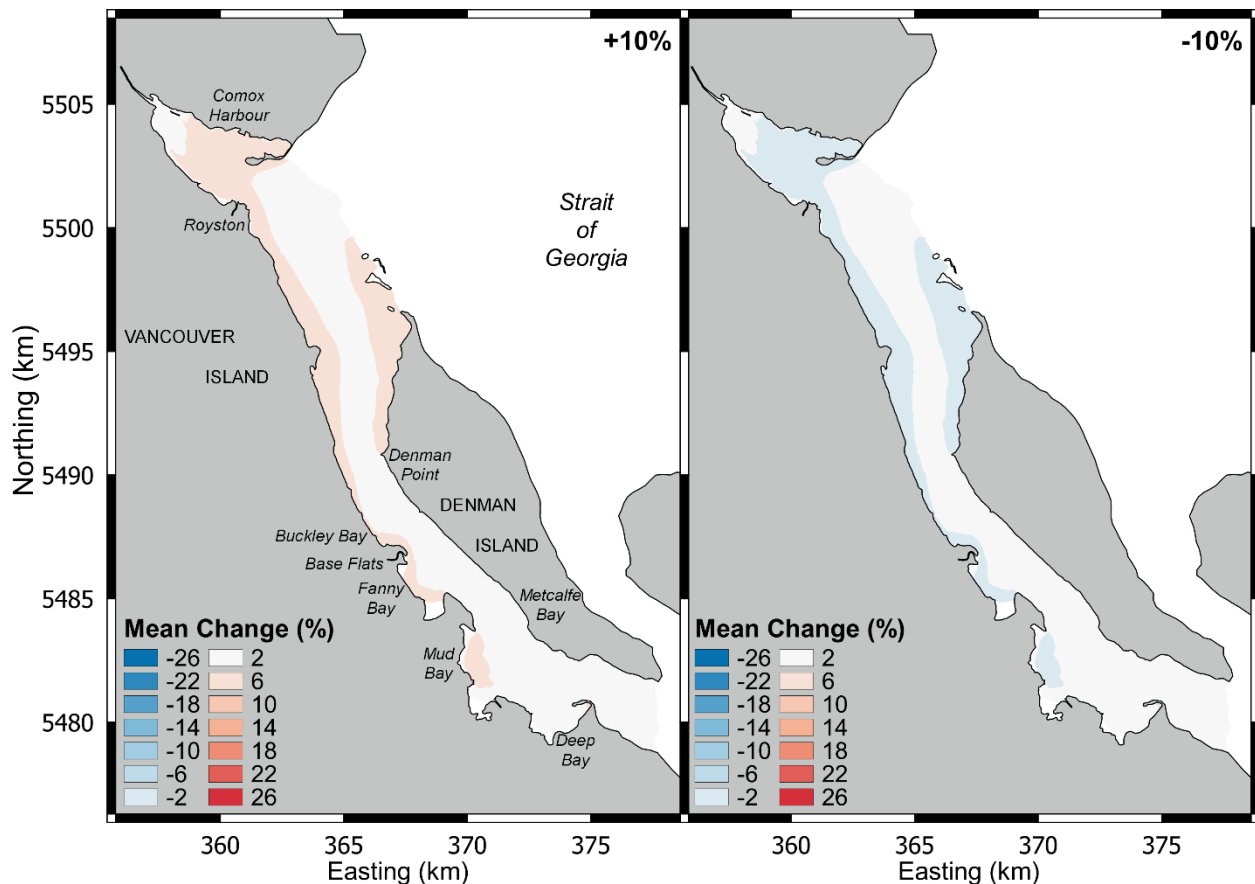
Figure C13: Maps of the temporal mean Sensitivity Index of nitrate concentration to changes in dissolved inorganic nitrogen inputs from the sediment (left: +10% input, right: -10% input).

10.5. ACKNOWLEDGMENTS

10.6. REFERENCES

Allen, S.E., and Wolfe, M.A. 2013. Hindcast of the timing of the spring phytoplankton bloom in the strait of Georgia, 1968-2010. Progr. Oceanogr. 115:6-13.

Barwell-Clarke, J., and Whitney, F. 1996. Institute of Ocean Sciences Nutrient Methods and Analysis. Can. Tech. Rep. Hydrogr. Ocean. Sci. 182:vi + 43 p.

Belley, R., Snelgrove, P.V.R., Archambault, P., and Juniper, S.K. 2016. Environmental Drivers of Benthic Flux Variation and Ecosystem Functioning in Salish Sea and Northeast Pacific Sediments. PLoS ONE. 113:1-26.

Biggs, M.I. 2015. Characteristics and status of the butter clam (*Saxidomus gigantea*) population at seal island, B.C. 1940-2013. MSc Thesis. Vancouver Island University. 119 p.

Cerco, C.F., and Cole, T. 1993. Three-dimensional eutrophication model of Chesapeake Bay. J. Env. Eng. 119 (6):1-16.

Chen, B., and Liu, H. 2010. Relationships between phytoplankton growth and cell size in surface oceans: Interactive effects of temperature, nutrients, and grazing. Limnol. Oceanogr. 55 (3):965-972.

DFO. 2015. Carrying capacity for shellfish aquaculture with reference to mussel aquaculture in Malpeque Bay, Prince Edward Island. DFO Can. Sci. Advis. Sec. Sci. Advis. Rep. 2015/003.

Filgueira, R., Comeau, L.A., Guyondet, T., McKindsey, C.W., and Byron, C.J. 2015. Modelling Carrying Capacity of Bivalve Aquaculture: A Review of Definitions and Methods. Meyers, R.A. (Ed), In: Encyclopedia of Sustainability Science and Technology pp. 1-33. Springer New York.

Filgueira, R., Guyondet, T., Comeau, L.A., and Sutherland, T.F. 2016. Dynamic Energy Budget DEB Models of Bivalve Molluscs Inhabiting British Columbia Coastal Waters: Review of Existing Data and Further Directions for Data Collection. In Can. Tech. Rep. Fish. Aquat. Sci. Vol. 3173. Vii + 28 p.

Flye-Sainte-Marie, J., Jean, F., Paillard, C., Ford, S., Powell, E., Hofmann, E., and Klinck, J. 2007. Ecophysiological dynamic model of individual growth of *Ruditapes philippinarum*. Aquaculture. 266 (14):130-143.

Fox, J., Behrenfeld, M.J., Haëntjens, N., Chase, A., Kramer, S.J., Boss, E., Karp-Boss, L., Fisher, N.L., Penta, W.B., Westberry, T.K., and Halsey, K.H. 2020. Phytoplankton Growth and Productivity in the Western North Atlantic: Observations of Regional Variability From the NAAMES Field Campaigns. Front. Mar. Sci. 7 (February):1-15.

Gemmell, B.J., Oh, G., Buskey, E.J., and Villareal, T.A. 2016. Dynamic sinking behaviour in marine phytoplankton: Rapid changes in buoyancy may aid in nutrient uptake. Proceedings of the Royal Society B: Biol. Sci. 283 (1840):20161126.

Gillespie, G.E., and Kronlund, A.R. 1999. A manual for intertidal clam surveys. Can. Tech. Rep. Fish. Aquat. Sci. 2270:144 p.

Gillespie, G.E., S.M. Bower, K.L. Marcus and D. Kieser. 2012. Biological synopsises for three exotic molluscs, Manila clam (*Venerupis philippinarum*), Pacific oyster (*Crassostrea gigas*) and Japanese scallop (*Mizuhopecten yessoensis*) licensed for aquaculture in British Columbia. DFO Can. Sci. Advis. Sec. Res. Doc. 2012/013. v + 97p.

Gower, J., and King, S. 2012. Use of satellite images of chlorophyll fluorescence to monitor the spring bloom in coastal waters. Int. J. Remot. Sens. 33 (23):7469-7481.

Gower, J., King, S., Statham, S., Fox, R., and Young, E. 2013. The Malaspina dragon: A newly-discovered pattern of the early spring bloom in the Strait of Georgia, British Columbia, Canada. Progr. Oceanogr. 115:181-188.

Harrison, P.J., Fulton, J.D., Taylor, F.J.R., and Parsons, T.R. 1983. Review of the biological oceanography of the Strait of Georgia: pelagic environment. Can. J. Fish. Aquat. Sci. 407:1064-1094.

Ingall, E., Kolowith, L., Lyons, T., and Hurtgen, M. 2005. Sediment carbon, nitrogen and phosphorus cycling in an anoxic fjord, Effingham Inlet, British Columbia. Americ. J. Sci. 3053:240-258.

Khangaonkar, T., Sackmann, B., Long, W., Mohamedali, T., and Roberts, M. 2012. Simulation of annual biogeochemical cycles of nutrient balance, phytoplankton blooms, and DO in Puget Sound using an unstructured grid model. Ocean Dyn. 629:1353-1379.

Kim, T., and Khangaonkar, T. 2012. An offline unstructured biogeochemical model UBM for complex estuarine and coastal environments. Env. Model. Software. 31:47-63.

Kooijman, S.A.L.M. 2010. Dynamic energy budget theory for metabolic organisation (3rd ed.). Cambridge, Cambridge University Press. 514 p.

Lännergren, C. 1979. Buoyancy of natural populations of marine phytoplankton. Mar. Biol. 54 (1):1-10.

Lavoie, M., McKindsey, C., Pearce, C., and Archambault, P. 2016. Influence of intertidal Manila clam *Venerupis philippinarum* aquaculture on biogeochemical fluxes. Aquac. Env. Int. 8:117-130.

Mackas, D., Galbraith, M., Faust, D., Masson, D., Young, K., Shaw, W., Romaine, S., Trudel, M., Dower, J., Campbell, R., Sastri, A., Bornhold Pechter, E.A., Pakhomov, E., and El-Sabaawi, R. 2013. Zooplankton time series from the strait of georgia: Results from year-round sampling at deep water locations, 1990-2010. Progr. Oceanogr. 115:129-159.

Moore, J K., and Villareal, T. A. 1996. Buoyancy and growth characteristics of three positively buoyant marine diatoms. Mar. Ecol. Progr. Ser. 1321 (3):203-213.

Morel, A., Huot, Y., Gentili, B., Werdell, P.J., Hooker, S.B., and Franz, B.A. 2007a. Examining the consistency of products derived from various ocean color sensors in open ocean (Case 1) waters in the perspective of a multi-sensor approach. Remot. Sens. Env. 111:69-88.

Morel, A., Gentili, B., Claustre, H., Babin, M., Bricaud, A., Ras, J., and Tièche, F. 2007b. Optical properties of the "clearest" natural waters. Limnol. Oceanogr. 521: 217-229.

Munroe, D. 2000. Habitat overlap of the varnish clam (*Nuttallia obscurata*) with other commercial clam species on Denman Island, B.C. Report submitted to DFO, Pacific Biological Station, Nanaimo, B.C. 14 p. (unpublished).

Parsons, T.R., LeBrasseur, R.J., and Barraclough, W.E. 1970. Levels of Production in the Pelagic Environment of the Strait of Georgia, British Colurnbia: A Review. J. Fish. Res. Board. Can. 27:1251-1264.

Parsons, T.R., Maita, Y., and Lalli, C.M. 1984. A Manual of Chemical and Biological Methods for Seawater Analysis. Pergamon Press, Oxford, UK. 173 p.

Richardson, T.L., and Cullen, J.J. 1995. Changes in buoyancy and chemical composition during growth of a coastal marine diatom: ecological and biogeochemical consequences. Mar. Ecol. Progr. Ser. 1281 (3):77-90.

Rigby, E.I. 2019. Springtime benthic fluxes in the Salish Sea : Environmental parameters driving spatial variation in the exchange of dissolved oxygen, inorganic carbon, nutrients, and alkalinity between the sediments and overlying water. Western Washington University. MSC thesis. 63 p.

Robert, R., Trut, G., and Laborde, J.L. 1993. Growth, reproduction and gross biochemical composition of the Manila clam *Ruditapes philippinarum* in the Bay of Arcachon, France. Mar. Biol.: Int. J. Life Oceans Coast. Waters. 116 (2):291-299.

Sutton, J.N., Johannessen, S.C., and Macdonald, R.W. 2013. A nitrogen budget for the Strait of Georgia, British Columbia, with emphasis on particulate nitrogen and dissolved inorganic nitrogen. Biogeosciences, 10 (11):7179-7194.

Winter, D.F., Banse, K., and Anderson, G.C. 1975. The dynamics of phytoplankton blooms in Puget Sound a fjord in the northwestern United States. Mar. Biol. 29:139-176.